Stony Brook University

Identification and characterization of the novel BAR-domain containing proteins, FAM92A and FAM92B, as interacting partners of the ciliary protein Chibby

A Dissertation Presented

by

Xingwang Chen

to

The Graduate School

in Partial Fulfillment of the

Requirements

for the Degree of

Doctor of Philosophy

in

Molecular and Cellular Pharmacology

Stony Brook University

August 2015

Stony Brook University

The Graduate School

Xingwang Chen

We, the dissertation committee for the above candidate for the

Doctor of Philosophy degree, hereby recommend

acceptance of this dissertation.

Ken-Ichi Takemaru, Ph.D.
Dissertation Advisor
Associate Professor, Department of Pharmacological Sciences

David Talmage, Ph.D.
Chairperson of Defense
Professor, Department of Pharmacological Sciences

Miguel Garcia-Diaz, Ph.D.
Associate Professor, Department of Pharmacological Sciences

Maurice Kernan, Ph.D.
Associate Professor, Department of Neurobiology and Behavior

This dissertation is accepted by the Graduate School

Charles Taber
Dean of the Graduate School

Abstract of the Dissertation

Identification and characterization of the novel BAR-domain containing proteins, FAM92A and FAM92B, as interacting partners of the ciliary protein Chibby

by

Xingwang Chen

Doctor of Philosophy

In

Molecular and Cellular Pharmacology

Stony Brook University

2015

Cilia are small hair-like projections extending from nearly all eukaryotic cell surfaces. Cilia are associated with critical cellular functions such as cellular motility as well as acting as the cellular antennae for signaling pathways and sensory functions. In recognition of this, there has been intense research to elucidate the molecular mechanism of ciliary formation and maintenance in order to understand the many and heterogeneous diseases (cilia-related diseases termed the ciliopathies) resulting from ciliary defects. Chibby (Cby) is an evolutionarily conserved coiled-coil protein that was initially isolated as an antagonist of the canonical Wnt/β-catenin signaling pathway. Generation of CbyKO mice revealed phenotypes characteristic of ciliopathic diseases.

Subsequently, it was revealed that Cby is a critical mediator of cilia formation through its ability to recruit membranous vesicles to the ciliary base. However, the molecular mechanism as to how exactly Cby facilitates recruitment and subsequent fusion of small vesicles to centrioles remains unclear.

In order to gain insight into the role of Cby in vesicle recruitment, I first examined Cby dynamics at the bases of cilia in order to gain insight into the role Cby plays in vesicle recruitment. The fluorescence recovery after photobleaching (FRAP) data indicates that Cby is localized to a region of the cilia that is not readily accessible thru free diffusion. Second, I compiled a comprehensive list of potential Cby interacting partners, with a focus on basal body proteins. The tandem affinity purification (TAP) technology was used to identify the novel Cby interacting partners FAM92A and FAM92B. Beyond the few studies that suggest that FAM92A plays a role in embryogenesis, little else is known about the function of the FAM92 family of proteins. Members of this family contain a putative BAR-domain. BAR-domains are a highly conserved domain that forms a crescent-shaped homodimer and is found in many proteins involved in membrane dynamics.

I characterized FAM92A and FAM92B as novel Cby interacting partners that localized to the base of cilia. The BAR-domain of FAM92A and FAM92B was sufficient for this interaction as well as the FAM92 proteins ability to homodimerize. In the absence of Cby, FAM92A and FAM92B localization to the base of cilia was disrupted. This suggests that Cby acts upstream of the FAM92 proteins, possibly recruiting the FAM92 proteins to the basal body. Additionally, siRNA mediated knockdown of FAM92A decreased cilia formation, which implicates the FAM92 proteins involvement in cilia

formation. Furthermore, ectopic expression of FAM92 and Cby induced membrane tubule-like structures. Overall, I have identified and characterized the BAR-domain containing proteins, FAM92A and FAM292B, as novel Cby interacting partners. The BAR-domain properties of FAM92 proteins could provide the crucial link between Cby's ability to recruit vesicles and the subsequent membrane fusion necessary for cilia formation.

Table of Contents

List of Figures

Chapter 1

Chapter 2

Chapter 3

List of Tables

List of Abbreviations

APC:	Adenomatous polyposis coli
BAR:	Bin/Amphiphysin/Rvs
BBIP10:	BBSome Interacting Protein 10 kDa
BBS:	Bardet-Biedl Syndrome
CCDC186:	Coiled-coil domain containing 186
CCP:	Clathrin-coated pit
CK1α:	Casein kinase I
CME:	Clathrin mediated endocytosis
Dvl:	Dishevelled
FRAP:	Fluorescence recovery after photobleaching
Fz:	Frizzled
GA:	Golgi-apparatus
GEF:	Guanine nucleotide exchange factor
GPCR:	G-protein-coupled receptor
Gro:	Groucho
GSK3:	glycogen synthase kinase 3
Hh:	Hedgehog
HTR6:	Serotonin receptor 6
IFT:	Intraflagellar transport
JBTS:	Joubert syndrome
LRP5/6:	Lipoprotein receptor related protein
MCHR1:	Melanin concentrating hormone receptor 1
MKS1:	Meckel
NPHP:	Nephronophthisis
PCD:	primary ciliary dyskinesia
PCM:	pericentriolar material
PIGEA-14:	polycystin-2 interacting Golgi- and endoplasmic reticulum-associated

PKD:	polycystic kidney disease
PKD2:	polycystin-2
Ptch:	Patched
SIM:	Structure Illumination Microscopy
SSTR3:	Somatostain receptor 3
TAP:	Tandem affinity purification
TCF/LEF:	T-cell factor/lymphoid enhancer factor
TGN:	Trans-Golgi network

Acknowledgments

First and foremost, I would like to thank my advisor and mentor, Dr. Ken-Ichi Takemaru, for his guidance and support throughout my graduate studies. The lessons that I have learn from my time in his laboratory, from experimental design, to data interpretation, and equally important, how to present the data to an audience is something I will always treasure. Thank you, Ken, for teaching me to always ask why and to always do the necessary research before attempting an answer.

I would like to thank my thesis committee, Dr. Miguel Garcia-Diaz, Dr. Maurice Kernan, and Dr. David Talmage for their time, effort and guidance. Thanks to Dr. Kernan for his insight on phylogenetic analyses on the convergent nature of ciliary proteins. Thanks to Dr. Garcia-Diaz for his help in teaching me the use of the 3D structure prediction program Phyre2 and the generous gift of TEV proteases.

Thanks to all the past and present members of the Takemaru-Li lab including Dr. Damon Love, Dr. Ada Mofunanya, Dr. Victoria Fischer, Dr. Michael Burke, Dr. Benjamin Cyge, Dex-Ann Brown-Grant, and Saul Siller for the advice, reagents, and conversations, both scientific and otherwise. Particularly, thanks to Dex-Ann for her advice on being a newly minted parent. Thanks to Saul for his help in providing the MTECs. Thanks to all members of the office staff of the Department of Pharmacological Science especially Odalis Hernandez, who go above and beyond to ensure our life as graduate student can be focused on science.

I would like to thank my family for everything. My parents, Zhong Zhou Chen and Liying Li, who worked and sacrificed so much so that their children can pursue their

dreams. My sister, Dr. Xia Chen, whose strength and wisdom is a continuing source of admiration and inspiration. My beautiful wife, Mei Chen, whose support, love and compassion has made me a better man and makes me strive to be a better husband. Last but not least, my daughter, Alessandra Chen, whose laughter fills my heart with a joy I have never experience before.

Chapter 1: General Introduction

1.1 Cilia

Cilia structure and function

Cilia are hair-like organelles that project from the surfaces of nearly all eukaryotic cell types. The structure of cilium comprises a cylindrical microtubule-based cytoskeleton, called the axoneme, surrounded by the specialized plasma membrane. Cilia are broadly classified into two main categories according to their axonemal composition as well as motility. The axoneme of the primary cilia contains a ring of nine microtubule doublets in a 9+0 arrangement, while that of the motile multi-cilia contains the nine microtubule doublets plus a central pair of microtubule singles in a 9+2 arrangement (Badano et al., 2006). The primary cilium is present on most mammalian cell types and was ignored for over a century as a vestigial organelle after discovery. Recently however, much progress has been made in elucidating the function of the primary cilium, which is now known to play crucial roles in mechanosensation, photoreception and intracellular signaling (Fliegauf et al., 2006; Goetz and Anderson, 2010; Steere et al., 2012; Roy, 2009). Motile multi-cilia are mainly found on epithelial cells that line the airways, reproductive tracts and ependymas. These cilia are important for generating the physical forces needed for clearing mucus from the airway, transporting ova from the ovary to the uterus and circulating cerebrospinal fluids in the brain. This two scheme classification is simplistic and can be misleading, as motile primary cilia and sensory multi-cilia types exist (Shah et al., 2009). An example of motile primary cilia is found in the node of vertebrate embryos. Nodal primary cilia has a classic 9+0 arrangement but also have dynein arms that moves the cilia in a rotational

motion to establish left-right asymmetry (Nonaka et al., 1998a; Wagner and Yost, 2000; Essner et al., 2002; Nonaka et al., 1998b).

The cilium is a complex structure with over 1200 different proteins identified by proteomic analysis, many of which are known to associate with the axoneme (Pazour et al., 2005; Goel et al., 2013; Gherman et al., 2006; Yuan and Sun, 2013; Rolland et al., 2014). The ciliary structure can be separated into 3 distinct subdomains, each with its own unique ultrastructure and protein composition. Going from the most proximal to the distal are the basal body, the transition zone, and the ciliary axoneme (Figure 1). The basal body and the surrounding pericentriolar material (PCM) serve as the platform on which cilia are built. In order for proper docking to the plasma membrane to occur, the mother centriole/basal body forms accessory structures, which include the sub-distal and distal appendages (Graser et al., 2007; Ishikawa et al., 2005; Avasthi and Marshall, 2012). Amongst the distal appendage proteins, Cep164 is thought to play a major role in maintaining the structural integrity of the distal appendage as well as the subsequent recruitment of Rab8-associated vesicles (Kim and Dynlacht, 2013a). Cep164 is also required for the removal of TTBK2 and CP110 which serve as a cap that must be removed before cellular differentiation and subsequent ciliogenesis can be initiated (Tanos et al., 2013). The PCM is the amorphous mass of proteins that surrounds the two centrioles and is responsible for microtubule nucleation and anchoring. Pericentriolar proteins such as Cep290 and PCM-1 are required for the efficient recruitment of Rab8, as depletion of these proteins resulted in a significant decrease in Rab8 localization at the cilium as well as a decrease in cilium formation (Kim et al., 2008; Lopes et al., 2011; Dammermann and Merdes, 2002; Craige et al., 2010).

The region between the basal body and the axoneme is termed the transition zone, and has been a major focus of research. Marking this region are the Y-link structures that connect each of the nine microtubule doublets with the ciliary membrane. Several studies have linked transition zone proteins to roles in regulating ciliary protein composition. As such, depletion of transition zone proteins such as MKS1, TCTN1-3, and JBTS results in severely stunted cilia (Awata et al., 2014; Chih et al., 2012). These studies implicate the transition zone as a ciliary gate, providing a physical and molecular barrier to regulate protein entry and exit from the cilium (Chih et al., 2012; Craige et al., 2010; Williams et al., 2011).

The ciliary axoneme comprises of the axoneme which is sheathed by specialized extensions of the plasma membrane. Primary cilia mediate various signaling pathways by transporting and regulating signaling components along the axoneme. In motile cilia, the axoneme contains the motor proteins and inner and outer dynein arms, which drive the coordinated beating of cilia to move fluid over the epithelial surface (Satir and Christensen, 2007). Additionally, the intraflagellar transport (IFT) machinery uses the microtubule tract of the axoneme to transport ciliary cargo to and from the ciliary tip.

Ciliopathies

Ciliopathies comprise a group of disorders associated with genetic defects that result in the abnormal function or formation of cilia (Waters and Beales, 2011; Hildebrandt et al., 2011; Fliegauf et al., 2007a; Brown and Witman, 2014). Because cilia are present on many cell types, a single underlying genetic defect can affect multiple tissues. One of the best characterized ciliopathies is primary ciliary dyskinesia (PCD),

which is also known as immotile cilia syndrome. PCD is a devastating inherited disorder characterized by chronic respiratory disease, male infertility, and *situs inversus* (Bush and Ferkol, 2006; Schidlow, 1994). The most frequent cause of PCD is the loss of function of the outer dynein arms. The outer dyneins arms are found at the outer microtubule doublets and are responsible for generating ciliary beating using energy derived from ATP hydrolysis (Pazour et al., 2006; Lee, 2011; Voronina et al., 2009a). As a result, PCD patients often exhibit chronic bronchitis and sinusitis due to inefficient mucus clearance by motile cilia in the nasal epithelium. *Situs inversus* is a condition in which the positioning of the internal organs are reversed (Pazour and Rosenbaum, 2002). During embryonic development, nodal cilia are responsible for generating the leftward fluid flow over the embryonic node, a transient embryonic cavity that forms at the end of the developing notochord, which ultimately determines left-right asymmetry. In the absence of this fluid flow to dictate orientation, the position of organs is randomized with an equal chance that the embryo will develop with a left-right or right-left orientation (Nonaka et al., 1998a; Wagner and Yost, 2000). Other manifestations of motile cilia dysfunction include embryonic lethality due respiratory dysfunction, reproductive sterility, and hydrocephalus (Badano et al., 2006; Waters and Beales, 2011).

In contrast, defects of primary ciliary manifest a broad range of phenotypes likely due to their presence on many different cell types and their role in signal transduction (Hildebrandt and Zhou, 2007; Fliegauf et al., 2007b; Waters and Beales, 2011; Hildebrandt et al., 2011). One of the most common phenotypes of primary ciliary dysfunction is the formation of renal cysts, a condition associated with polycystic kidney

disease (PKD), Bardet-Biedl syndrome (BBS), Meckel syndrome (MKS), and nephronophthisis (NPHP) (Hildebrandt and Zhou, 2007; Pedersen et al., 2008; Jin and Nachury, 2009; Kim and Dynlacht, 2013a). The most prevalent of these disorders, PKD is amongst the most common life-threatening inheritable diseases, affecting over 12.5 million people worldwide (Brown and Witman, 2014). Primary cilia are thought to function in the renal epithelium as environmental sensors that regulate cell growth and differentiation, and their dysfunction results in abnormal cell proliferation and the consequent production of renal cysts (Badano et al., 2006). NPHP is an autosomal recessive cystic kidney disease and the most frequent cause of end stage renal failure in children (Hildebrandt and Zhou, 2007). It is characterized by the formation of corticomedullary cysts, interstitial fibrosis and renal insufficiency. Mutations in 11 different genes, *NPHP1-11*, are known to cause NPHP (Hildebrandt and Zhou, 2007; Wolf and Hildebrandt, 2011). Retinitis pigmentosa is another ciliopathy associated with primary ciliary defects. Primary cilia of the photoreceptor cells are responsible for connecting and trafficking of proteins from the inner segment to the outer segment, and their dysfunction leads to degenerative eyes and eventual blindness (Badano et al., 2006). Other primary cilia-related ciliopathies include Senior-Loken syndrome, MKS, BBS, and Joubert syndrome (JBTS), which manifest clinical phenotypes including *situs inversus*, polydactyly, deafness, mental retardation, and cysts of the kidney, liver and pancreases (Gunay-Aygun, 2009; Adams et al., 2007; Tobin and Beales, 2009; Sharma et al., 2008).

Primary cilia in signal transduction

To understand the cause of a ciliopathy phenotype, it is important to examine the biological processes at the cellular level that are perturbed under disease conditions. Located on the ciliary membrane are receptors, ion channels, effector proteins and transcription factors that mediate extracellular signals to control basic cellular processes both during embryonic development and adult homeostasis (Lienkamp et al., 2012; Dafinger et al., 2011; Nusse et al., 2008; Goetz and Anderson, 2010). The significance of primary cilia in early vertebrate development was first revealed in the a genetic study that demonstrated that the cilium is critical for survival and fate determination of the mouse embryo (Goetz and Anderson, 2010). Important developmental signaling pathways such as the Hh signaling and Wnt/β-catenin signaling pathways have all been shown to be dependent on cilia (Goetz and Anderson, 2010; Huangfu et al., 2003; Lienkamp et al., 2012; Jones et al., 2008). Consequently, ciliopathies often manifest in pathologies that are related to signal transduction pathways.

The Hh pathway is dependent on primary cilia for signaling (Huang and Schier, 2009; Huangfu et al., 2003; Satir and Christensen, 2007). Hh signaling is a highly conserved and ubiquitous pathway regulates a variety of cellular processes including cell fate specification and cell proliferation (Waters and Beales, 2011; Jacob and Lum, 2007; Jiang and Hui, 2008). In the unstimulated state Patched (Ptch), a transmembrane Hh receptor found at the ciliary membrane, represses activation of Smoothened (Smo), a G-protein coupled receptor found around the base of cilia (Milenkovic et al., 2009). Upon Hh binding to Ptch, Smo is then able to translocate to the ciliary membrane to activate Gli2. Gli2, a transcription factor, usually found at the ciliary tip, then translocate to the nucleus where it activates Hh target gene expression (Milenkovic et al., 2009).

Genetic studies showed that intraflagellar transport (IFT) proteins are required for Hh signaling, specifically the translocation of Gli2 from the ciliary tip to the nucleus (Huangfu et al., 2003; Kim et al., 2010; Ocbina et al., 2009).

The Wnt/β-catenin pathway regulates development, stem cell pluriopotency and cell fate determination (Klaus and Birchmeier, 2008; Pinto and Clevers, 2005). The Wnt proteins are a family of 19 highly conserved, secreted glycoproteins that act as ligands for receptor mediated signaling, most notably in this case for the Frizzled (Fz) family of G-protein coupled receptors (Angers and Moon, 2009; Nusse et al., 2008). In the absence of Wnts, cytoplasmic β-catenin is recruited and phosphorylated by a 'destruction complex' comprised of the tumor suppressor *adenomatous polyposis coli* gene product (APC), Axin, casein kinase 1α (CK1α), and glycogen synthase kinase 3 (GSK3). The phosphorylated β-catenin is rapidly ubiquitylated and targeted for degradation by the 26S proteasome. The suppressed level of β-catenin allows the transcriptional repressor Groucho (Gro) to bind to the T-cell-specific factor/lymphoid enhancer-binding factor (TCF/LEF) transcription factors, preventing the expression of Wnt/β-catenin target genes (Behrens et al., 1996). The Wnt/β-catenin pathway is activated upon Wnt ligand binding to Fz and its co-receptors, low-density lipoprotein receptor related protein 5 and 6 (LRP5/6) (Angers and Moon, 2009). This binding recruits Dishevelled (Dvl) and axin proteins via interaction with Fz and LRPs, thereby preventing the formation of the β-catenin phosphorylating 'destruction complex' (Clevers, 2006). β-Catenin accumulates in the cytoplasm and translocates to the nucleus. Nuclear β-catenin displaces with Gro from TCF/LEF transcription factors and activates Wnt target genes (Behrens et al., 1996).

There have been substantial interests in the relationship between cilia and Wnt signaling. Nephrocystin-2, the product of the *NPHP2/inversin* gene, has been shown to block Dvl's ability to activate Wnt signaling by targeting it for degradation (Simons et al., 2005; Lienkamp et al., 2012). Kif3a, an essential component of the anterograde motor kinesin 2, has been shown to regulate Wnt signaling by restricting CK1α phosphorylation of Dvl (Corbit et al., 2008). Additionally, it has been reported that the suppression of *BBS4*, which encodes a basal body protein that is a core component of the BBSome complex, led to a disruption in proteasomal targeting with a concomitant accumulation of cytoplasmic β-catenin (Gerdes et al., 2007). Cumulatively, these data suggest that basal body proteins are important regulators of Wnt signaling (Corbit et al., 2008; Lienkamp et al., 2012; Gerdes et al., 2007).

However, other studies have shown that mutants for ciliary genes fail to show the phenotypes characteristic of Wnt signaling defects. In zebrafish, a mutants deficient in *Ift88* lacks cilia, but shows no apparent defects in Wnt-dependent developmental processes or in expression of known Wnt target genes (Huang and Schier, 2009). Another study showed that expression of the Wnt target gene *Axin2* and a transgenic Wnt reporter is normal in mouse embryos lacking ciliary genes such as *ift88, ift72,* or *kif3a* (Ocbina et al., 2009). Interestingly, Cby was initially characterized as a β-catenin antagonist and through generation of CbyKO mice, it was found that Cby also has a role in cilia formation. In airway epithelia and MEFs, mutations of the *Cby* gene result in mild up-regulation of Wnt responses (Voronina et al., 2009b). In reconciliation of these two contrasting analyses, it is possible that the role of cilia in the canonical Wnt pathway might be cell type-specific and more subtle than its effect on the Hh signaling pathway.

1.2 Ciliogenesis

Initiation of cilia formation

Centrosomes are non-membrane bound organelles located in close proximity to the nucleus. The centrosome comprises a mother and a daughter centriole that together with the PCM forms a microtubule organizing complex (MTOC) to generate the mitotic spindle pole in dividing cells. The mother centriole is distinguishable from the daughter centriole by the presence of fibrous distal and subdistal appendages which are crucial for initiation of cilia formation. Ciliogenesis of both primary and multi-ciliated cells is thought to largely follow similar pathways with a key difference in how centrioles are generated (Marshall et al., 2005; Vladar and Stearns, 2007). In primary ciliated cells, centrioles duplicate using existing centrioles as templates, while multi-ciliated cells must undergo additional template-independent steps to generate hundreds of centrioles.

Ciliogenesis occurs through an ordered series of steps (Sorokin, 1968; Ishikawa and Marshall, 2011; Hagiwara et al., 2000). First, the mother centriole acquires various accessary structures such as distal and subdistal appendages to mature into the basal body. Distal appendage protein Cep164 triggers ciliogenesis by recruiting TTBK2, which is required for the removal of centriole capping protein, CP110, and recruitment of IFT proteins (Cajánek and Nigg, 2014; Graser et al., 2007). The basal body then migrates towards the cell surface (Tanos et al., 2013; Graser et al., 2007; Joo et al., 2013). The distal appendages are thought to transform into the transition fibers upon docking to the apical membrane as revealed by transmission electron microscopy (TEM) (Sorokin, 1968; Graser et al., 2007). During the migration, the distal appendage of the mother centriole associates with post-Golgi vesicles, which fuse to each other and flatten prior

to fusion the plasma membrane (Sorokin, 1962). The removal of the centriolar capping proteins, CP110 and CPAP, from the distal end of the basal body is a prerequisite for elongation of the axoneme (Tsang et al., 2008; Tanos et al., 2013; Schmidt et al., 2009). Next, the basal body nucleates the outgrowth of axonemal microtubules, which protrude beneath an extension of the plasma membrane giving rise to the mature axoneme. The delivery of ciliary components from the cytoplasm to the cilium is mediated by members of the Arf and Rab family of small GTPases (Chavrier and Goud, 1999; Knödler et al., 2010).

The IFT particles move along the polarized microtubule axoneme from the base of the cilium towards the ciliary tip and back to the base. The microtubule motor protein kinesin provides the anterograde movement while the retrograde movement is carried out by the dynein motor proteins (Pazour and Rosenbaum, 2002; Pedersen and Rosenbaum, 2008). IFT can be separated into six distinct phases. First, the IFT machinery and its cargo are assembled at the transition fiber, which links the basal body and the membrane around the neck of the cilium, to form the IFT particles (Deane et al., 2001). Second, the IFT-B sub-complex mediates anterograde movements towards the ciliary tip and alterations in kinesin or IFT-B subunits have been shown to block cilia formation (Rosenbaum and Witman, 2002). The third and fourth steps involve a complex series of poorly understood events including the unloading of anterograde cargos, switching of the anterograde for retrograde transport machinery and loading of the retrograde cargos to the IFT-A sub complex. Fifth, IFT-A is thought to act in retrograde movement towards the base of the cilium and perturbations of retrograde trafficking typically result in short, bulged cilia (Pedersen and Rosenbaum, 2008).

Finally, step six is the disassembly of the IFT machinery. The IFT machinery is important for transporting not only the ciliary components needed for axonemal assembly, but also for components of the Hh signaling pathway and possibly the Wnt signaling pathway (Corbit et al., 2008; Pedersen and Rosenbaum, 2008).

Ciliary vesicle trafficking

The delivery of ciliary proteins to the cilia necessitates their sorting and packing into carrier vesicles, the docking and fusion of vesicles with the base of the cilium and transport from the ciliary base to the tip (Rosenbaum, 2002). The specificity of membrane targeting and fusion is critical for proper flow of cargos within the cell. The Rab family of small GTPases mediate the tethering of vesicle cargos to their targeted membrane (Zerial and McBride, 2001). Rab8, which has been detected in the ciliary membrane, functions in trafficking of vesicles from the trans-Golgi network (TGN) to the base of the cilium (Moritz et al., 2001; Yoshimura et al., 2007). Rab8 is activated by the guanine nucleotide exchange factor Rabin8, which is activated by another member of the Rab family, Rab11. The activated form of Rab11 stimulates the GEF activity of Rabin8 towards Rab8 (Knödler et al., 2010; Wang et al., 2012; Westlake et al., 2011).

The BBSome is an octamer complex of ciliary proteins consisted of seven highly conserved Bardet-Biedl syndrome (BBS) proteins BBS1, BBS2, BBS4, BBS5, BBS7, BBS8, BBS9 and BBSome interacting protein of 10 kDa (BBIP10) (Loktev et al., 2008; Nachury et al., 2007). The BBSome recruited by the Arf-like GTPase Arl6-GTP to form a BBSome coat complex that can sort the ciliary receptor somatostatin receptor 3 (Sstr3) to the cilia by using Sstr3's own ciliary targeting sequence (Jin et al., 2010). Mice

lacking either BBS2 or BBS4 protein possess seemingly normal primary cilia but the Sstr3 and melanin-concentrating hormone receptor 1 (Mchr1) fail to localize to cilia (Berbari et al., 2008a). BBS4 is thought to act as a bridging factor between PCM-1 and the microtubule motor protein, dynein, to bring proteins to the base of cilia (Nachury et al., 2007; Kim et al., 2004). BBIP10 has been shown to be required for ciliogenesis and is thought to stabilize cytoplasmic microtubule polymerization surrounding the basal body through acetylation (Loktev et al., 2008). Taken together, not only does the BBSome serves as delivery vehicle of ciliary proteins to the base of the cilia but also anchors and organizes these BBSome-coated vesicles for transport into the ciliary axoneme.

Although there is no strong consensus for ciliary targeting sequences found in all ciliary proteins, some share a ciliary localization sequence. Rhodopsin, polycystin-1 and polycystin-2 share a “VxPx” motif which when mutated, disrupts their localization to the basal body (Mazelova et al., 2009). G-protein coupled receptors (GPCRs) that localize to the ciliary membrane including Sstr3, serotonin receptor 6 (Htr6), and Mchr1 share a consensus sequence “Ax[S/A]xQ” in the third intracellular loop that may comprise a ciliary localization sequence. Mutations to the A and Q residues result in a significant decreases in ciliary localization (Berbari et al., 2008b; a). Furthermore, post-translational modifications have been shown to be necessary for ciliary membrane localization. For instance, palmitoylation of a critical cysteine residue in the cytoplasmic tail of fibrocystin is required for sorting into the ciliary membrane by Rab8a (Follit et al., 2010). In other cases, post-translational modification of ciliary proteins is necessary for

the recruitment of other ciliary proteins such as SUMOylation of the small GTPase Arl13b is required for polycystin-2 entry into the cilium (Li et al., 2012).

The process by which ciliary targeted vesicles fuse with the periciliary membrane remains poorly understood, although it is likely to be similar to the canonical fusion events that occur throughout the cell and across species, and uses a number of highly conserved proteins. These proteins include soluble NSF (N-ethylmaleimide-sensitive factor) attachment protein receptors (SNAREs), the ATP-driven chaperone NSF/Sec18p, its partner proteins αSNAP/Sec17p, and the large family of Rab GTPases and Arl proteins (Chia and Gleeson, 2014). Rab proteins act as a molecular switch through their GTPase activity, to recruit cytosolic effector molecules required for docking on the appropriate target membrane (Zerial and McBride, 2001). After the transport vesicle is tethered to its targeted membrane, the formation of a stable ternary SNARE complex docks the transport vesicle onto the target membrane (Price et al., 2000). The binding of highly specific cognate vesicles and target membrane SNAREs is the central event in docking of membranes before fusion (Hay and Scheller, 1997; Rothman and Warren, 1994). The docked vesicle then fuses with the target membrane to deliver its content. Loss of membrane tethers can result in disrupted membrane transport, and can affect the organization and identity of cellular compartments. Thus the role of membrane tethers and fusion in bridging membranes is important for understanding ciliary vesicular trafficking as well as ciliogenesis.

1.3 Chibby (Cby)

Characterization of Cby as a β-catenin interacting protein

Cby is a highly conserved 15 kDa protein that contains a coiled-coil domain necessary for homodimerization (Mofunanya et al., 2009). Cby was first identified in a Ras-recruitment screen in yeast for proteins that directly binds to the C-terminal activation domain of β-catenin (Takemaru et al., 2003). β-Catenin is a 94 kDa protein, composed of 12 armadillo repeats flanked by unique N- and C-terminal regions, that exhibit transcriptional activating activity. β-Catenin is a crucial component of the Wnt/β-catenin signaling pathway. Its role in the Wnt/β-catenin pathway is to bind to the DNA-bound T-cell factor/lymphoid enhancer factor (TCF/LEF) transcriptional factors and to act as a coactivator to stimulate the downstream expression of Wnt target genes (Behrens et al., 1996; Brunner et al., 1997). Cby inhibits the Wnt/β-catenin-mediated transcriptional activation by competing with LEF-1 for binding to β-catenin.

Cby as a shuttling protein

Cby regulates the Wnt/β-catenin pathway and accomplishes this through two distinct molecular mechanisms: 1) Cby competes with TCF/LEF transcriptional factors for β-catenin binding in the nucleus thus preventing Wnt target gene expression (Takemaru et al., 2009). 2) Cby facilitates the nuclear export of β-catenin by forming a stable tripartite complex with 14-3-3 chaperone proteins, thus decreasing the overall level of nuclear β-catenin proteins (Li et al., 2008). As such, Cby harbors both nuclear localization signal (NLS) and nuclear export signal (NES) motifs, which allow it to constitutively shuttle between the nucleus and cytoplasm (Li et al., 2010). Cby's ability to form a homodimer is required for its efficient nuclear import, but not its ability to bind to β-catenin or its ability to translocate to the cytoplasm (Mofunanya et al., 2009).

Cby in development and disease

Aberrant Wnt signaling has been implicated in several cancer types particularly in colorectal cancer, as mutations in this pathway can be found in nearly all colorectal patients (Sebio et al., 2014; Bienz and Clevers, 2000; Giles et al., 2003). As such, it is of great interest to examine whether Cby functions as a tumor suppressor in colorectal cancer. One study demonstrated that in a series of 36 colorectal tumors, no mutations were detected for the Cby promoter region suggesting that Cby's possible role as a tumor suppressor is weak at best (Gad et al., 2004). Another study showed that while no Cby mutations were found in any of the examined colon carcinoma cell lines, Cby mRNA expression was strongly down-regulated when compared to normal colon epithelial cells (Schuierer et al., 2006). In contrast to the *in vitro* data, quantitative RT-PCR and gene chip analyses of Cby mRNA levels in colorectal carcinoma tumor samples did not show any significant differences from the adjacent non-cancerous tissues (Schuierer et al., 2006). While these studies suggest that Cby may not function as a tumor suppressor in colorectal cancer, it remains possible that Cby may be involved in the pathogenesis of other cancer types. For example, it was observed that colon carcinoma cell lines had reduced expression of Cby, and that ectopically expressed Cby was able to suppress the growth of SW480 colon cancer cells (Schuierer et al., 2006; Fischer et al., 2012).

Wnt/β-catenin signaling has been shown to be important for cardiomyocyte development, as the inhibition of this pathway is necessary for cardiomyocyte differentiation, proliferation and repair (Barandon et al., 2003; Foley and Mercola, 2005). Cby is ubiquitously expressed in early stages of embryonic stem cell differentiation and

is upregulated during cardiomyocyte differentiation (Singh et al., 2007). Overexpression of Cby promotes but its knockdown inhibits cardiac differentiation. Another known effect of the activated Wnt/β-catenin pathway is the inhibition of adipocyte differentiation in 3T3-L1 pre-adipocyte cells as well as mouse embryonic stem cells. When Cby was overexpressed, it stimulated adipogenesis, while depletion of Cby by RNAi inhibited adipocyte differentiation (Li et al., 2007). Taken together, these data suggest that Cby is critical for development through its activity as a Wnt/β-catenin antagonist.

Cby in ciliogenesis

In order to gain further insight into Cby's role in development, Cby-knockout mice were generated (Voronina et al., 2009b). One phenotype that became readily apparent was that Cby knockout mice were prone to develop rhinitis and sinusitis. Further investigation revealed that the underlying cause was their inability to clear mucus from the nasal cavity effectively. Ultrastructural analysis by transmission electron microscope (TEM) indicated a significant decrease in the number of motile cilia in the nasal epithelium, likely resulting from defective basal body docking to the apical cell surface (Love et al., 2010; Voronina et al., 2009a). In addition to its role in motile cilia formation, Cby is also required for primary cilia formation as Cby knockdown resulted in a significant decrease in the number of cilia in mammalian cultured cells (Lee et al., 2014).

Using super-resolution microscopy and immuno-TEM, it was revealed that Cby clusters as a ring at the transition fibers and the proximal region of the transition zone of the mature cilia (Burke et al., 2014). In the absence of Cby, there was a marked

decrease in the number of ciliary vesicles at the distal appendage of mother centrioles. The proposed model by which Cby mediates ciliogenesis is that Cby is first recruited to the distal appendage of the mother centriole by the distal appendage protein Cep164 (Burke et al., 2014). Cby then associates with the membrane trafficking component Rabin8, a guanine nucleotide exchange factor (GEF) for the small GTPase Rab8, to promote the recruitment of Rab8 associated vesicles necessary for ciliary assembly (Burke et al., 2014). How exactly Cby promotes efficient recruitment and subsequent fusion of small vesicles to form the ciliary vesicles remain poorly understood.

Cby has also been shown to interact with the C-terminal region of polycystin-2 (PKD2), a commonly mutated gene product in polycystic kidney disease patients (Hidaka et al., 2004). The study also identified the *cis*-Golgi protein GM130 as another interacting partner for Cby (Hidaka et al., 2004). Thus, Cby was named as “PIGEA-14” (polycystin-2-interating Golgi- and endoplasmic reticulum-associated) protein in this study. Polycystin-2 plays a role in mechanosensation in renal cilia (Nauli and Zhou, 2004; Pazour et al., 2002). Interestingly, co-expression of Cby and polycystin-2 in HeLa cells resulted in a redistribution of Cby and polycystin-2 to the trans-Golgi network, which suggests that Cby plays an important role in regulating the intracellular localization of polycystin-2 and possibly other intracellular proteins.

1.4 BAR-domain proteins

The plastic nature of cellular membranes, such as the ciliary membrane, is essential for cellular function in secretion, cell signaling, and development (Suetsugu, 2010; Frost et al., 2009; Habermann, 2004). It is therefore important to understand the mechanism by which flat membranes are transformed into cylindrical and vesicles

membranes for intracellular cargo trafficking. Membrane curvature is recognized as a highly regulated event and is not a passive property of the membrane. Lipid bilayer curvature is aided by protein structures. A prominent example is clathrin, which is involved in cellular endocytosis and is known to attach to adaptor protein complexes inducing greater membrane curvature (Daumke et al., 2014; Qualmann et al., 2011).

BAR-domain proteins are a group of proteins that can affect membrane curvature (Frost et al., 2009; Mim and Unger, 2012). BAR proteins, so named after its founding protein members, Bin, Amphiphysin, and Rvs, are responsible for both sensing and inducing membrane curvature. Although BAR proteins lack a characteristic sequence motif in their primary structure, members of the BAR domain superfamily have a highly conserved tertiary structure. BAR proteins contain a dimerization motif consisting of three α-helices of 250-280 amino acids, which form a rigid banana-shaped or crescent-shaped structure with positively charged residues are distributed along the membrane-interacting concave face (Habermann, 2004; Peter et al., 2004; Shinozaki-Narikawa et al., 2006). The formation of homodimers, and in some cases heterodimers, is crucial for their function. Genetic mutation to key residues that ablate homodimer formation renders BAR domain non-functional.

Phosphorylation of the BAR domain has been demonstrated to exhibit autoinhibitory effects, preventing binding, bending and impairing oligomerization (Mim and Unger, 2012). The phosphorylation of the F-BAR protein Cdc15 causes it to adopt a “closed” or autoinhibited conformation while dephosphorylation leads to an “open” or elongated conformation (Roberts-Galbraith and Gould, 2010). The association of the rigid banana-shaped structures with the phospholipid bilayer through electrostatic

interactions causes local deformation that will facilitate the binding of additional BAR proteins, thereby generating a positive-feedback loop for curvature propagation (Frost et al., 2009).

Some BAR proteins function directly in vesicle formation and membrane bending, while others act as effectors of small GTPases (Chavrier and Goud, 1999; Habermann, 2004). BAR proteins can be categorized based on their BAR domain structure into N-BAR, F-BAR and the I-BAR domain proteins. N-BAR domain contains an N-terminal amphipathic helix, which is used as a 'wedge' to induce curvature in the membrane that is further stabilized by BAR protein binding to the membranes (Gallop et al., 2006). The N-BAR domain preferentially binds to highly curved membranes and includes proteins such as amphiphysin, arfaptin, and sorting nexins (Gallop et al., 2006). The F-BAR domain, like the N-BAR, also contains the N-terminal amphipathic helix but is thought to function more towards dimer formation than curvature induction (Frost et al., 2008). The F-BAR domain is present in many proteins involved in membrane trafficking and is frequently linked to cytoskeletal dynamics (Roberts-Galbraith and Gould, 2010). I-BAR domains, also known as IRSp53-MIM homology domains, bind phosphoinositide-rich membranes with high affinity to induce a negative membrane curvature and include proteins such as IRSp53, MIM, ABBA, and IRTKS (Suetsugu, 2010; Zhao et al., 2011).

Clathrin-mediated endocytosis (CME) illustrates how BAR proteins acting in conjunction are necessary for a vital cellular process. Endocytosis is the cellular process by which cells internalize portions of the plasma membrane along with extracellular materials. This process is known to require specific spatial and temporal recruitment of BAR proteins. CME is nucleated by the assembly of the F-BAR protein

FCHO, AP-2 and clathrin at $PI(4,5)P_2$ enriched plasma membranes which are generated by phosphatidylinositol 4-phosphate 5-kinase type I (PIPKI) (Di Paolo and De Camilli, 2006). Conversion of $PI(4,5)P_2$ to $PI(3,4)P_2$ by C2α (PI3KC2α) is required to recruit the PX-domain containing BAR proteins SNX9/18, which further induce curvature to form a mature clathrin coated pit (CCP). This facilitates constriction of the pit to form a droplet shape. $PI(3,4)P_2$ is then converted to PI(3)P by PI4-phosphate which recruits the highly curved BAR domain proteins endophilin and amphiphysin to assemble around the constricted vesicle neck for further constriction and recruitment of the GTPase dynamin (Gallop et al., 2006; Peter et al., 2004). The final membrane fission is accomplished by dynamin GTP hydrolysis located at the neck of the pit (Chi et al., 2014; Daumke et al., 2014). BAR proteins are recruited to the CME sequentially and is in part regulated by the membrane composition. An important feature of this pathway is the ordered recruitment of increasing curved BAR protein to reach the final dynamin-mediated fission (Mim and Unger, 2012; Qualmann et al., 2011).

Here, I have characterized the BAR-domain containing proteins, FAM92A and FAM92B, as basal body proteins that interact with Cby. My work demonstrated a role for FAM92A in cilia formation, as well as Cby's importance in facilitating the FAM92 proteins function. This interaction could provide vital clues as to how Cby is able to facilitate the membrane vesicle docking and fusion event that is critical for proper cilia formation.

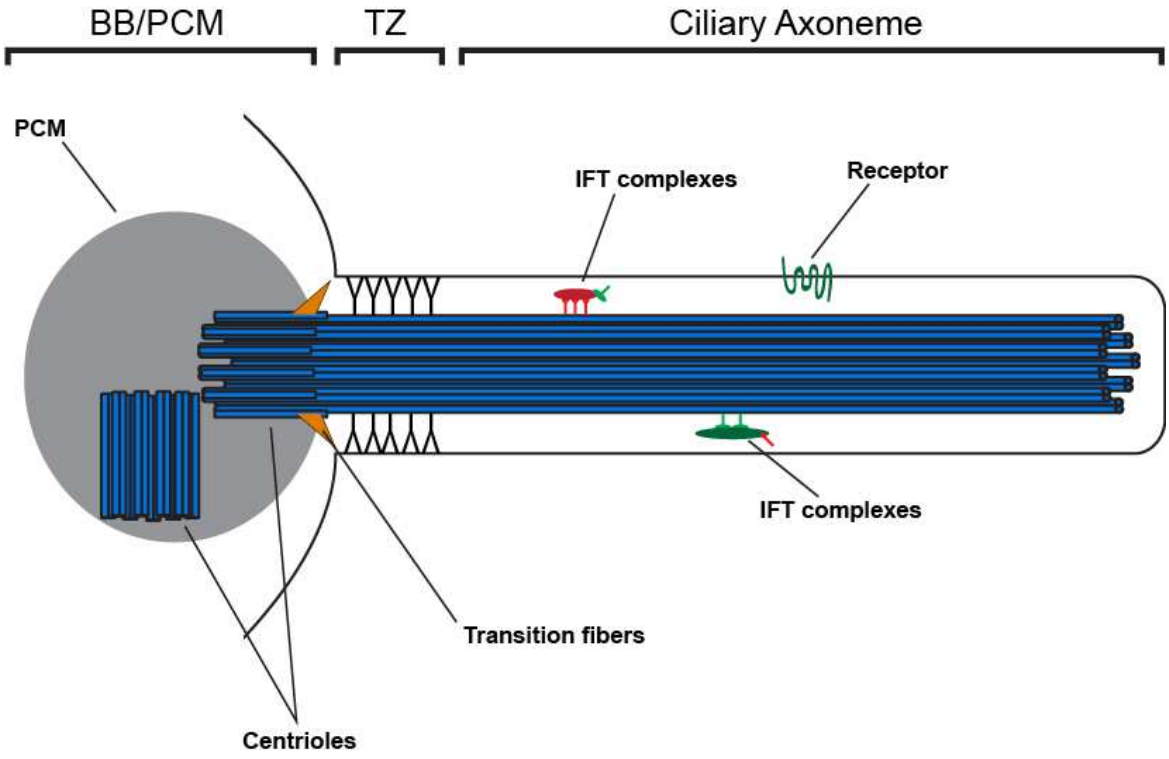

Figure 1: The ciliary structure.

The IFT particles carrying ciliary components and signal transduction travel along the ciliary axoneme. The receptors for the various signaling pathways localized to the ciliary membrane. The Y-link and the presence of ciliary gate proteins denote the transition zone. The mother and daughter centrioles are surrounded by the PCM, which is responsible for microtubule nucleation and anchoring.

Chapter 2: Cby Dynamics at the Base of the Cilia

2.1 Introduction

The initial steps of primary cilia assembly have been compiled using detailed TEM analyses of epithelial cells, fibroblasts and other cell types that possess primary cilia (Dawe et al., 2007; Sorokin, 1968). These steps include the docking of a Golgi-derived ciliary vesicle (CV) to the distal appendage of the mother centriole, the fusion of secondary vesicles to form the sheath surrounding the elongating axoneme and finally the fusion of the axoneme-bound membrane with the plasma membrane (Pedersen et al., 2008; Seeley and Nachury, 2010; Kim and Dynlacht, 2013b). The importance of distal appendage proteins (DAPs) such as cenexin/ODF2, Cep164, Cep83, SCLT1, FBF1, and Cep89 in vesicle docking and fusion events have been highlighted in numerous studies (Tanos et al., 2013; Graser et al., 2007; Ishikawa et al., 2005). Loss of these DAPs has been shown to block ciliogenesis at the centriole-to-membrane docking stage.

In characterizing Cby as a ciliary component, it was determined that Cby is a DAP that facilitates the efficient docking of Rab8 positive vesicles and is necessary for the CV formation at the distal appendage of basal bodies (Steere et al., 2012; Voronina et al., 2009b). Additionally, the continued Cby localization at the base of mature cilia suggests that Cby is also involved in ciliary maintenance and function. To elucidate Cby's role, I examine Cby dynamics at the basal body and whether this dynamics is responsible for the re-establishment of the basal body after microtubule depolymerization. Some basal body components such Spag6 exhibited a dynamic exchange regardless of the basal body assembly status, while others such as Sas6a

exhibited stable and dynamic exchange during basal body assembly (Pearson et al., 2009b). It was further suggested that protein localization at distinct basal body structural domains correlated with specific dynamic properties (Pearson et al., 2009a). Here I intended to show Cby dynamics at the base of cilia in mature RPE1 cells, and the existence of a pericentriolar pool of Cby that is likely responsible for the dynamism in a microtubule-dependent manner.

2.2 Materials and methods

Cell line and culture

hTERT-RPE1 cells (ATCC) and HEK293T cells (ATCC) were used. All cells were maintained at 37°C in 5% CO_2. All cells were cultured in complete media, comprising DMEM (Gibco) supplemented with 10% (v/v) fetal bovine serum (FBS) (Gibco) and 1% (v/v) penicillin-streptomycin (Gibco). To induce ciliation, confluent cells were placed in serum-starvation media, comprising DMEM supplemented with 1% (v/v) penicillin-streptomycin for 18-48 hr.

Plasmids

pEF1α-IRES-EGFP-FLAG-hCby (IRES-EGFP-Flag-hCby) has been previously described (Burke et al., 2014). The 2nd generation lentiviral vector backbone pEF1α-IRES-EGFP was a gift of Nurit Ballas (Stony Brook University, Stony Brook, NY), and was originally generated by Ihor Lemischka (Mount Sinai Medical Center, New York, NY).

pLenti-EGFP-hCby was generated by sub-cloning EGFP-hCby into pEF1α-IRES-EGFP with the original IRES-EGFP cassette removed. hCby was amplified using

Expand High Fidelity PCR System (Roche) with the following primers:

hCby-Eco-Sfi-5'

5'-TCAGGAATTCGGCCATTACGGCCATGCCTTTCTTTGGGAATAC-3'

hCby-Xba-Not-Sfi-3'

5'-TCAGTCTAGAGCGGCCGCGGCCGAGGCGGCCTCATTTTCTCTTCCGGCTGA-3'

Following amplification, PCR products were purified using Cycle-Pure Kit (Omega-Bio-Tek). Purified fragments and vectors were digested for 1 hr at 50°C by SfiI endonuclease (NEB) in NEBuffer 4. Digested fragments and vectors were resolved on a 1% agarose gel and appropriate bands excised, followed by purification using QIAEX II Gel Extraction Kit (Qiagen). Ligation reactions were performed with a 3:1 ratio of insert to vector using T4 ligase (NEB) for 1 hr at 25°C. Ligation products were transformed into DH5α *E. coli* competent cells (NEB), plated on LB agar plates containing 150 µg/mL ampicillin (Sigma) and grown overnight at 37°C. Colonies were grown in liquid culture for minipreps and sent for sequencing with the following primer that anneals upstream of the cloning site:

IRES-EGFP-F: 5'-TTCTCAAGCCTCAGACAGTG-3'

Lentiviral production and infection

Viral particles were generated by co-transfecting a pEF1α-IRES-EGFP-backbone transfer vector with ENV, a 2nd generation lentiviral envelope plasmid, and PAX, a 2nd generation lentiviral packaging plasmid (gifts from Orlando Scharer, Stony Brook University, Stony Brook, NY) (1:1:1) into ~70% confluent HEK293T cells and the virus

containing media were collected at 48 hr, 72 hr, and 96 hr post-transfection. Infections of ~70% confluent RPE1 cells were performed using a 1:1 mixture of viral media and complete media overnight. Infection was repeated as needed and immunofluorescence microscopy was used to visually confirm positive infection based on GFP expression.

Fluorescence recovery after photobleaching (FRAP)

FRAP imaging was performed using Zeiss LSM 510 META NLO Two-Photon Laser Scanning Confocal Microscope System equipped with a cell chamber system with temperature and carbon dioxide control (Zeiss). The microscope was fitted with a 100x [1.4 numerical aperture (NA), oil] objective. RPE1 cells were infected with pLenti-EGFP-hCby and checked for GFP expression. Infected RPE1 cells were seeded on a 3.5 mm glass bottom plate (MatTek) and serum-starved for 48 hr for proper localization of EGFP-hCby proteins. Infected cells were imaged before bleaching (pre-bleach), then bleached within a region of interest (ROI) at the basal body using a single pulse of the 488 nm laser at 100% for 1 sec. Time-lapse images were recorded immediately post-bleach at 0 min, 1 min, 5 min, 10 min, 15 min, 20 min, 25 min, and 30 min. Basal body fluorescence intensities were measured using ImageJ (NIH) and the background fluorescence as defined by a ROI at time 0 was subtracted. All fluorescence intensities were normalized to the pre-bleached level as 100%. Images were captured using the Zeiss LSM 510 META imaging software and cropped using Adobe Photoshop software. Microsoft Excel was used for curve fitting analyses.

Cold exposure assays for microtubule depolymerization and repolymerization

All cells were fixed using 1:1 methanol/acetone mixture for 10 min on ice. RPE1 cells were infected with pEF1α-IRES-EGFP-Flag-hCby lentiviruses, seeded on coverslips, and incubated for 72 hr for optimal protein expression. Ciliation was induced for 18 hr. For control, cells were fixed immediately after ciliation. For microtubule recovery assays, cells were placed on ice for 30 min to depolymerize the microtubule network (Dafinger et al., 2011). Repolymerization of the microtubules was initiated by incubating cells in 37°C media and stopped by fixation at the indicated time points.

Antibodies

All antibodies were diluted in antibody diluent (5% BSA and 0.1% Triton X-100 in PBS). Primary antibodies used were mouse anti-Cby 27-11 (1:100) previously described (Cyge et al., 2011), rabbit anti-CCDC186 (1:300, Sigma), and mouse anti-acetylated α-tubulin (1:10,000, Sigma). Secondary antibodies used were DyLight 488 or 549-conjugated goat anti-mouse and anti-rabbit (1:300, Jackson ImmunoResearch).

Immunofluorescence imaging

Fixed samples were washed with PBS prior to blocking in 4% (v/v) goat serum (Gibco) in antibody diluent for 1 hr at room temperature. The samples were then incubated with primary antibody overnight at 4°C, and washed with PBS before a second blocking step with goat serum in diluent for 1 hr at room temperature. The samples were incubated with fluorescent secondary antibody for 1 hr at room temperature, washed with PBS and incubated in DAPI (nuclear stain) for 1 min. They were further washed with PBS before finally mounted on a cover glass with Fluoromount G (Southern Biotech), an anti-fade medium. Immunofluorescence imaging

was performed on a Leica DMI6000B microscope equipped with Leica DFC300 FX camera and LAS AF Version 2.6 software.

2.3 Results

The dynamics of Cby protein were monitored using fluorescence recovery after photobleaching (FRAP), which has been successfully used to examine both the dynamics and stable incorporation of centrosomal proteins (Pearson et al., 2009a; Moss et al., 2007; Varmark et al., 2007; Hirayama et al., 2008). To this end, I generated lentiviruses expressing EGFP-Cby fusion protein which were used to infect RPE1 cells. RPE1 cells are commonly used in the study of primary cilia, as they ciliate readily upon serum-starvation. The benefit of this system was the ability to visually confirm Cby production based on EGFP expression. The infected cells were then seeded on a glass bottom plate, grown to confluence and serum-starved to induce ciliation. Live-cell fluorescence microscopy revealed a single strong punctate signal of EGFP-Cby, presumably at the basal body (Figure 2A). As FRAP was initiated, I observed a slow recovery of EGFP-Cby signal intensities, with a maximum recovery intensity of ~60% of the pre-bleached fluorescence intensity at the 30 min mark with a half-life of ~4.26 min (Figure 2B). The slow recovery can be explained by Cby localization to the ciliary transition zone, which is thought to limit the free diffusion of non-ciliary proteins into the cilium (Chih et al., 2012; Klinger et al., 2014).

IFT20 is a Golgi-associated protein required for ciliary assembly. Strong reduction of IFT20 levels has been shown to prevent ciliary assembly, whereas moderate reduction did not block ciliary assembly but did reduce the amount of polycystin-2 localization to the ciliary membrane (Follit et al., 2006). It has been

proposed that IFT20 functions in the trafficking of ciliary membrane proteins from the Golgi apparatus to the cilium (Follit et al., 2006). Interestingly, Cby has been shown to co-localize extensively with IFT20 in early differentiation stages of tracheal ciliated cells and these subcellular compartments may represent pools of post-Golgi vesicles potentially involved in the assembly of centrioles (Burke et al., 2014). To examine whether the recovery of Cby is derived from the pool of post-Golgi vesicles, I performed cold exposure assays. The ice-cold condition induces depolymerization of the microtubule network, an effect that can be readily reversed by placing the cells back in normal culture media (Cassimeris et al., 1986). By repolymerizing the microtubule network, we can establish a starting time point and observe the migratory pattern of ciliary proteins to the basal body along the newly polymerized microtubule tracks (Dafinger et al., 2011; Lopes et al., 2011). The reassembly of the microtubule network to pre-treatment level occurred within 20 min post-cold exposure (Cassimeris et al., 1986).

To track the movement of Cby, I generated lentiviruses expressing Flag-tagged-Cby to infect RPE1 cells. Positive infection was visually confirmed using immunofluorescence microscopy. Infected cells were grown to confluence, and then serum-starved to induce ciliation. These cells were then placed on ice to induce microtubule depolymerization. As the cells recovered post-cold exposure, I observed an interesting pericentriolar localization pattern for Cby (Figure 3). This pattern is similar to the localization patterns found for centriolar satellite proteins, which include non-membranous 70-100 nm granules scattered around the basal body (Kubo et al., 1999; Barenz et al., 2011). Cep290, a known component of both the centriolar satellite and basal body, exhibits numerous puncta around the basal body in response to microtubule

repolymerization after nocodazole treatment (Kim et al., 2008). Taken together, this raises the possibility that Cby may also be trafficked to the basal body in a microtubule-dependent manner.

The Golgi apparatus (GA) is important for primary cilia formation, as it is believed to provide the ciliary components necessary for the maturation of the distal appendage into a ciliary vesicle. Alterations in the integrity and position of the Golgi apparatus have been shown to result in ciliary defects (Asante et al., 2013; Hurtado et al., 2011). Just as important are the microtubule networks, which provide the mechanism for proteins to be trafficked from the GA to the primary cilium through polarized vesicle trafficking (Hsiao et al., 2012). To examine whether Cby localization to the basal body is microtubule-dependent, I performed an immunofluorescence co-staining for Cby and CCDC186, a Golgi protein marker. At 3 min post-cold exposure, I observed a Cby localization pattern peripheral to GA, in some instances forming a pattern surrounding the Golgi apparatus (Figure 3, right panels). Taken together, these results imply Cby is trafficked to the basal body in a microtubule-dependent manner. Additionally, the disruption of the microtubule network did not completely ablate the localization of Cby at the base of the cilium, further suggesting that at least a fraction of Cby localized to a region of the cilium that is not affected by microtubule depolymerization.

2.4 Discussion

Characterizing Cby dynamics is critical for understanding its role Cby in various aspects of cilia formation and function. Cby acts in the formation of cilia through its interactions with Cep164 and Rab8-associated vesicles to form the ciliary vesicles (Burke et al., 2014). However Cby's role in mature ciliary function is less clear. By using

super-resolution microscopy, it was determined that Cby localized to the distal appendage/transition fibers in mature cilia (Burke et al., 2014). This region is referred to as the ciliary gate as it regulates the flow of proteins into and out of the ciliary axoneme (Benzing and Schermer, 2011; Craige et al., 2010; Szymanska and Johnson, 2012). What role Cby plays in the sorting and regulation of membrane vesicles into the ciliary axoneme remains unclear.

Cby function in ciliary maintenance might be an extension of its ability to facilitate the recruitment of Rab8 associated vesicles, specifically its ability to shuttle the necessary ciliary components to the distal appendage or ciliary gate. Here we have shown a population Cby remains dynamic in ciliated cells, and the likely source of this active exchange is a pool of Cby localized peripherally to the GA. The peripheral-GA Cby localization pattern is similar to the localization pattern observed for centriolar satellite (XPCM-1 positive dots) after nocodazole treatment (Kubo et al., 1999). As the microtubule repolymerization progresses, there was a concentrating effect of the centriolar satellite around the centrosome, again similar to what was observed for Cby cold exposure assays. Centriolar satellite-associated proteins are an excellent candidate to mediate the dynamic function of basal bodies, a key function of which is targeting centriolar and pericentriolar materials from the cytoplasm to the basal body along microtubule tracts (Barenz et al., 2011; Kubo et al., 1999). Investigating the connection between Cby and the pericentriolar materials may give us a clue as to how Cby dynamics are important for ciliary maintenance.

In many respects, Cby functions in a pathway similar to the coiled-coil domain containing 41 (CCDC41) protein. CCDC41 is stably incorporated into the distal end of

the mother centriole where it co-localizes with Cep164 and reportedly the depletion of CCDC41 inhibited ciliogenesis at the ciliary vesicle docking step (Joo et al., 2013). In addition, a pool of CCDC41 localizes to the GA and physically interacts with IFT20 (Joo et al., 2013). CKδ is another protein that localizes to the centrosome, *trans*-Golgi network (TGN), and cytoplasmic vesicles (Behrend et al., 2000; Greer and Rubin, 2011). CK1δ functions to coordinate the positioning and activity of multiple ciliary effectors, such as Rab11a, Rab8a, Cep290, PCM1, and IFT20 to mediate the transport of polycystin-2 and other membrane cargo from the Golgi to the basal body and the nascent cilium (Greer et al., 2014). I examined the possibility of Cby localizing to the GA, by performing immunofluorescence co-staining of Cby with a number of *cis, medial, trans* GA protein marker (data not shown). Cby was only localized peripherally to the GA. This raises the possibility that Cby exists in a region post-GA and serves to sort and shuttle vesicles containing ciliary components to the ciliary gate, where it delivers its cargo by fusing with the ciliary membrane. The transient nature of protein trafficking, as well as the harsh nature of fixative used could explain why we were unable to observe any pericentriolar Cby localization previously. The microtubule repolymerization assay might be further explored to optimize the conditions in which endogenous Cby proteins enrich in sufficient quantity to be detectable by antibodies.

The data above suggest that Cby might be required for the efficient trafficking of vesicles between the GA and the centrosomal compartments in primary ciliated cells, which is necessary for ciliary maintenance. While Cby does not have an established centrosomal targeting sequence like those found in ODF2/cenexin (Huber et al., 2008), Cby does have a well-characterized function in protein shuttling. The process involves

Cby physically interacting with 14-3-3 protein forming a stable tripartite complex to facilitate β-catenin nuclear export, thereby suppressing β-catenin-mediated transcriptional activation (Li et al., 2008). Subsequently it was found that Cby contains both a nuclear localization signal (NLS) and nuclear export signal (NES) motif and constitutively shuttles between the nucleus and cytoplasm (Li et al., 2010). A clue might lie in an observation from *Cby-/-* MTECs, where the initial vesicles are found localized to the distal appendage but at a much reduced level compared to *Cby+/+* MTECs (Burke et al., 2014). This suggests that while vesicles may be able to localize to the distal appendage, Cby is required for the subsequent vesicle fusion or stabilization to form the ciliary vesicle. Additionally, SCLT1 a component of DAP has been shown to interact with the membrane coat protein clathrin, which raises the possibility that centrioles might directly associate with clathrin-coated vesicles (Tanos et al., 2013; Liu et al., 2005)

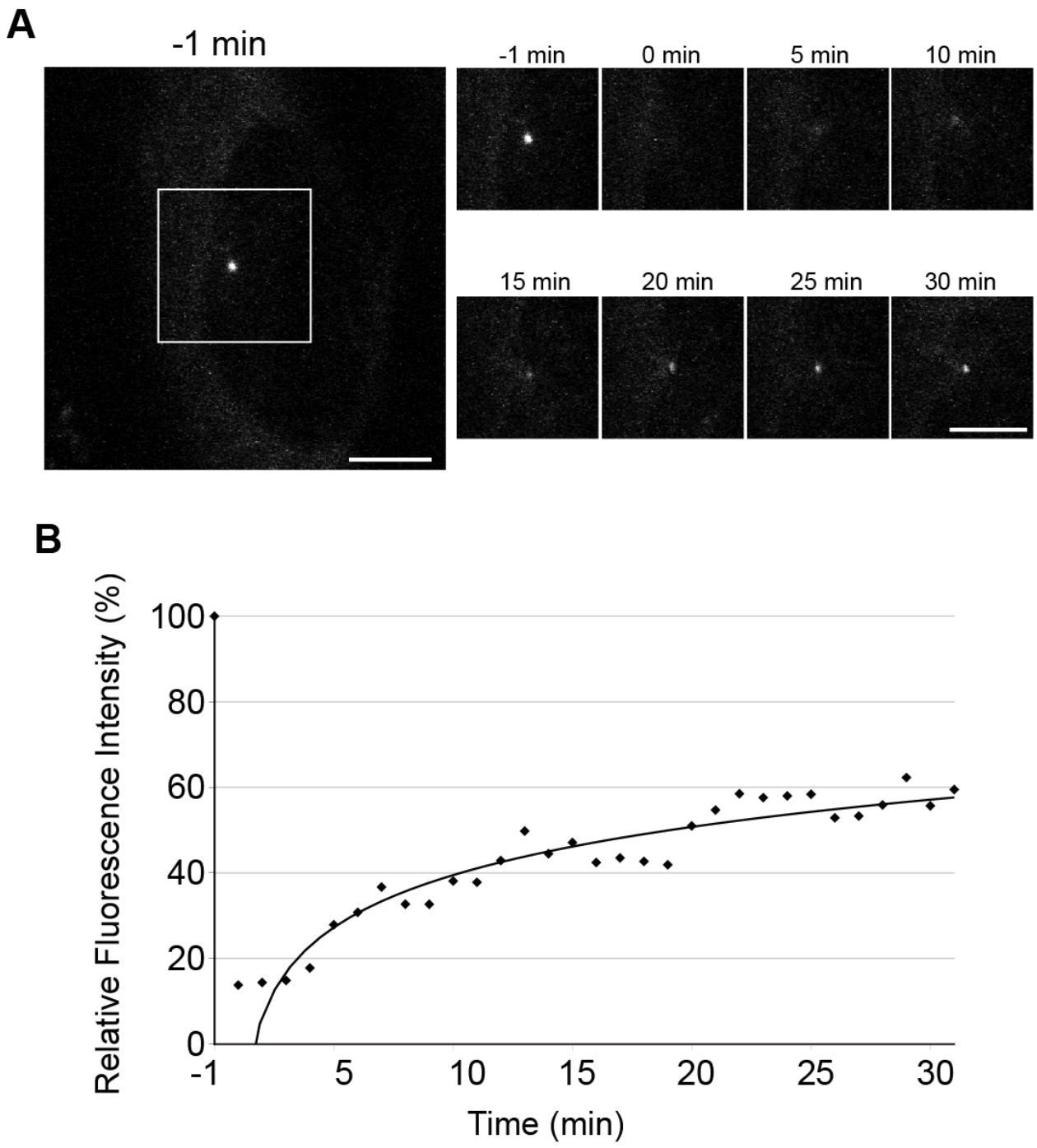
A
-1 min
-1 min
0 min
5 min
10 min
15 min
20 min
25 min
30 min
B
Relative Fluorescence Intensity (%)
100
80
60
40
20
0
-1
5
10
15
20
25
30
Time (min)

Figure 2. Cby dynamics at the base of cilia.

(A) Fluorescence recovery after photobleaching (FRAP) assays were performed for EGFP-Cby in RPE1 cells. RPE1 cells were infected with lentiviruses expressing EGFP-Cby, grown to confluence and serum starved to induce ciliation for 18 hr prior to photobleaching. The left image shows the localization of EGFP-Cby at the basal body. Images of the boxed area were taken before and after photobleaching at the indicated time-points. Scale bars, 5 μm.

(B) Kinetic profile of EGFP-Cby fluorescence recovery at the basal body. The fluorescence recovery intensity at the basal body was measured at the indicated time-points and normalized to the pre-bleach fluorescence at time -1 min (100%) with background subtracted.

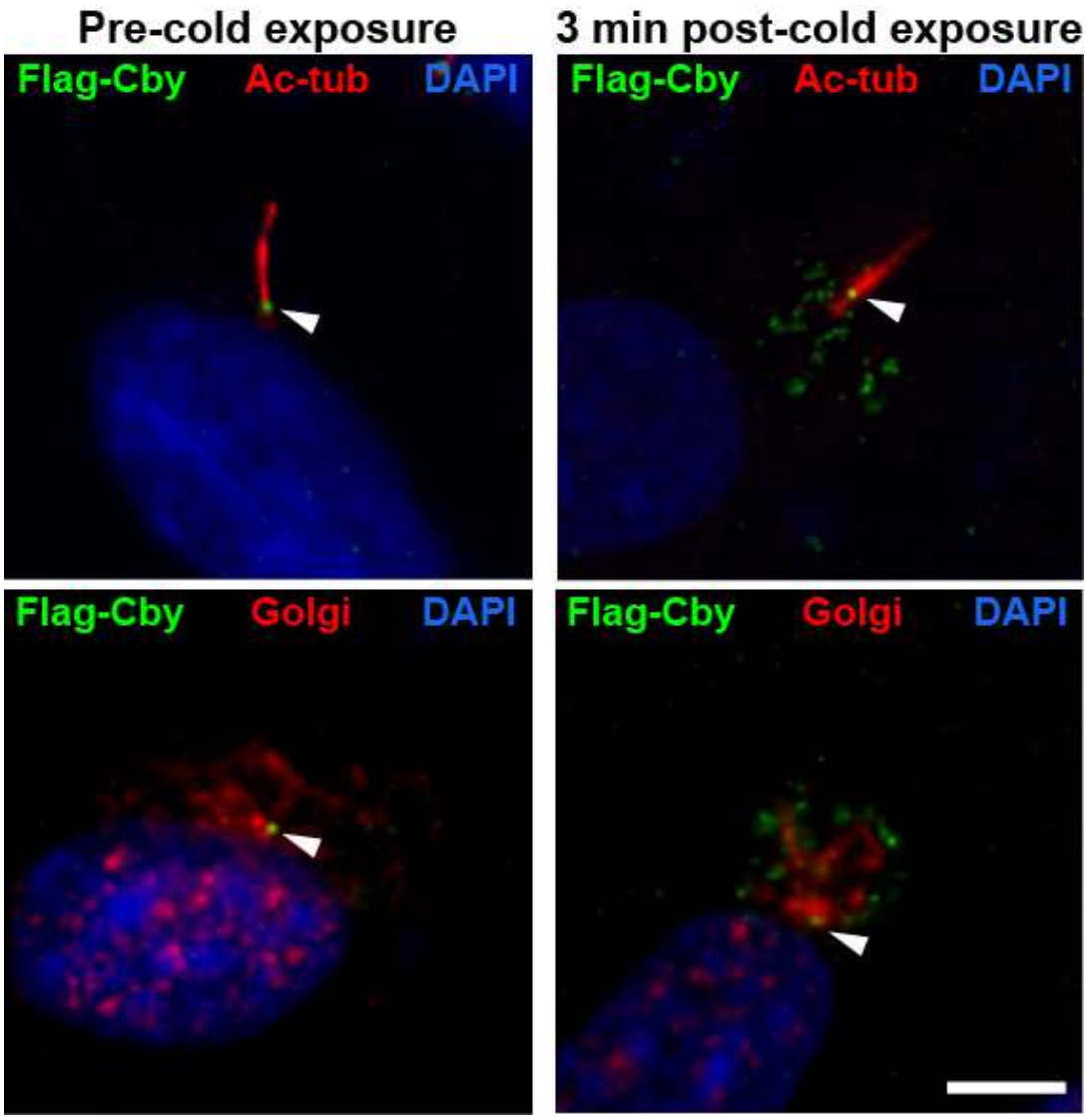

Figure 3. Cby clusters near the Golgi apparatus after cold exposure.

RPE1 cells were infected with lentiviruses expressing Flag-Cby and serum starved for 18 hr to induce ciliation. Cells were then either fixed (pre-cold exposure) or placed on ice for 30 min to depolymerize the microtubule network and then allowed to recover for 3 min (3 min post-cold exposure) before fixation. Immunofluorescence staining was performed using 27-11 Cby antibody (green) and acetylated α-tubulin (Ac-tub) antibody for cilia (red) or CCDC186 antibody for *cis*-medial Golgi (red). Nuclei were detected by DAPI (blue). The arrowheads indicate Cby protein at the basal body. Scale bar, 5 μm.

Chapter 3: Identification and Characterization of BAR-Domain Containing Proteins, FAM92A and FAM92B, as Novel Interacting Partners of Cby

3.1 Introduction

Tandem Affinity Purification (TAP)

Using super-resolution microscopy, it was demonstrated that Cby protein localizes as a ring-like cluster at the proximal region of the transition zone of mature cilia (Burke et al., 2014). It is thought that this population of Cby is crucial for cilia formation. Cby promotes efficient recruitment and fusion of Rab8-positive vesicles to form a ciliary vesicle at the distal end of centrioles, likely by stabilizing the Cep164-Rabin8 complex (Burke et al., 2014). TEM studies of CbyKO ciliated cells revealed that while Cby is not essential for vesicle attachment to the distal appendage, it is necessary for efficient vesicle stabilization and fusion (Burke et al., 2014). However, the precise molecular function of Cby in ciliogenesis is not fully understood.

Affinity purification was successful in identifying 14-3-3ζ and 14-3-3ε as Cby interacting partners (Li et al., 2008). The study used a maltose-binding protein (MBP)-Cby fusion protein in a pull-down assay from HEK293T cell lysates and was critical for revealing a second mechanism by which Cby inhibits β-catenin signaling by physically shuttling β-catenin out of the nucleus and into the cytoplasmic compartment (Takemaru et al., 2009; Li et al., 2008). To gain further insight into the molecular function of Cby in ciliogenesis, I utilized the tandem affinity purification (TAP) technology (Puig et al., 2001). The TAP strategy was pivotal in the identification and characterization of the BBSome complex (Nachury, 2008). The TAP technology allows for a rapid purification of protein complexes from relatively small number of cells, and is often combined with

mass spectrometry for a comprehensive profile of potential interacting partners. TAP was first used in yeast in 1997 by Bertrand Seraphin and colleagues and was later adapted for mammalian cells (Rigaut et al., 1999; Cheeseman and Desai, 2005). The TAP tag used in my experiment consists of a protein A moiety followed by a TEV protease cleavage site and a calmodulin-binding peptide (CBP) fused to the N-terminus of Cby, or to EGFP as negative control (Figure 3A). The TAP tag used in the identification of the BBSome consisted of GFP followed by a TEV cleavage site and an S-tag (Cheeseman and Desai, 2005). This highlights the versatility of the technology, as different tags can be experimented with for the optimal result. The goal of my project in this chapter is to identify novel Cby interacting partners with a focus on possible basal body proteins, and explore their function in the formation and maintenance of cilia.

3.2 Materials and methods

Cell line and culture

hTERT-RPE1 (RPE1) cells (ATCC), HEK293T cells (ATCC), COS7 (ATCC), and Flp-In T-Rex HEK293 cells (Invitrogen) were used. Preparation of mouse tracheal epithelial cells (MTECs) and mouse embryonic fibroblasts (MEFs) has been previous described (Burke et al., 2014; Li et al., 2007).

All cells were maintained at 37°C in 5% CO_2. All cells were cultured in complete media, comprising DMEM (Gibco) supplemented with 10% FBS (Gibco) and 1% penicillin-streptomycin (Gibco). To induce ciliation, ~80% confluent cells were placed in DMEM and 1% penicillin-streptomycin for 18-48 hr.

Plasmids

pcDNA3-ProtA-TEV-CBP (pcDNA-TAP) is an N-terminally tagged TAP fusion protein vector and was used to transfect HEK Flp-In T-Rex HEK293 cells together with the Flp-recombinase expression vector pOG44 (Invitrogen) to establish stable cells expressing TAP-Cby according to the manufacturer's instructions. pCS2+Flag-Cby, pCS2+Flag-CbyC, pCS2+Flag-Cby4A, and pMAL-c2E-MBP-Cby vectors have been previously described (Burke et al., 2014; Mofunanya et al., 2009; Takemaru et al., 2003).

All the FAM92 expression constructs below were constructed by PCR-based cloning using human FAM92A and FAM92B cDNA purchased from Dana Farber/Harvard Cancer Center (Harvard University, Boston, MA) as template.

HA-FAM92A plasmid was generated by amplifying a FAM92A cDNA with the following primers and sub-cloning into the BamHI and XhoI restriction sites of pCS2+HA expression vector.

hFAM92A_Bam5': 5'-TCAGGGATCCATGAGGCGCACCCTGGAAAA-3'

hFAM92A_Xho3': 5'-TCAGTCTAGATTACTTAAGAAAATTTTCTTCTTC-3'

HA-FAM92B plasmid was generated by amplifying a FAM92B cDNA with the following primers and subcloned into the BamHI and XhoI restriction sites of pCS2+ expression vector.

hFAM92B_Bam5': 5'-TCAGGGATCCATGAACATCGTCTTCTCCAG-3'

hFAM92B_Xho3': 5'-TCAGCTCGAGTTAGAGAGAATGTCCTGGAA-3'

HA-FAM92A-BAR plasmid was generated by amplifying a FAM92A-BAR cDNA corresponding to the amino acid positions 1-220 with the following primers and subcloned into the BamHI and XhoI restriction sites of pCS2+HA expression vector.

hFAM92A1-Bam-5': 5'-TCAGGGATCCATGAGGCGCACCCTGGAAAA-3'

92A-220-Xho3': 5'-TCAGCTCGAGTTAAACCTCTAAATCTTCATCTT-3'

HA-FAM92B-BAR plasmid was generated by amplifying a FAM92B-BAR cDNA corresponding to the amino acid positions 1-217 with the following primers and subcloned into the BamHI and XhoI restriction sites of pCS2+HA expression vector.

hFAM92B_Bam5': 5'-TCAGGGATCCATGAACATCGTCTTCTCCAG-3'

92B-217-Xho3': 5'-TCAGCTCGAGTTACAGTAGATCCCTCTCCAGGT-3'

Flag-FAM92A plasmid was generated by amplifying a FAM92A cDNA with the following primers and subcloned into the EcoRI and XhoI restriction sites of pCD-βG-Flag expression vector.

hFAM92A_Eco5': 5'-TCAGGAATTCAATGAGGCGCACCCTGGAAAA-3'

hFAM92A_Xho3': 5'-TCAGTCTAGATTACTTAAGAAAATTTTCTTCTTC-3'

Flag-FAM92B plasmid was generated by amplifying a FAM92B cDNA with the following primers and subcloned into the EcoRI and XhoI restriction sites of pCD-βG-Flag expression vector.

hFAM92B_Eco5': 5'-TCAGGAATTCAATGAACATCGTCTTCTCCAG-3'

hFAM92B_Xho3': 5'-TCAGCTCGAGTTAGAGAGAATGTCCTGGAA-3'

His-FAM92A plasmid was generated by amplifying a FAM92A cDNA with the following primers and subcloned into the BamHI and NotI restriction sites of pET28a expression vector (Novagen).

hFAM92A1-Bam-5': 5'-TCAGGGATCCATGAGGCGCACCCTGGAAAA-3'

hFAM92A1-Not-3': 5'-TCAGGCGGCCGCTTAGAGAGAATGTCCTGGAA-3'

pEF1α-IRES-EGFP-Flag-FAM92A plasmid was generated by amplifying a Flag-FAM92A cDNA with the following primers and subcloned into the SfiI restriction sites of pEF1α-IRES-EGFP lentiviral vector:

Sfi1-Flag 5': 5'-GAATTCGGCCATTACGGCCACCATGGATTACAAGGATGA-3'

hFAM92A-Sfi3': 5'-
GAATTCGGCCGAGGCGGCCTTACTTAAGAAAATTTTCTTCTTC-3'

pEF1α-IRES-EGFP-Flag-FAM92A-BAR plasmid was generated by amplifying a Flag-FAM92A-BAR cDNA with the following primers and subcloned into the SfiI restriction sites of pEF1α-IRES-EGFP lentiviral vector:

Sfi1-Flag 5': 5'-GAATTCGGCCATTACGGCCACCATGGATTACAAGGATGA-3'

hFAM92A-BAR-Sfi3': 5'-
GAATTCGGCCGAGGCGGCCTTAAACCTCTAAATCTTCATCTT-3'

pEF1α-IRES-EGFP-Flag-FAM92B plasmid was generated by amplifying a Flag-FAM92B cDNA with the following primers and subcloned into the SfiI restriction sites of pEF1α-IRES-EGFP lentiviral vector:

Sfi1-Flag 5': 5'-GAATTCGGCCATTACGGCCACCATGGATTACAAGGATGA-3'

hFAM92A-Sfi3': 5'-
GAATTCGGCCGAGGCGGCCTTACTTAAGAAAATTTTCTTCTTC-3'

GFP-FAM92A plasmid was generated by amplifying a FAM92A cDNA with the following primers and subcloned into the BamHI and XhoI restriction sites of pCS2+GFP-BB expression vector:

hFAM92A1-Bam-5': 5'-TCAGGGATCCATGAGGCGCACCCTGGAAAA-3'

hFAM92A1-Xho-3-2': 5'-TCAGCTCGAGTTACTTAAGAAAATTTTCTTCTTC-3'

GFP-FAM92B plasmid was generated by amplifying a FAM92B cDNA with the following primers and subcloned into the BamHI and XhoI restriction sites of pCS2+GFP-BB expression vector:

hFAM92B_Bam5': 5'-TCAGGGATCCATGAACATCGTCTTCTCCAG-3'

hFAM92B_Xho3': 5'-TCAGCTCGAGTTAGAGAGAATGTCCTGGAA-3'

FAM92A-Flag plasmid was generated by amplifying a FAM92A cDNA with the following primers and subcloned into the BamHI and XhoI restriction sites of pCS2+C-Flag expression vector:

hFAM92A-Bam-ACC-5': 5'-TCAGGGATCCACCATGAGGCGCACCCTGGAAAA-3'

92A1-nonstop-Xho3': 5'-TCAGCTCGAGCTTAAGAAAATTTTCTTCTTCTGT-3'

FAM92B-Flag plasmid was generated by amplifying a FAM92B cDNA with the following primers and subcloned into the BamHI and XhoI restriction sites of pCS2+C-Flag expression vector:

h92B-BamACC5': 5'-TCAGGGATCCACCATGAACATCGTCTTCTCCAG-3'

92B-nonstop-Xho3': 5'-TCAGCTCGAGGAGAGAATGTCCTGGAAGCA-3'

Molecular cloning was performed as described in Chapter 2: Materials and Methods following the restriction digest recommended by the manufacturer's instructions (NEB).

Transfection

Transfection of HEK293T and COS7 cells: HEK293T cells were directly seeded in 6-well plates, while COS7 cells were seeded on coverslips in 6-well plates and transfected at ~70% confluency. Transfection of plasmid DNA was performed using Expressfect (Denville) according to the manufacturer's recommendation. After overnight transfection, the cells were either collected for subsequent experiments or replenished with fresh media and grown for a maximum of 48 hr.

siRNA knockdown of FAM92A: RPE1 cells were maintained in complete media and seeded on coverslips one day before transfection with siRNA using Lipofectamine RNAiMAX (Invitrogen) according to the manufacturer's protocol and repeated four times for optimal knockdown effectiveness. Knockdown of FAM92A was performed with Silencer Select Pre-Designed siRNA FAM92A S225646 (Sigma), while control knockdown was performed with Silencer Select Negative Control (Sigma).

Lentiviral production and infection

Lentiviral production and infection were performed as described in Chapter 2: Materials and Methods.

Antibodies

Immunofluorescence imaging: All antibodies were diluted in antibody diluent (5% BSA and 0.1% Triton X-100 in PBS). Primary antibodies used were mouse anti-Flag (1:300, Sigma), mouse anti-Cby 8-2 (1:100, in house) previously described (Cyge et al., 2011), mouse anti-acetylated α-tubulin (1:10,000, Sigma), rabbit anti-GFP (1:300, in house), rabbit anti-FAM92A (1:300, Sigma), rabbit anti-FAM92B (1:300, Sigma), and mouse anti-γ-tubulin (1:300, Sigma). Secondary antibodies used were DyLight 488-, DyLight 549-, and DyLight 649-conjugated anti-rabbit, anti-mouse, anti-mouse IgG1, anti-mouse IgG2a, and anti-mouse IgG2b (1:300, Jackson ImmunoResearch).

Western blotting: All antibodies were diluted in 5% milk in TBST (50 mM Tris-HCl, pH 7.4, 150 mM NaCl, 0.1% Tween 20). Primary antibodies used were rabbit anti-FAM92A (1:1000, Sigma), mouse anti-GAPDH (1:5000, Meridian), rabbit anti-FAM92B (1:1000, Sigma), mouse anti-Flag (1:1000, Sigma), rat anti-HA (1:1000, Roche), rabbit anti-His (1:1000, Santa Cruz), and rabbit anti-Cby3041 (1:300, in house) previously described (Takemaru et al., 2003). Secondary antibodies used were horseradish peroxidase (HRP)-conjugated goat anti-rat, goat anti-rabbit, and goat anti-mouse (1:5000, Jackson ImmunoResearch).

Tandem affinity purification (TAP)

HEK293 cell lines for inducible expression of TAP-tagged proteins: HEK293 cell lines expressing TAP-GFP or TAP-Cby were generated using the HEK 293 Flp-In T-Rex system (Invitrogen). These cells allow rapid generation of stable cell lines expressing a protein of interest under the control of a tetracycline-inducible promoter. This inducible system allows for adjustment of protein expression levels similar to physiological expression levels by titrating tetracycline doses. To generate the cell lines stably expressing the TAP-tagged proteins, 1 μg TAP plasmid was co-transfected with 9 μg the pOG44 Flp recombinase plasmid (Invitrogen) into HEK293 Flp-In T-Rex cells. Cells were selected for about 4 weeks in standard medium containing 200 μg/ml hygromycin (Invitrogen) and 15 μg/ml blasticidin (Invitrogen), and all colonies were pooled yielding a polyclonal TAP cell line.

Preparation of cell extracts: TAP-Cby- or TAP-GFP-expressing HEK293 cells were plated in twenty 15-cm dishes, grown to ~60% confluence and induced with 0.02 μg/mL tetracycline, which yielded expression levels similar to that of the endogenous protein (data not shown). After 48 hr of induction, cells were washed three times with ice-cold PBS and resuspended in 10 mL TAP lysis buffer (10% glycerol, 50 mM HEPES-KOH, pH 8.0, 100 mM KCl, 2 mM EDTA, 0.1% NP-40, 2 mM DTT, Protease Inhibitor Cocktail (Sigma), 10 mM NaF, 0.25 mM NaOVO3, 5 nM okadaic acid, 5 nM calyculin A, and 50 mM β-glycerolphosphate). Two cycles of freeze-thaw, alternating between liquid nitrogen and 37°C water bath, was performed to improve protein recovery. Cell extracts were cleared by centrifugation at 10,000 rpm for 15 min at 4°C for subsequent tandem affinity purification.

Tandem affinity purification: All subsequent steps were performed at 4°C, unless indicated otherwise, and all centrifugation involving beads was spun at 2,000 rpm for 5 min. The cleared supernatant was mixed with 150 µL IgG Sepharose (Sigma), previously equilibrated with TAP lysis buffer, and incubated for 4 hr with gentle agitation. The incubated beads were pelleted and first washed with TAP lysis buffer then washed with TEV buffer (10 mM HEPES-KOH, pH 8.0, 150 mM NaCl, 0.1% NP-40, 0.5 mM EDTA, and 1 mM DTT). Next, the beads were resuspended in 300 µL TEV buffer with addition of 10 µL TEV protease (a gift from Dr. Miguel Garcia-Diaz, Stony Brook University, Stony Brook, NY) and incubated for 4 hr on a rotator. After centrifugation, the supernatant containing Cby protein complexes was collected and the beads were washed with calmodulin-binding buffer (10 mM β-mercaptoethanol, 10 mM HEPES-KOH, pH 8.0, 125 mM KCl, 1 mM MgOAc, 1 mM imidazole, 0.1% NP-40, and 2 mM $CaCl_2$) three times, with the supernatant collected each time. The supernatant was pooled, mixed with 1/250 volume of 1 M $CaCl_2$ and 150 µL calmodulin beads (Stratagene), pre-equilibrated with calmodulin-binding buffer, and incubated for 90 min. The beads were washed with calmodulin-binding buffer, then with calmodulin-rinsing buffer (50 mM ammonium bicarbonate, 75 mM NaCl, 1 mM MgOAc, 1 mM imidazole, and 2 mM $CaCl_2$). For elution, 100 µL of calmodulin-elution buffer (50 mM ammonium bicarbonate and 2 mM EGTA) was added and incubated at 37°C for 5 min. The elution process was repeated two more times for a total elution volume of 300 µL.

Silver staining: After SDS-PAGE, the gel was stained using SilverQuest Silver Staining Kit (Invitrogen) according to the manufacturer's protocol. Briefly, the gel was fixed with 100 mL of fixative for 20 min with gentle agitation then washed in 30% ethanol

for 10 min. The gel was placed in 100 mL in Sensitizing solution for 10 min before a wash in 30% ethanol then in 100 mL of ultrapure water. Next, the gel was incubated in 100 mL of Staining solution for 15 min then washed with ultrapure water for 30 sec. For detection, the gel was immersed in 100 mL of Developing solution for 4-8 min. Once the desired band intensity was reached, 10 mL of Stopper solution was directly applied to the Developing solution, followed by agitation for 10 min for a complete stop. The gel was washed with 100 mL of ultrapure water for 10 min and stored at 4°C.

Mass spectrometry analysis: The TAP eluates were loaded on 8% NuPage Tri-Acetate midi gel (Life Technologies) and run for 10-15 min to ensure that proteins entered the separating gel. The gel was removed, washed with ultrapure water, and subjected to silver staining. As soon as a band was visible, Stopper solution was applied. The gel was placed on a clean sheet of transparencies and cut with a clean razor blade before placing in a pre-washed centrifuge tube. The gel section was submitted to the Stony Brook Proteomics Center for protein identification by mass spectrometry. Matrix assisted laser desorption ionization-time of flight (MALDI-TOF) mass spectrometer was used. In summary, the mass spectrometer created charged peptides and then uses the mass-to-charge ratio of the peptides to predict its amino acid sequence. Based on the amino acid sequence of the peptide, we are able to obtain the likely identity of the protein.

Protein sequence alignment

FAM92A and FAM92B amino acid sequences were obtained by searching the NCBI databases. The alignment algorithms used were CLUSTALW (Thompson et al.,

1994) and manually adjusted with SeaView (Gouy et al., 2010). Protein sequence alignments were prepared with Adobe Illustrator for presentation.

Protein expression in bacteria and *in vitro* pull-down assays

MBP-fusion protein and His-fusion protein were expressed and purified as previously described (Mofunanya et al., 2009). Briefly, an MBP-Cby expression construct was transformed into *E. coli* BL21 cells, while a His-human FAM92A expression construct was transformed into *E. coli* BL21 DE3 cells. Bacteria were grown at 37°C to an optical density of 0.6 at 600 nm as measured by Spectronic-20. Induction of protein expression was achieved with 0.5 mM isopropyl-1-thio-β-galactopyranoside (IPTG) (Sigma) for 3 hr at 30°C. MBP fusion proteins were purified using amylose resin (NEB) and His fusion protein was purified using Ni-NTA His-Bind Resin (Novagen). Purified proteins were dialyzed with dialysis buffer (20 mM HEPES-KOH, pH 7.9, 100 mM NaCl, 1 mM EDTA 0.1% NP-40 and 10% glycerol). The concentrations of proteins were estimated visually on SDS-PAGE gels stained with Coomassie Brilliant blue (Sigma) and compared to protein standards (Invitrogen).

In vitro binding assays were performed as previously described (Mofunanya et al., 2009). Briefly, equal amounts of MBP or MBP-Cby fusion protein were incubated with His-FAM92A at 4°C for 1 hr in 30 µL of protein binding buffer (PBB) (20 mM HEPES pH 7.9, 20% glycerol, 0.5 mM EDTA, 100 mM NaCl, 6 mM $MgCl_2$, and 0.1% NP-40). After incubation, 20 µL of amylose resin pre-equilibrated in PBB was added and incubated at 4°C for 1 hr. The beads were pelleted and washed with PBB three times and subjected to SDS-PAGE and western blotting.

Co-immunoprecipitation and western blotting

Co-immunoprecipitation: Transfected HEK293T cells were washed with PBS and pelleted at 2,000 rpm for 5 min. The cells were resuspended in IPB Lysis buffer (20 mM Tris-HCl, pH 8.0,135 mM NaCl, 2.5 mM $MgCl_2$, 1 mM EGTA, 1% Triton X-100, and 10% glycerol, freshly supplemented with Roche complete protease inhibitor cocktail) and incubated at room temperature for 10 min. The lysates were cleared by centrifugation using a Microfuge 22R centrifuge (Beckman Coulter) at 12,000 rpm for 30 min at 4°C. Supernatants were incubated with 2 µg anti-Flag antibody overnight at 4°C with gentle agitation, followed by 2 hr incubation with Protein A- and Protein G-Sepharose beads (Roche). Beads were then centrifuged and washed with IPB Lysis buffer. Bound proteins were eluted from the collected beads by adding an equal volume of 2x SDS gel-loading buffer (100 mM Tris-HCl, pH 6.8, 4% SDS, 0.2% bromophenol blue, 20% glycerol, and 200 mM β-mercaptoethanol) and boiling at 95°C for 5 min, and subjected to SDS-PAGE.

Western blotting: Boiled protein samples were resolved on either a 12% or 15% SDS -PAGE gel and transferred to nitrocellulose membranes for immunoblotting. Following incubation with horseradish peroxidase (HRP)-conjugated secondary antibody, HyGlo chemiluminescent substrates (Denville) were added and HyBlot CL films (Denville) were used to detect bands. Films were developed by a Konica Medical Film Processor SRX-101A.

Immunofluorescence imaging

Immunofluorescence staining was performed as described in the Materials and Methods section in Chapter 2. Images were acquired using a Leica DMI6000B research microscope equipped with Leica DFC300 FX camera and LAS AF Version 2.6 software. Confocal imaging was performed on a Zeiss LSM 510 META NLO Laser Scanning Confocal Microscope with a 100x C-Apochromat objective lens (1.4 NA, oil) using the Zeiss LSM 510 META imaging software (version 4). Super-resolution imaging was conducted using a Nikon Structured Illumination Microscopy (N-SIM) equipped with a CFI SR Apochromat TIRF 100x oil objective (1.49 NA, oil), and 488 and 561 nm lasers. Images were taken with an EMCCD camera and NIS-Elements software (Nikon). All images were prepared with Adobe Photoshop and Illustrator.

RT-PCR

Total RNA was extracted from tissue culture cells using QIAshredder (Qiagen) and RNeasy Plus Kit (Qiagen) according to the manufacturer's protocols. cDNA was synthesized from the RNA using High-Capacity cDNA Reverse Transcription Kit (Applied Biosystems) and used as template for PCR reactions. The PCR products were visualized by agarose gel electrophoresis. The primer sequences for the indicated mRNA of interest are listed below.

FAM92A

H92AqPCR_Forward: 5'-GCAACACTCACAGCAAGGAA-3'

H92AqPCR_Reverse: 5'-ACGACTTGTTCGGCTAGCAT-3'

FAM92B

H92BqPCR_Forward: 5’-CAAGCAGCTCATCGACTTTG-3’

H92BqPCR_Reverse: 5’-TAGAGCTTCAGGGGGTTGAC-3’

GAPDH

hGAPDH_Forward: 5’-ACCACAGTCCATGCCATCAC-3’

hGAPDH_Reverse: 5’-CGCTGTTGAAGTCAGAGGAG-3’

Quantification of Primary Cilia

Primary cilia were scored individually on a given field. The percentage of ciliated cells was calculated based on the number of ciliated cells divided by the total number of cells. Independent transfection was performed at least three times and a minimum of 100 cells were counted for each siRNA transfection. Student’s t-test and SEM analysis was done using Excel (Microsoft).

3.3 Results

Identification of FAM92A as a potential interacting partner for Cby

HEK293 cells were stably transfected with either TAP-Cby or TAP-GFP tetracycline-inducible expression vectors to create stable cell lines. For optimal purification, the protein of interest should be expressed at or close to its physiological levels (Puig et al., 2001). To achieve this, TAP-Cby stable cells were subjected to different concentrations of tetracycline. We choose a tetracycline concentration of 0.02 µg/mL that induced TAP-Cby at levels closest to endogenous Cby as assessed by western blotting (data not shown). Several small scale TAP procedures were performed

to optimize the protocol with different concentration of KCl and different incubation times with IgG beads.

Silver-staining of TAP-Cby elution showed several unique bands when compared to the control TAP-GFP lane (Figure 4B). The eluates from both TAP-Cby and TAP-GFP were run on a Tris-Acetate gel for approximately 10 min, only to ensure that the proteins had entered the separating gel. The protein bands were visualized by silver-staining, cut out, and sent for mass spectrometry. Mass spectrometry generated a list of potential Cby-interacting partners (Table 1). The list includes the 14-3-3 proteins, 14-3-3ε and 14-3-3ζ, which helps to serve as positive controls, as they are known strong interactors for Cby (Li et al., 2008). Amongst the Cby-specific interactors, FAM92A raised a great deal of interest based on literature and database researches. The literature searches yielded limited yet interesting information about the function of FAM92A. One study characterized a *Xenopus* homologue of FAM92A, xVAP019, showing that it plays an important role in embryonic development. Interestingly, the database searches revealed that FAM92A contains a putative BAR-domain. BAR-domain proteins are known to function in secretory vesicle fusion and signal transductions (Ren et al., 2006). It is possible that by characterizing FAM92A, and its potential interaction with Cby, I might be able to provide the molecular mechanism by which Cby is able to stabilize and mediate vesicle fusion at the base of cilia.

The Bin/Amphiphysin/Rvs (BAR) domain of Family with sequence similarity 92 (FAM92)

FAM92A belongs to the family with sequence similarity 92 (FAM92) containing the Bin/Amphiphysin/Rvs (BAR), which has two family members, FAM92A and FAM92B. The BAR domains are dimerization, lipid binding and curvature sensing modules found in many different proteins with diverse functions including organelle biogenesis, membrane trafficking or remodeling, and cell division and migration (Habermann, 2004; Frost et al., 2009; Mim and Unger, 2012). The functions of BAR-domain proteins that caught my interest were the organelle biogenesis and membrane trafficking abilities since Cby has been shown to be involved in these biological processes. A ClustalW sequence alignment of human FAM92A and FAM92B amino acids revealed a highly conserved BAR domain region with a short N-terminal region and a longer C-terminal tail (Figure 5). The highly conserved nature of the BAR domain suggests that FAM92A and FAM92B might share similar functionality.

To examine whether the BAR domain of FAM92A and FAM92B is conserved across species, we performed an alignment of FAM92A and FAM92B homologues from a variety of organisms (Figures 6 and 7). The BAR domain region was highly conserved across species, although interestingly FAM92B homologues were found only in vertebrates (Figure 7). To further investigate if FAM92A and Cby interactions play a role in cilia formation, we asked if a correlation exists between the presence of FAM92A and Cby genes and cilia. Reciprocal BLASTP analysis was performed using FAM92A amino acid sequences from ciliated/flagellated multicellular and unicellular eukaryotes. To summarize the data, we generated a simple phylogenetic tree containing ciliated/flagellated representatives of the metazoa, fungi, plants, and excavata (Figure 8). Interestingly, both FAM92A and Cby were absent in *C. elegans,* a model organism

often used for sensory cilia research but lacks the motile cilia (Bae and Barr, 2008; Inglis et al., 2007). FAM92A and Cby homologues co-exist in many animals containing motile cilia, except for the bikonts *Selaginella moellendorffii* and *Trichomonas vaginalis*, in which FAM92A homologues were absent.

Physical interaction between Cby and FAM92 proteins

Interactions between FAM92 proteins and Cby were examined using co-immunoprecipitation assays (Figure 9B). Briefly, Flag-tagged Cby was co-transfected with HA-tagged FAM92 proteins, the lysate were immunoprecipitated with Flag antibody then immunoblotted with HA antibody. Both HA-tagged FAM92A and HA-tagged FAM92B were shown to co-immunoprecipitate with Flag-tagged Cby. To further refine this, I sought to determine which region or domain of these proteins is responsible for their interactions. The BAR domain of FAM92A and FAM92B was tested for its ability to interact with Cby (Figure 9A and C). HA-tagged FAM92A-BAR and HA-tagged FAM92B-BAR were shown to co-immunoprecipitate with Flag-tagged Cby. I also examined the region of Cby responsible for its interaction with FAM92A-BAR by using two different Cby mutants (Figure 9D). The hCbyC mutant contains the C-terminal half of Cby (aa 64-126) harboring its coiled-coil domain that is responsible for its dimerization and basal body localization (Hidaka et al., 2004; Burke et al., 2014; Mofunanya et al., 2009). The hCby4A mutant contains the leucine to alanine point mutations at residues 77, 84, 91, and 98 within the coiled-coil motif that is defective in homodimerization as well as its ability to localize to the basal body (Burke et al., 2014; Mofunanya et al., 2009). HA-tagged FAM92A-BAR was shown to co-immunoprecipitate with the Flag-tagged Cby4A mutant, but not with the hCbyC mutant. A third hCby

mutant that encodes the N-terminal residues (1-63) was tested but I was unable to detect its expression in the cell lysate (data not shown). To examine whether FAM92A and Cby interaction was direct, a MBP pull-down assay using bacterially expressed and purified FAM92A and Cby proteins showed that the interaction between FAM92A and Cby was direct. Overall these results suggest that the BAR-domain of FAM92A and FAM92B is sufficient for its interaction with Cby. The N-terminal portion of Cby might be required for its direct interaction with FAM92A-BAR.

FAM92A and FAM92B homodimerize via their BAR domain but do not heterodimerize

On the basis of structural studies of the BAR-domain containing proteins, Arfaptin-2 and Amphiphysin, dimerization is thought to be critical for the function of BAR proteins (Habermann, 2004). Amphiphysin dimerization is thought to be necessary for its ability to sense and/or induce membrane bending (Peter et al., 2004). Arfaptin-2 forms a homodimer, which is a prerequisite for its binding to small GTPases that is critical for its functions (Tarricone et al., 2001). Heterodimers are mostly formed between closely related family members, such as Amphiphysin I and II as well as APPL1 and 2 (Habermann, 2004; Ramjaun et al., 1999; Miaczynska et al., 2004). The F-BAR family of proteins, srGAP1, srGAP2, and srGAP3, have been shown to heterodimerize (Coutinho-Budd et al., 2012). Heterodimerization is also possible in some distant members of the BAR-domain family. Amphiphysin II heterodimerizes with Snx4, an interaction thought to be linked to the early steps of endocytosis to intracellular transport (Leprince, 2003).

To examine whether FAM92A and FAM92B have the ability to homodimerize and/or heterodimerize, different forms of tagged FAM92A and FAM92B were subjected to co-immunoprecipitation assays. Flag-tagged FAM92A was able to co-immunoprecipitate with HA-tagged FAM92A, as did Flag-tagged FAM92B with HA-tagged FAM92B (Figure 10A). However, HA-tagged FAM92A was not able to co-immunoprecipitate with Flag-tagged FAM92B. Next, I wanted to determine if the BAR-domain was sufficient for its dimerization ability. Flag-tagged FAM92A co-immunoprecipitate with HA-tagged FAM92A-BAR, as did Flag-tagged FAM92B with HA-tagged FAM92B-BAR (Figure 10B). Taken together, these results indicates that FAM92A and FAM92B can homodimerize via their BAR-domain, but do not appear to heterodimerize.

FAM92A and FAM92B co-localize with Cby at the basal body

The Human Protein Atlas (HPA) database indicated FAM92A protein expression is found in most tissues, usually with moderate to strong cytoplasmic positivity with a granular staining pattern (http://www.proteinatlas.org/ENSG00000188343-FAM92A1/tissue). Renal glomeruli, glial cells, and smooth and skeletal muscle cells were weakly stained or negative. The HPA database indicates that FAM92B protein expression was found at the basal part of cilia in respiratory epithelia as well as oviduct, while other normal tissues were negative for FAM92B expression (http://www.proteinatlas.org/ENSG00000 153789-FAM92B/tissue).

Based on the specific interaction of FAM92A and FAM92B with Cby, it raised the interesting possibility of FAM92A and FAM92B as potential basal body proteins. The

RPE1 cell line is often used in studies of ciliary proteins, as they ciliate readily by serum starvation. To examine FAM92A and FAM92B localization, I infected RPE1 cells with lentiviruses expressing Flag-tagged FAM92 proteins. Both Flag-tagged FAM92A and FAM92B co-localize with Cby at the centrioles in cycling RPE1 cells (Figure 11). Interestingly, they appear to localize to only one of the two centrioles, similar to Cby. Cby is known to localize to the distal end of the mother centriole (Lee et al., 2014; Steere et al., 2012), which suggests that both FAM92 proteins are also mother centriole proteins. In ciliated RPE1 cells, Flag-tagged FAM92A and FAM92B co-localized with Cby at the base of cilia. Since the BAR-domain of FAM92A is sufficient for its interaction with Cby, I sought to determine whether the BAR-domain is also sufficient for its localization. Flag-tagged FAM92A was able to co-localize with Cby at the base of cilia (Figure 11).

Expression of endogenous FAM92A and FAM92B mRNA in both cycling and ciliated RPE1 cells was examined using RT-PCR (Figure 12A). The levels of FAM92B mRNA were lower compared to FAM92A, as it required more PCR cycles for the FAM92B PCR products to be detectable. One concern I had with using the commercially available antibodies for FAM92A and FAM92B is potential cross-reactivity. The antigen sequence used for generating the FAM92A and FAM92B antibody was found within the BAR-domain, where the FAM92 proteins shared significant homology. To evaluate this, HEK293T cells were transfected with N-terminally Flag-tagged FAM92A and FAM92B. Antibodies were specific to their target protein (Figure 12B). This was repeated using C-terminally Flag-tagged FAM92A and FAM92B to the ensure location of the tag did not interfere with antibody recognition. Finally, immuno-staining

for FAM92A and FAM92B was performed in ciliated RPE1 cells. The results confirmed co-localization of FAM92A with Cby at the base of cilia (Figure 12C). The FAM92B antibody did not show any significant signals at the centrosome (data not shown). It is possible that FAM92B expression is tissue-specific, or its expression is below the detection threshold for the antibody.

To examine whether FAM92A and FAM92B localization pattern is similar in multi-ciliated cells, we isolated and infected mouse tracheal epithelial cells (MTECs) with Flag-tagged FAM92 lentiviruses at the time of seeding, followed by differentiation of MTECs at the air-liquid interface (ALI). Immuno-staining showed that both Flag-tagged FAM92A and FAM92B co-localize with Cby (Figure 13A). Following the establishment of the ALI, MTECs will simultaneously generate hundreds of centrioles that will serve as the basal body of the motile cilia (Vladar and Brody, 2013). Accordingly, genes important for centriole biogenesis and cilia formation are upregulated. To examine whether FAM92 expressions were upregulated, RT-PCR was performed on mRNA taken from MTECs at ALId0, 4, and 14. The results indicate that FAM92A and FAM92B gene expression remains constant throughout MTEC differentiation (Figure 13B). Finally immuno-staining was performed for endogenous FAM92A and FAM92B in fully ciliated MTECs. Both FAM92A and FAM92B co-localize with Cby in multi-ciliated cells in MTEC cultures (Figure 13C).

These findings suggest that FAM92A is expressed in both primary ciliated and multi-ciliated cells and co-localizes with Cby at the basal body. FAM92B expression is either tissue specific as it is expressed in multi-ciliated MTECs but not in primary ciliated RPE1 cells, or its expression is below detection threshold. Overall these localization

studies, along with the Cby interaction studies, indicate FAM92A and FAM92B as novel basal body proteins.

Super-resolution fluorescence microscopy reveals that FAM92A localizes in a ring pattern with Cby at the ciliary base

Conventional light microscopy has been useful in providing an approximate localization of centrosomal proteins, but the dimensions of centrioles are close to the optical resolution limit of 200 nm (Schermelleh et al., 2010; Sonnen et al., 2012). This made gathering information about the spatial organization of centrosomal components difficult. The recent development of super-resolution fluorescence microscopy techniques has made it possible to resolve beyond the optical resolution of 200 nm. Structure Illumination Microscopy (SIM) can improve the resolution obtained by conventional confocal microscopy by a factor of 2, which can provide structural information at a resolution of ~200 nm in both X and Y axes (Gustafsson et al., 2008; Jost and Heintzmann, 2013).

In order to understand FAM92A's localization at the base of cilia in relation to Cby, immuno-staining images of endogenous Cby and FAM92A were taken with SIM. For these images, MTECs was induced to differentiation by establishing the ALI. Cells were fully differentiated at ALId14. The SIM images revealed that FAM92A co-localizes with Cby in a ring-like pattern (Figure 14A). The axial cross-section image indicated that both FAM92A and Cby localize to the same plane. As Cby was shown to localize to the transition fibers, this suggest that FAM92A also localizes to the transition fibers (Figure 14B).

FAM92A and FAM92B localization to the basal body is disrupted in the absence of Cby

Cby is recruited to the distal appendages by the distal appendage protein Cep164 (Burke et al., 2014). To examine whether FAM92 proteins act upstream or downstream of Cby, we used mouse embryonic fibroblasts (MEFs) isolated from both CbyWT and CbyKO embryos. These MEFs, like RPE1 cells, can be induced to ciliate through serum starvation. Endogenous FAM92A and FAM92B mRNA expression in both cycling and ciliated MEFs was confirmed using RT-PCR. The mRNA levels of FAM92A and FAM92B remained constant in both CbyWT and CbyKO MEFs in cycling and ciliated states (Figure 15A). In serum-starved CbyKO MEFs, the localization of FAM92A to the γ-tubulin-positive basal body was undetectable (Figure 15B). To confirm this in multi-ciliated cells, immunofluorescence staining of MTECs was performed. FAM92A and FAM92B localization at the basal body was severely reduced in multi-ciliated cells in the absence of Cby (Figure 15C). This suggests that Cby acts upstream of FAM92 proteins and is most likely to recruit FAM92 proteins to the basal body.

FAM92A knockdown results in a decrease in the level of ciliation

The characterization of FAM92A as a novel basal body protein and its interaction with Cby raises the question of whether FAM92A is required for cilia formation. To examine this, I proceeded to knockdown FAM92A expression in RPE1 cells using siRNA-mediated gene silencing. Briefly, RPE1 cells were subjected to 4 rounds of siRNA transfection over the course of 4 days. These cells were then serum-starved to induce ciliation. Cell lysates were then collected for western blot analysis. The FAM92A

siRNA-treated cells had significantly lower levels of FAM92A protein compared to the scrambled siRNA-treated negative control (Figure 16B). By counting the number of cilia, as denoted by acetylated α-tubulin staining, over the number of basal body, as denoted by γ-tubulin staining, in a given field I was able to determine the level of ciliation. Knockdown of FAM92A decreased the overall levels of ciliation in RPE1 cells (Figure 16A). Over 85% of cells were ciliated in the scramble siRNA group, while only 68% of cells were ciliated in FAM92A siRNA group (Figure 16C). This represented a significant decrease in ciliation suggests that FAM92A does play a role in cilia formation.

Ectopic expression of FAM92 and Cby induces membrane tubule-like structures

The universal and minimal BAR domain is a dimerization, membrane-binding, and curvature-sensing module (Peter et al., 2004). The BAR-domain dimer, with its crescent-shaped that contains positively charged residues distributed along its concave face, binds preferentially to curved membrane thus able to act as a sensor of membrane curvature (Peter et al., 2004; Habermann, 2004; Mim and Unger, 2012; Gallop et al., 2006). Some BAR-domain proteins contains additional domains that will induce membrane curvature (Ramjaun et al., 1999). Ectopic expression of BAR domain proteins are able to drive membrane curvature to form a higher ordered helical arrays of membrane to form membrane tubules and vesicles (Shinozaki-Narikawa et al., 2006; van Weering et al., 2010). Amphiphysin-1 has been shown to tubulate membranes when overexpressed in COS cells (Yin et al., 2009; Zhao et al., 2013). Endophilin A, which is involved in the clathrin pathway, has also been shown to tubulate membrane (Renard et al., 2015; Boucrot et al., 2015; Gallop et al., 2006).

Accordingly, BAR domain are classified by the degree of curvature that they can sense and/or induce. N-BAR domain are BAR domains with an N-terminal amphipathic helix that can insert itself into the phosopholipids of the membrane to act as a wedge to drive membrane curvature, tubulate and form vesicles (Peter et al., 2004; Gallop et al., 2006; van Weering et al., 2010). F-BAR domain dimers are less curved than N-BAR domains, however they are involved in driving and/or sensing extremely positive membrane curvatures and can form either broad or narrow membrane tubules (Roberts-Galbraith and Gould, 2010; Dharmalingam et al., 2009; Suetsugu, 2010). I-BAR domain dimers are relatively flat and instead of inducing positive curvature, will induce negative curvature in membranes (Millard et al., 2005; Mattila et al., 2007). I-BAR domain proteins induce plasma membrane protrusions rather than invagination and can stabilize tubules by binding to the inner surface of the membranes (Mattila et al., 2007; Millard et al., 2005; Suetsugu, 2010)

To examine whether FAM92 proteins share this ability to tubulate membranes, GFP-tagged FAM92A and FAM92B were expressed in COS7 cells. Diffuse cytoplasmic staining was observed in both of the FAM92A and FAM92B expressing cells (Figure 17). However when FAM92A was co-expressed with Cby, I observed strong FAM92A accumulation in puncta surrounded by a ring of Cby. When FAM92B was co-expressed with Cby, I observed the formation of membrane tubulation. This suggests that FAM92B is able to tubulate membrane but only in the presence of Cby.

3.4 Discussion

Identification of FAM92 proteins as novel Cby interacting partners.

In characterizing the FAM92 proteins as Cby-interacting partners, I found that the BAR-domain was sufficient for their interactions with Cby. The C-terminal portion of Cby did not immunoprecipitate with the BAR-domain of FAM92A, but the Cby mutant lacking the homodimerization ability did. Cby exists predominantly as a homodimer, which is required for its efficient nuclear import (Mofunanya et al., 2009). Additionally, Cby contains a nuclear localization signal in its C-terminal portion (Li et al., 2010). This suggests that FAM92A-BAR domain interaction with Cby is dependent on the N-terminal portion of Cby.

Many BAR-domain proteins have shown the ability to homodimerize (Habermann, 2004). Some closely related BAR-domain family members have also shown the ability to heterodimerize (Habermann, 2004). Given the homology between the two FAM92 proteins their ability to heterodimerize was a surprise. The molecular basis for why some BAR domains can only homodimerize while other BAR domains can also heterodimerize is unclear. One study suggests compatibility issues based on different amino acid residues at the dimer interface (Dislich et al., 2011). SNX33 forms homodimers but not heterodimers with its closets homologs SNX9 and SNX18. However mutating some key amino acids in SNX9, it allowed SNX9 to heterodimerize with SNX33 (Dislich et al., 2011). The inability to heterodimerize could indicate different cellular function for the two FAM92 proteins. Further work would be needed to identify the key amino acid residues in the FAM92 dimer interfaces.

FAM92 proteins in ciliogenesis

Based on my findings above, Cby recruits FAM92A and FAM92B to the base of

cilia. Cby itself is recruited to the distal appendage by Cep164 (Burke et al., 2014). There, Cby interacts with Rabin8, the GEF for Rab8, which serves to recruit Rab8-positive vesicles to the maturing ciliary vesicle (Burke et al., 2014). It is possible that FAM92A and FAM92B are recruited to the basal body as a component of the Rab8-positive vesicles, and that in the absence of Cby, the vesicles containing the FAM92 are not recruited to the base of cilia.

BAR-domain proteins have been implicated in ciliary function. The ArfGAP with SH3 domain, ankyrin repeat and PH domain 1 (ASAP1) is a BAR-domain protein with a crucial role in rhodopsin transport. Rhodopsin, the light sensitive receptor protein, is sorted at the *trans*-Golgi network (TGN) into the membrane enclosed rhodopsin transport carriers (RTC), and delivered to the primary cilia and cilia-derived sensory organelles (Deretic and Wang, 2012a). The formation of the rhodopsin-Arf-ASAP1 complex at the TGN results in membrane deformation and release of the RTC (Deretic and Wang, 2012b). ASAP1 likely mediates membrane deformation through its BAR domain while mediating GTP-hydrolysis on Arf4, which then dissociates from the TGN (Wang et al., 2012; Nie and Randazzo, 2006; Nie et al., 2006). Another example is the F-BAR domain protein syndapin I. Syndapin I is a lipid binding and membrane curvature-sensing spatial organizer that is thought to associate with membrane areas prone to cilia formation (Qualmann and Kelly, 2000). Syndapin I recruits Cobl which contains three Wiskott-Aldrich homology 2 (WH2) domains for actin-binding and nucleation (Ahuja et al., 2007). Together, the syndapin I/Cobl complex is thought to prime the location for formation of cilia through local changes in membrane topology.

Based on the function of ASAP1, it raises the interesting possibility that FAM92 proteins also act at the TGN to serve the link and free the vesicles for delivery to the ciliary compartment. In this model, FAM92 would be sorted with Rab8, Rab11, IFT20, and other ciliary components into vesicles that are then trafficked to the base of cilia (Figure 18). There, FAM92A binds Cby and stabilizes the vesicle for subsequent fusion.

The knockdown of FAM92A did yield a significant decrease in ciliation, although the effect was only moderate. This could be explained by genetic redundancy, that in the absence of FAM92A, FAM92B or possibly other proteins are able to substitute for FAM92A. It is also possible that FAM92A is required for the early stages of cilia formation, and that perhaps its effect is more significant at earlier time points. The duration of serum starvation has been known to have a significant impact on ciliation in CbyKO MEFs. At 24 hr, CbyWT MEFs ciliated at 45%, while CbyKO MEFs ciliated at 5%. However, at the 72 hr mark, CbyKO MEFs were able to ciliate up to 30% compared to CbyWT 55% ciliated (Lee et al., 2014).

Formation of membrane tubule-like structures by FAM92 and Cby proteins

The ability to tubulate membrane is a known characteristic of BAR-domain proteins (Peter et al., 2004; Zhao et al., 2013; Shinozaki-Narikawa et al., 2006). Under normal physiological conditions, membrane tubulation does not occur. The deformation of membrane is an energetically prohibitive process but when there is a high concentration of BAR-domain proteins, usually ectopically expressed, this barrier becomes surmountable (Wang et al., 2009; Gallop and McMahon, 2005). The proposed model by which BAR domain tubulates membrane is the binding of one BAR-domain

protein produces a local curvature, which attracts another BAR-domain protein and so on (van Weering et al., 2010), until the BAR-domain polymerizes into a helical coat that is held together by lateral and tip-to-tip interactions (Frost et al., 2008). Using Cryo-EM reconstructions, it revealed that the BAR proteins are arranged in a lattice of spiral rows (Frost et al., 2009; Yin et al., 2009).

FAM92A and FAM92B appear to only contain the putative BAR domain. Some BAR-domain proteins contain an N-terminal, amphipathic helices that act as a wedge to induce membrane curvature, while others induce curvature through electrostatic and intermolecular interactions (Wang et al., 2009). FAM92A and FAM92B by themselves were unable to induce membrane tubulation. Only with the addition of Cby was tubulation possible. This could suggest that Cby stabilizes the polymerization of FAM92 dimers needed to form the higher ordered lattice structure. Cby could be responsible for accumulating enough FAM92 proteins so that a critical mass is reach for membrane tubulation to occur spontaneous. Overall the membrane tubulation assay confirms the FAM92 as BAR-domain proteins.

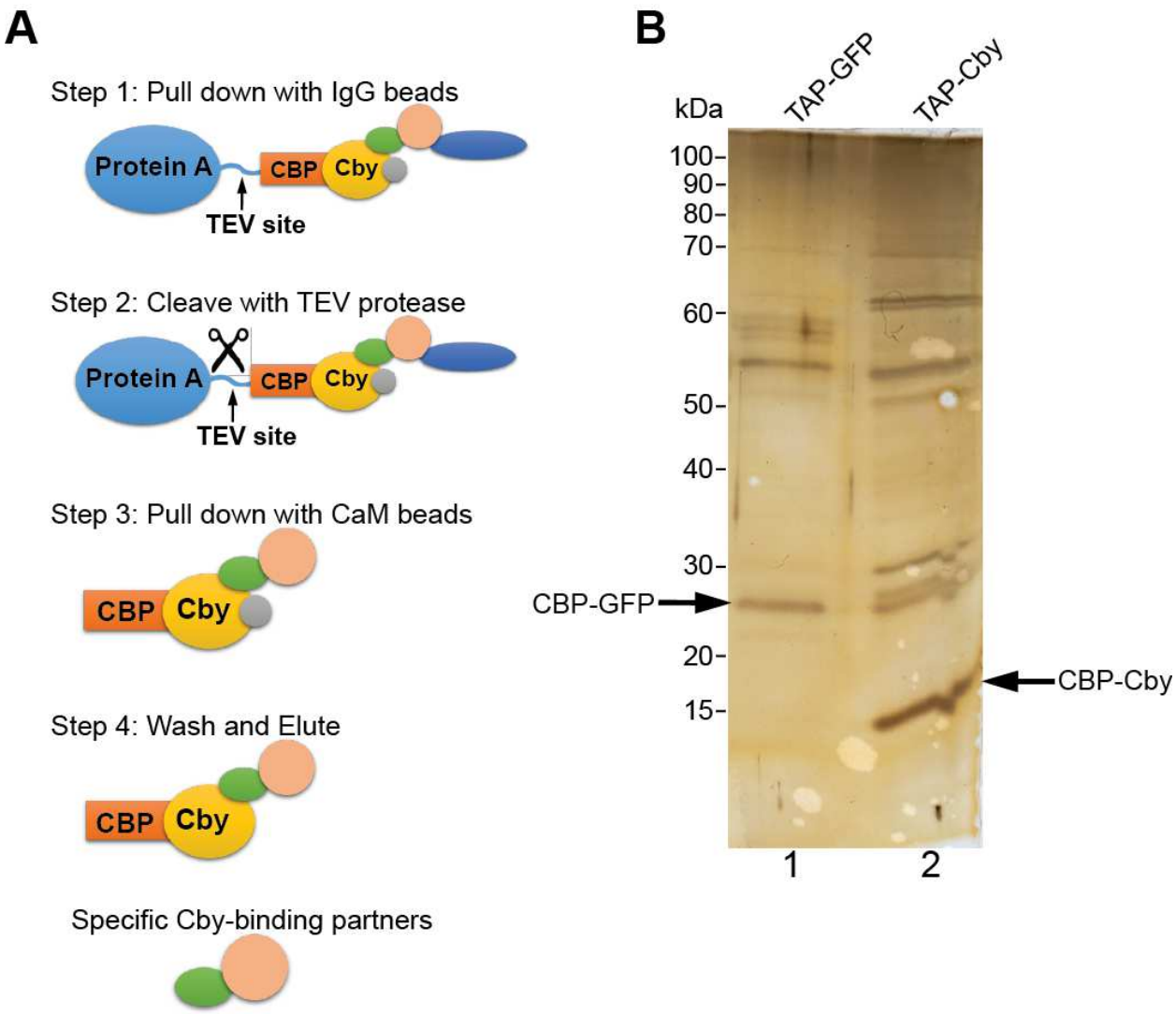

Figure 4. Tandem affinity purification of novel Cby-binding partners.

(A) Schematic representation of the tandem affinity purification (TAP) protocol. The TAP tag consists of three components: a protein A moiety acting as an immunoglobulin G (IgG)-binding domain, a tobacco etch virus (TEV) protease cleavage site, and a calmodulin (CaM)-binding peptide (CBP). TAP-Cby and TAP-GFP expressed in HEK 293 cells were purified using IgG agarose beads (Step 1), followed by the cleavage of the protein A moiety by TEV protease (Step 2). Next, the remaining multi-protein complexes were further purified using CaM Sepharose beads (Step 3). Finally, CBP-Cby and specific Cby-binding partners were eluted with EGTA (Step 4).

(B) The final TAP elutions were resolved on a 4-20% gradient SDS-PAGE gel and visualized by silver staining. TAP-GFP was used as negative purification control. The positions of molecular weight marker bands are indicated on the left. The arrows indicate bands for CBP-GFP in lane 1 and CBP-Cby in lane 2. The samples were analyzed by tandem mass spectrometry (LC-MS/MS) and identified proteins are listed in Table 1.

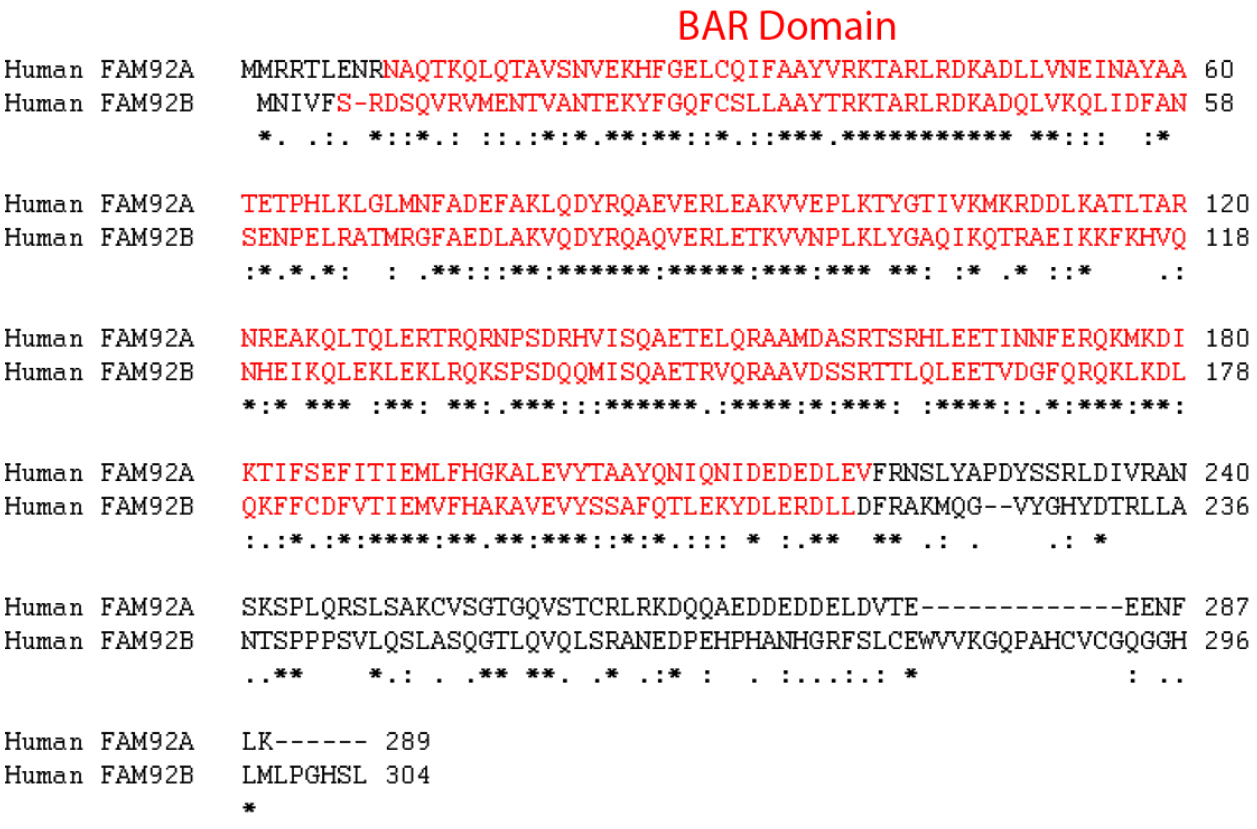

Figure 5. Alignment of human FAM92A and FAM92B amino acid sequences.

Amino acid sequence alignment of human FAM92A and FAM92B was performed using ClustalW. The highly conserved BAR domains are highlighted in red. Amino acids residues that are identical in both FAM92 family member are marked with an asterisks, conserved and semi-conserved substitution are marked with a colon and period, respectively.

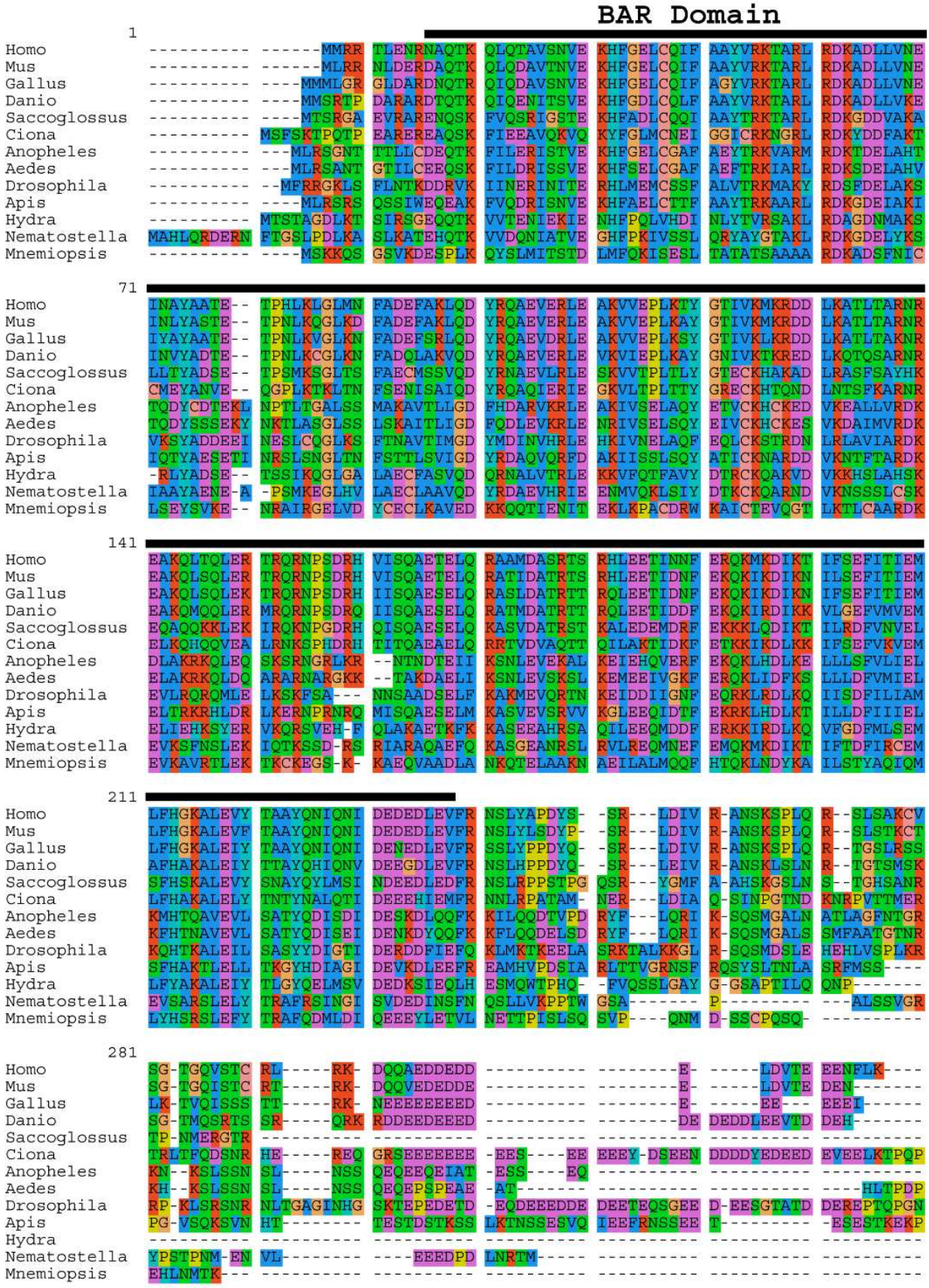
BAR Domain
1
Homo ---------- ------MMRR TLENRNAQTK QLQTAVSNVE KHFGELCQIF AAYVRKTARL RDKADLLVNE
Mus ---------- ------MLRR NLDERDAQTK QLQDAVTNVE KHFGELCQIF AAYVRKTARL RDKADLLVNE
Gallus ---------- ----MMMLGR GLDARDNQTR QIQDAVSNVE KHFGELCQIF AGYVRKTARL RDKADLLVNE
Danio ---------- ----MMSRTP DARARDTQTK QIQENITSVE KHFGDLCQLF AAYVRKTARL RDKADLLVKE
Saccoglossus ---------- ----MTSRGA EVRARENQSK FVQSRIGSTE KHFADLCQQI AAYTRKTARL RDKGDDVAKA
Ciona ---------- MSFSKTPQTP EAREREAQSK FIEEAVQKVQ KYFGLMCNEI GGICRKNGRL RDKYDDFAKT
Anopheles ---------- ---MLRSGNT TTLLCDEQTK FILERISTVE KHFGELCGAF AEYTRKVARM RDKTDELAHT
Aedes ---------- ---MLRSANT GTILCEEQSK FILDRISSVE KHFSELCGAF AEFTRKIARL RDKSDELAHV
Drosophila ---------- --MFRRGKLS FLNTKDDRVK IINERINITE RHLMEMCSSF ALVTRKMAKY RDSFDELAKS
Apis ---------- ----MLRSRS QSSIWEQEAK FVQDRISNVE KHFAELCTTF AAYTRKAARL RDKGDEIAKI
Hydra ---------- MTSTAGDLKT SIRSGEQQTK VVTENIEKIE NHFPQLVHDI NLYTVRSAKL RDAGDNMAKS
Nematostella MAHLQRDERN FTGSLPDLKA SLKATEHQTK VVDQNIATVE GHFPKIVSSL QRYAYGTAKL RDKGDELYKS
Mnemiopsis ---------- ----MSKKQS GSVKDESPLK QYSLMITSTD LMFQKISESL TATATSAAAA RDKADSFNIC
71
Homo INAYAATE-- TPHLKLGLMN FADEFAKLQD YRQAEVERLE AKVVEPLKTY GTIVKMKRDD LKATLTARNR
Mus INLYASTE-- TPNLKQGLKD FADEFAKLQD YRQAEVERLE AKVVEPLKAY GTIVKMKRDD LKATLTARNR
Gallus IYAYAATE-- TPNLKVGLKN FADEFSRLQD YRQAEVDRLE AKVVEPLKSY GTIVKLKRDD LKATLTAKNR
Danio INVYADTE-- TPNLKCGLKN FADQLAKVQD YRQAEVERLE VKVIEPLKAY GNIVKTKRED LKQTQSARNR
Saccoglossus LLTYADSE-- TPSMKSGLTS FAECMSSVQD YRNAEVLRLE SKVVTPLTLY GTECKHAKAD LRASFSAYHK
Ciona CMEYANVE-- QGPLKTKLTN FSENISAIQD YRQAQIERIE GKVLTPLTTY GRECKHTQND LNTSFKARNR
Anopheles TQDYCDTEKL NPTLTGALSS MAKAVTLLGD FHDARVKRLE AKIVSELAQY ETVCKHCKED VKEAALVRDK
Aedes TQDYSSSEKY NKTLASGLSS LSKAITLIGD FQDLEVKRLE NRIVSELSQY EIVCKHCKES VKDAIMVRDK
Drosophila VKSYADDEEI NESLCQGLKS FTNAVTIMGD YMDINVHRLE HKIVNELAQF EQLCKSTRDN LRLAVIARDK
Apis IQTYAESETI NRSLSNGLTN FSTTLSVIGD YRDAQVQRFD AKIISSLSQY ATICKNARDD VKNTFTARDK
Hydra -RLYADSE-- TSSIKQGLGA LAECFASVQD QRNALVTRLE KKVFQTFAVY DTRCKQAKVD VKKHSLAHSK
Nematostella IAAYAENE-A -PSMKEGLHV LAECLAAVQD YRDAEVHRIE ENMVQKLSIY DTKCKQARND VKNSSSLCSK
Mnemiopsis LSEYSVKE-- NRAIRGELVD YCECLKAVED KKQQTIENIT EKLKPACDRW KAICTEVQGT LKTLCAARDK
141
Homo EAKQLTQLER TRQRNPSDRH VISQAETELQ RAAMDASRTS RHLEETINNF ERQKMKDIKT IFSEFITIEM
Mus EAKQLSQLER TRQRNPSDRH VISQAETELQ RATIDATRTS RHLEETIDNF EKQKIKDIKN ILSEFITIEM
Gallus EAKQLSQLEK TRQRNPSDRH IISQAESELQ RASLDATRTT RQLEETIDNF EKQKIKDIKN IFSEFITIEM
Danio EAKQMQQLER MRQRNPSDRQ IISQAESELQ RATMDATRTT RQLEETIDDF EKQKIRDIKK VLGEFVMVEM
Saccoglossus EQAQQKKLEK IRQKNPGDRH QISQAESELQ KASVDATRST KALEDEMDRF EKKKLQDIKT ILRDFVNVEL
Ciona ELKQHQQVEA LRNKSPHDRH TITQAEAELQ RRTVDVAQTT QILAKTIDKF ETKKIKDLKK IFSEFVKVEM
Anopheles DLAKRKQLEQ SKSRNGRLKR --NTNDTEII KSNLEVEKAL KEIEHQVERF EKQKLHDLKE LLLSFVLIEL
Aedes ELAKRKQLDQ ARARNARGKK --TAKDAELI KSNLEVSKSL KEMEEIVGKF ERQKLIDFKS LLLDFVMIEL
Drosophila EVLRQRQMLE LKSKFSA--- NNSAADSELF KAKMEVQRTN KEIDDIIGNF EQRKLRDLKQ IISDFILIAM
Apis ELTRKRHLDR LKERNPRNRQ MISQAESELM KASVEVSRVV KGLEEQIDTF EKRKLHDLKT ILLDFIIIEL
Hydra ELIEHKSYER VKQRSVEH-F QLAKAETKFK KASEEAHRSA QILEEQMDDF ERKKIRDLKQ VFGDFMLSEM
Nematostella EVKSFNSLEK IQTKSSD-RS RIARAQAEFQ KASGEANRSL RVLREQMNEF EMQKMKDIKT IFTDFIRCEM
Mnemiopsis EVKAVRTLEK TKCKEGS-K- KAEQVAADLA NKQTELAAKN AEILALMQQF HTQKLNDYKA ILSTYAQIQM
211
Homo LFHGKALEVY TAAYQNIQNI DEDEDLEVFR NSLYAPDYS- -SR---LDIV R-ANSKSPLQ R--SLSAKCV
Mus LFHGKALEVF TAAYQNIQNI DEDEDLEVFR NSLYLSDYP- -SR---LDIV R-ANSKSPLQ R--SLSTKCT
Gallus LFHGKALEIY TAAYQNIQNI DENEDLEVFR SSLYPPDYQ- -SR---LDIV R-ANSKSPLQ R--TGSLRSS
Danio AFHAKALEIY TTAYQHIQNV DEEGDLEVFR NSLHPPDYQ- -SR---LEIV R-ANSKLSLN R--TGTSMSK
Saccoglossus SFHSKALEVY SNAYQYLMSI NDEEDLEDFR NSLRPPSTPG QSR---YGMF A-AHSKGSLN S--TGHSANR
Ciona LFHAKALELY TNTYNALQTI DEEEHIEMFR NNLRPATAM- NER---LDIA Q-SINPGTND KNRPVTTMER
Anopheles KMHTQAVEVL SATYQDISDI DESKDLQQFK KILQQDTVPD RYF---LQRI K-SQSMGALN ATLAGFNTGR
Aedes KFHTNAVEVL SATYQDISEI DENKDYQQFK KFLQQDELSD RYF---LQRI K-SQSMGALS SMFAATGTNR
Drosophila KQHTKALEIL SASYYDIGTI DERDDFIEFQ KLMKTKEELA SRKTALKKGL R-SQSMDSLE HEHLVSPLKR
Apis SFHAKTLELL TKGYHDIAGI DEVKDLEEFR EAMHVPDSIA RLTTVGRNSF RQSYSLTNLA SRFMSS----
Hydra LFYAKALEIY TLGYQELMSV DEDKSIEQLH ESMQWTPHQ- -FVQSSLGAY G-GSAPTILQ QNP-------
Nematostella EVSARSLELY TRAFRSINGI SVDEDINSFN QSLLVKPPTW GSA------- P--------- ---ALSSVGR
Mnemiopsis LYHSRSLEFY TRAFQDMLDI QEEEYLETVL NETTPISLSQ SVP----QNM D-SSCPQSQ- ----------
281
Homo SG-TGQVSTC RL-----RK- DQQAEDDEDD ---------- --------E- -----LDVTE EENFLK----
Mus SG-TGQISTC RT-----RK- DQQVEDEDDE ---------- --------E- -----LDVTE DEN-------
Gallus LK-TVQISSS TT-----RK- NEEEEEEEED ---------- --------E- -----EE--- EEEI------
Danio SG-TMQSRTS SR-----QRK RDDEEDEEED ---------- --------DE DEDDLEEVTD DEH-------
Saccoglossus TP-NMERGTR ---------- ---------- ---------- ---------- ---------- ----------
Ciona TRLTFQDSNR HE-----REQ GRSEEEEEEE -EES----EE EEEY-DSEEN DDDDYEDEED EVEELKTPQP
Anopheles KN--KSLSSN SL-----NSS QEQEEQEIAT -ESS----EQ ---------- ---------- ----------
Aedes KH--KSLSSN SL-----NSS QEQEPSPEAE -AT------- ---------- ---------- ----HLTPDP
Drosophila RP-KLSRSNR NLTGAGINHG SKTEPEDETD -EQDEEEDDE DEETEQSGEE D-EESGTATD DEREPTQPGN
Apis PG-VSQKSVN HT-------- TESTDSTKSS LKTNSSESVQ IEEFRNSSEE T--------- -ESESTKEKP
Hydra ---------- ---------- ---------- ---------- ---------- ---------- ----------
Nematostella YPSTPNM-EN VL-------- ----EEEDPD LNRTM----- ---------- ---------- ----------
Mnemiopsis EHLNMTK--- ---------- ---------- ---------- ---------- ---------- ----------

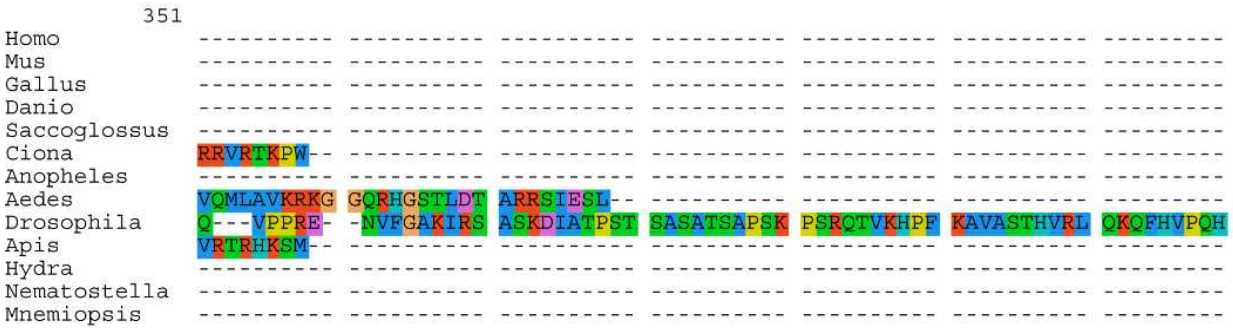

Figure 6. Evolutionary conservation of FAM92A proteins across species.

FAM92A protein sequences were aligned using ClustalW and manually adjusted using SeaView. The conserved BAR domain is indicated by the black bar. Each of the eight classes of amino acids is represented by a distinct color. Note that only a partial sequence was available for *Saccoglossus kowalevskii*.

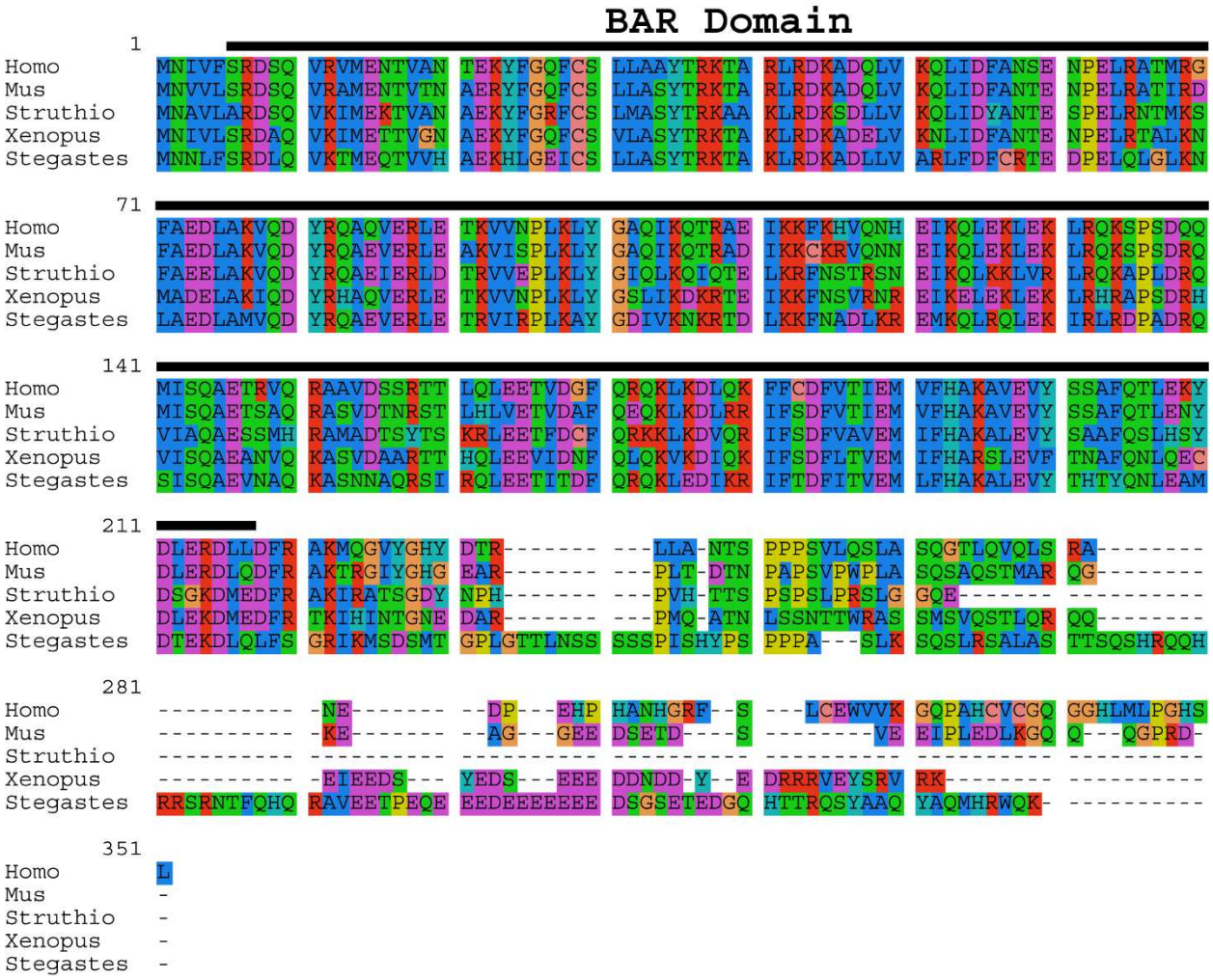

Figure 7. Evolutionary conservation of FAM92B proteins across species.

FAM92B protein sequences were aligned using ClustalW and manually adjusted using SeaView. The conserved BAR domain is indicated by the black bar. Each of the eight classes of amino acids is represented by a distinct color. Note that FAM92B homologues are found only in vertebrates.

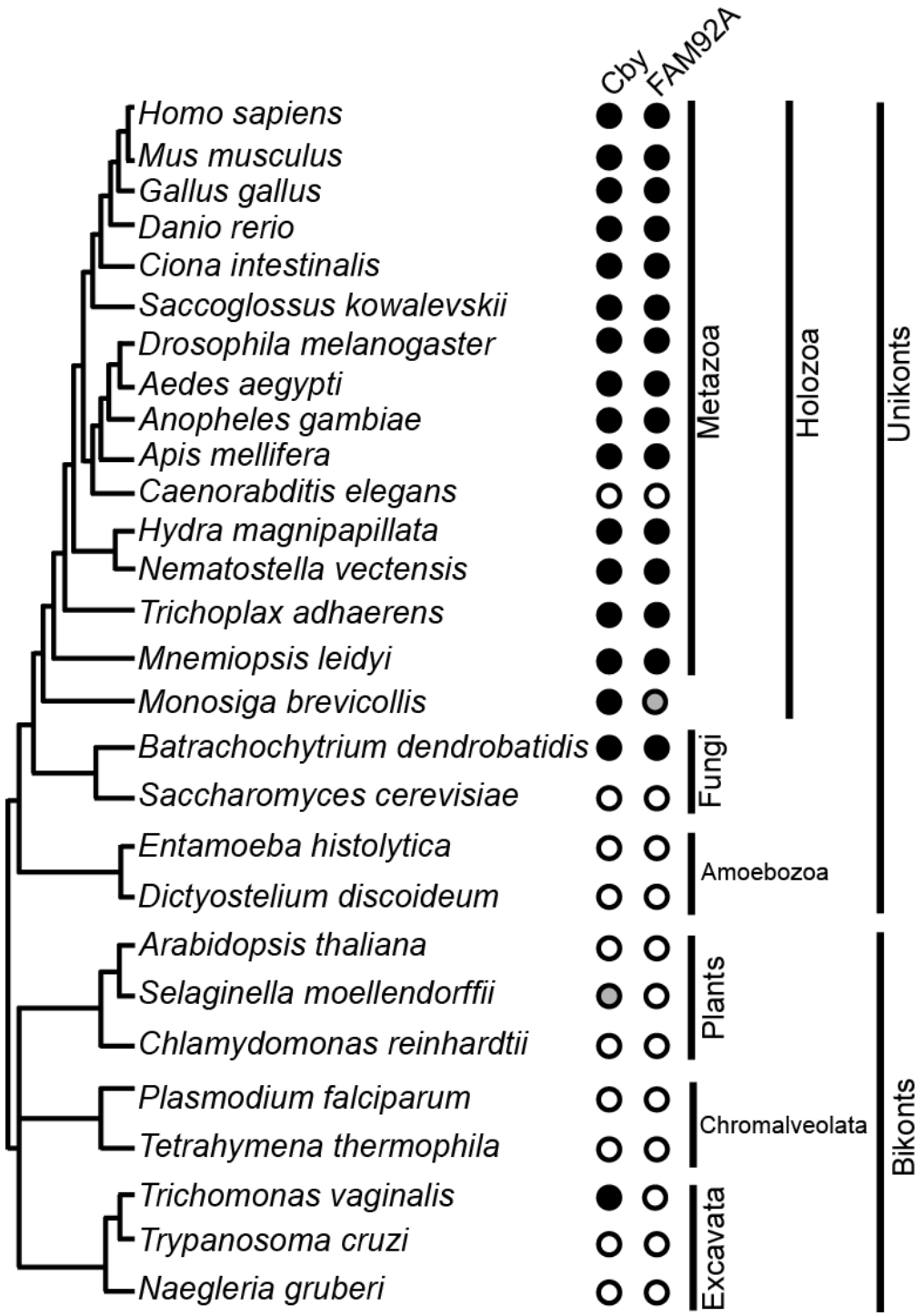
Cby
FAM92A
Homo sapiens
Mus musculus
Gallus gallus
Danio rerio
Ciona intestinalis
Saccoglossus kowalevskii
Drosophila melanogaster
Aedes aegypti
Anopheles gambiae
Apis mellifera
Caenorabditis elegans
Hydra magnipapillata
Nematostella vectensis
Trichoplax adhaerens
Mnemiopsis leidyi
Monosiga brevicollis
Batrachochytrium dendrobatidis
Saccharomyces cerevisiae
Entamoeba histolytica
Dictyostelium discoideum
Arabidopsis thaliana
Selaginella moellendorffii
Chlamydomonas reinhardtii
Plasmodium falciparum
Tetrahymena thermophila
Trichomonas vaginalis
Trypanosoma cruzi
Naegleria gruberi
Metazoa
Fungi
Amoebozoa
Plants
Chromalveolata
Excavata
Holozoa
Unikonts
Bikonts

Figure 8. Phylogenetic analysis of FAM92A and Cby.

Cby and FAM92A homologues are found in many animals containing motile cilia (black circles). Interestingly, both are present in *Drosophila melanogaster* but absent in *Caenorabditis elegans* (white circle). A probable Cby homologue is found *Selaginella moellendorffii* (gray circle). *Monosiga brevicollis* has a Cby homologue as well as a protein containing a BAR domain with weak homology to the BAR domain of FAM92A proteins. FAM92A and Cby co-exist in many species except for the bikonts *Selaginella moellendorffii* and *Trichomonas vaginalis* in which FAM92A homologues are missing.

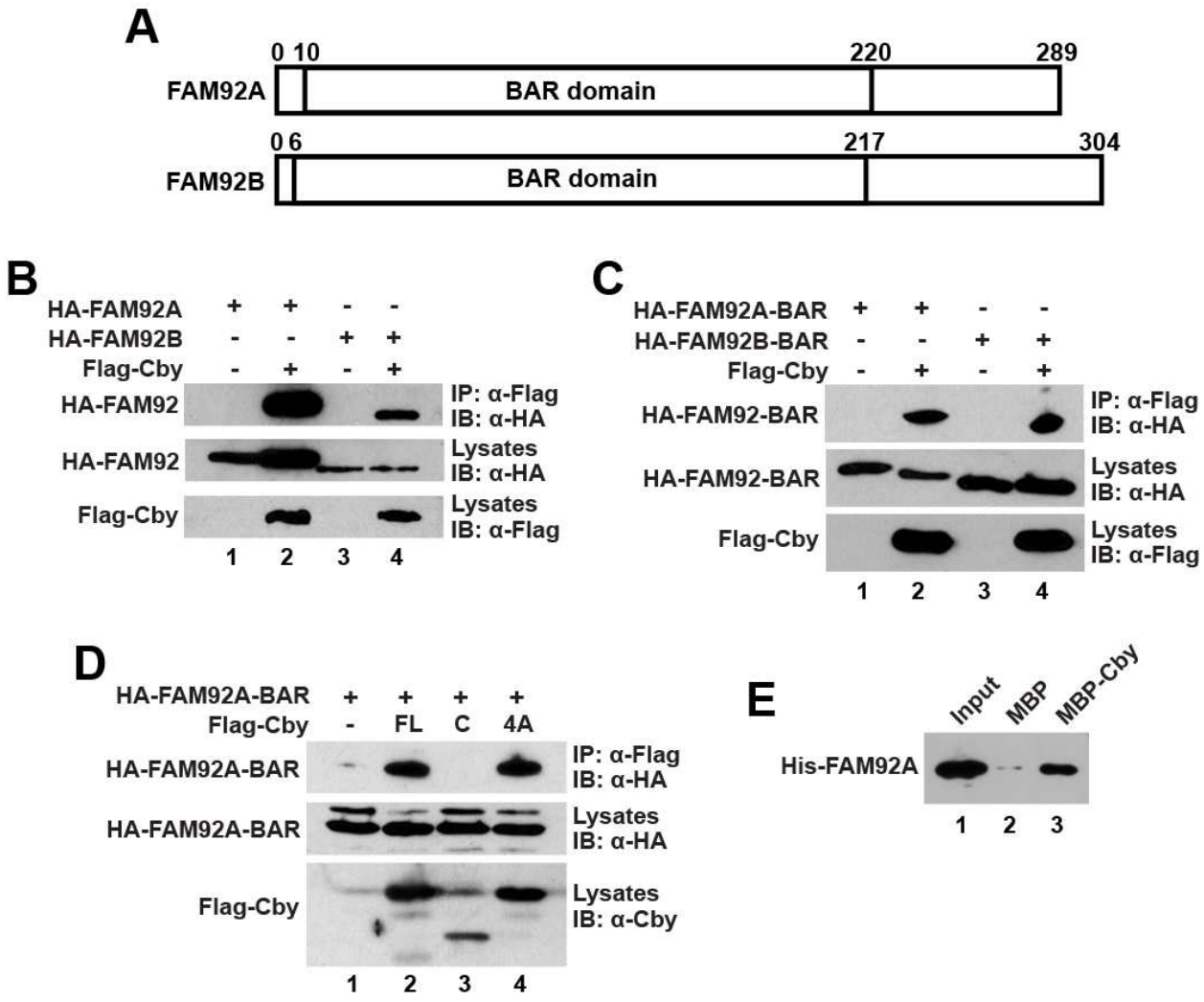

Figure 9. Physical interaction between Cby and FAM92 proteins.

(A) Schematic representation of human FAM92A and FAM92B proteins. The numbers indicate the amino acid position of the BAR domain.

(B) HEK293T cells were transiently transfected with the indicated combinations of expression plasmids for Flag-Cby and HA-tagged FAM92A or FAM92B. Total cell lysates were immunoprecipitated with anti-Flag antibody and detected with anti-HA antibody. Total cell lysates were also probed with either anti-HA or anti-Flag antibody to determine levels of protein expression. Cby interacts with both FAM92A (lane 2) and FAM92B (lane 4).

(C) HEK293T cells were transiently transfected with the indicated combinations of expression plasmids for Flag-Cby and HA-tagged BAR domain of FAM92A or that of FAM92B. Total cell lysates were immunoprecipitated with anti-Flag antibody and detected with anti-HA antibody. Total cell lysates were also probed with either anti-HA

or anti-Flag antibody to examine protein expression levels. The BAR domain of FAM92A (lane 2) and FAM92B (lane 4) is sufficient for Cby binding.

(D) HEK293T cells were co-transfected with expression plasmids for HA-FAM92A-BAR and Flag-tagged full-length Cby (Cby-FL), C-terminal half of Cby (CbyC), or Cby4A mutant (Cby4A) with leucine to alanine point-mutations at residues 77, 84, 91, and 98 which ablates Cby homodimerization. Total cell lysates were immunoprecipitated with anti-Flag antibody and detected with anti-HA antibody. Total cell lysates were also detected with either anti-HA or anti-Cby antibody to assess levels of protein expression. The BAR domain of FAM92A interacts with Cby4A (lane 4), but not with C-terminal portion of Cby (lane 3), suggesting that the N-terminal region of Cby might be involved in the interaction with FAM92A.

(E) MBP pull-down assays were performed using bacterially expressed and purified proteins to test their direct interaction *in vitro*. His-FAM92A was pulled down with MBP-Cby but not with MBP alone, indicating that FAM92A directly interacts with Cby.

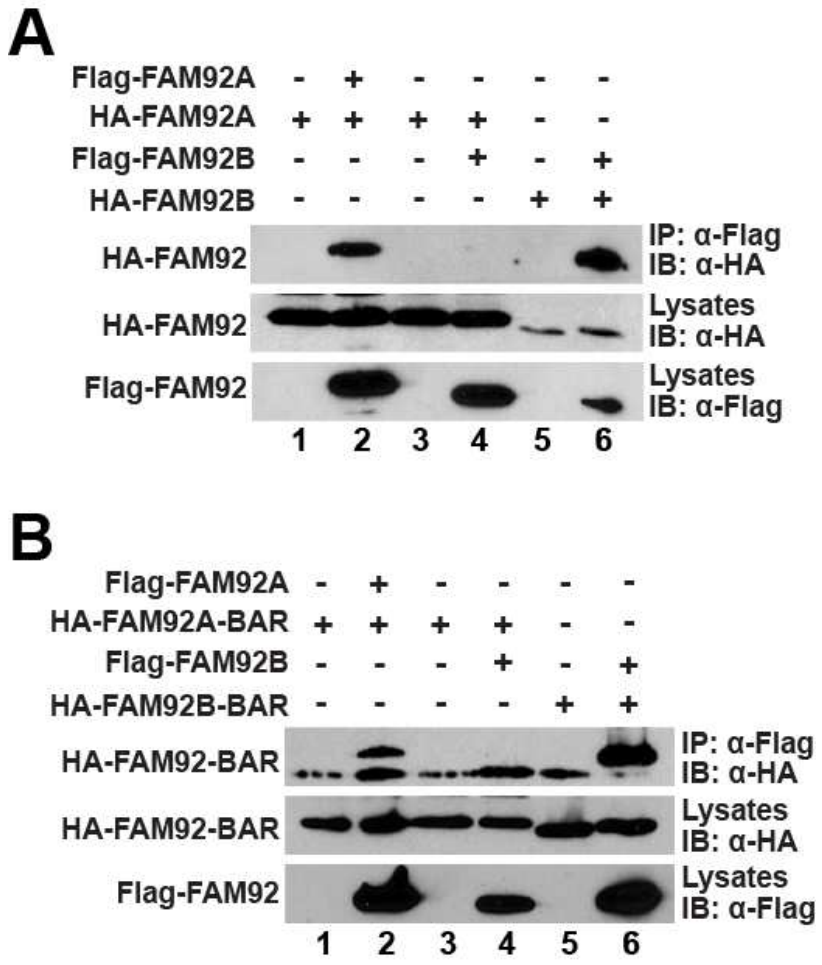

Figure 10. FAM92A and FAM92B homodimerize via their BAR domain but do not heterodimerize.

(A) HEK293T cells were transiently transfected with the indicated combination of expression plasmids for Flag- and HA-tagged FAM92 proteins. Total cell lysates were immunoprecipitated with anti-Flag antibody and detected with anti-HA antibody. Total cell lysates were also probed with either anti-HA or anti-Flag antibody to determine levels of protein expression. FAM92A (lane 2) and FAM92B (lane 6) showed ability to form homodimers but not heterodimer (lane 4).

(B) HEK293T cells were transiently transfected with the indicated combination of expression plasmids for Flag-tagged FAM92 proteins and HA-tagged FAM92-BAR proteins. Total cell lysates were immunoprecipitated with anti-Flag antibody and detected with anti-HA antibody. Total cell lysates were also probed with either anti-HA or anti-Flag antibody to determine levels of protein expression. BAR domain of FAM92A (lane 2) and FAM92B (lane 6) is sufficient for homodimer formation. No heterodimer was detected (lane 4).

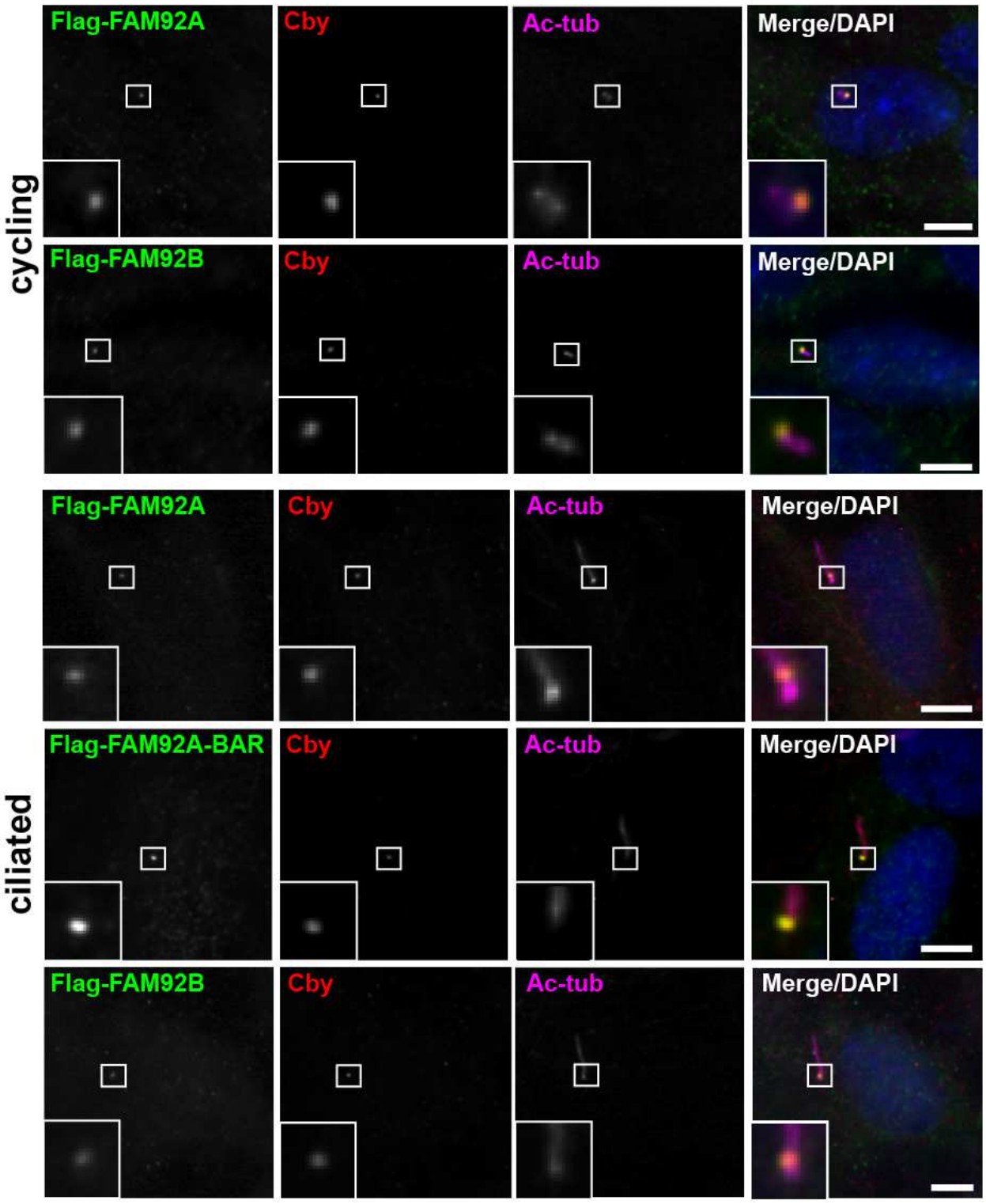
cycling
ciliated
Flag-FAM92A
Cby
Ac-tub
Merge/DAPI
Flag-FAM92B
Cby
Ac-tub
Merge/DAPI
Flag-FAM92A
Cby
Ac-tub
Merge/DAPI
Flag-FAM92A-BAR
Cby
Ac-tub
Merge/DAPI
Flag-FAM92B
Cby
Ac-tub
Merge/DAPI

Figure 11. Ectopic FAM92 proteins co-localize with Cby at the mother centriole in cycling cells and at the base of cilia in cells with primary cilia.

RPE1 cells were infected with the indicated Flag-FAM92 lentiviruses and either fixed as cycling cells at low confluency or serum-starved for 18 hr to induce ciliation. Immunofluorescence staining was performed with antibodies against Flag tag for FAM92 (green), Cby (red), and acetylated α-tubulin (Ac-tub) for cilia (purple). Nuclei were detected by DAPI (blue). Both FAM92A and FAM92B were detected at the mother centriole with Cby in cycling cell and at the base of cilia in ciliated cells. The FAM92A-BAR domain also co-localized to the mother centriole. Scale bar, 5 μm.

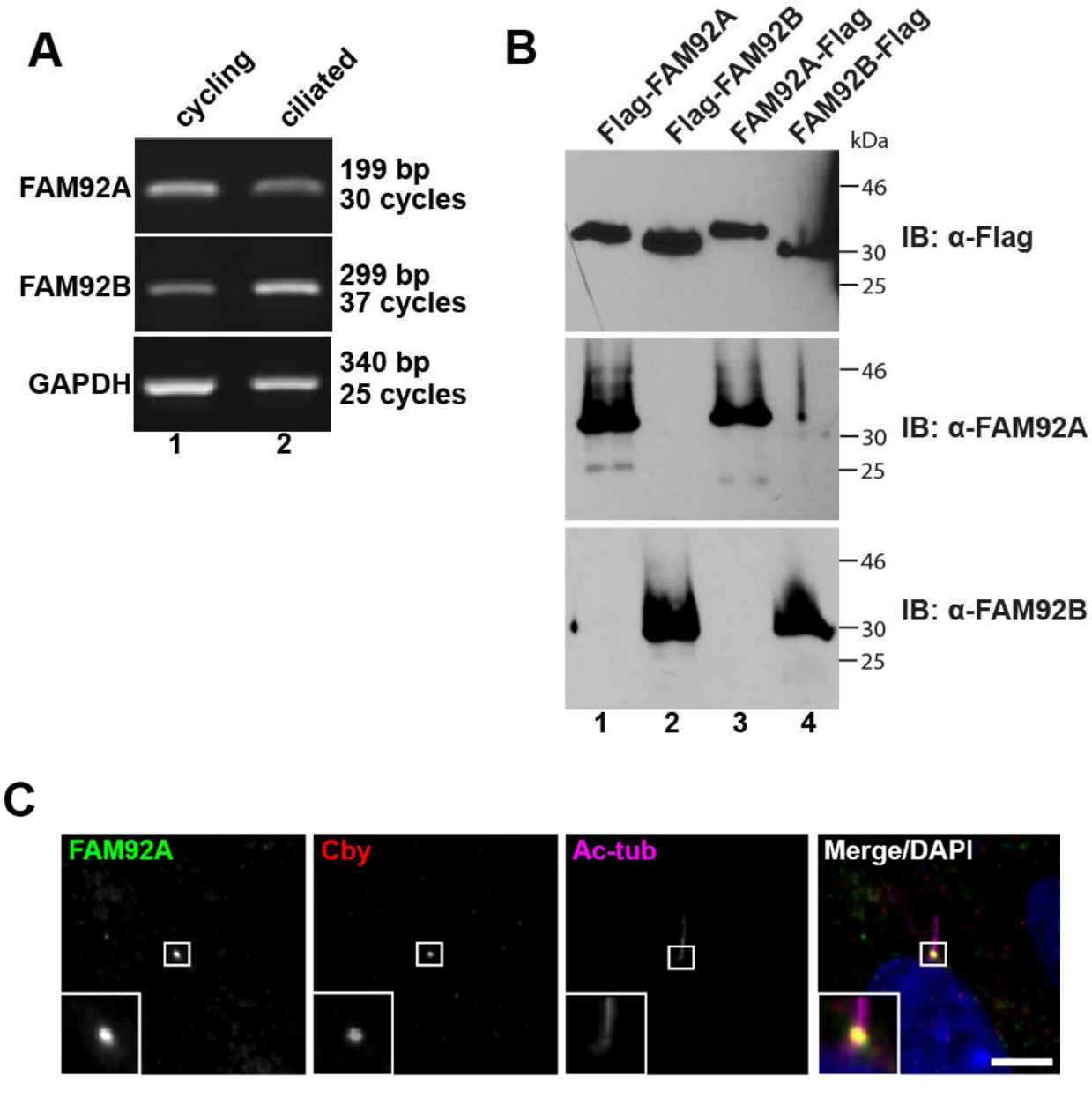

Figure 12. Endogenous FAM92A co-localize with Cby at the base of cilia.

(A) Expression of FAM92A and FAM92B was analyzed by RT-PCR in cycling and ciliated RPE1 cells. GAPDH was used as an internal control. FAM92B PCR products were detectable at higher PCR cycle numbers, suggesting that its mRNA expression level is low.

(B) FAM92A and FAM92B antibodies were evaluated their specificity and cross-reactivity using western blotting. Lysates were collected from HEK293T cells expressing either N-terminally tagged Flag-FAM92A (lane 1) or Flag-FAM92B (lane 2), or C-terminally tagged FAM92A-Flag (lane 3) or FAM92B-Flag (lane 4), followed by western blotting using anti-Flag, anti-FAM92A, or anti-FAM92B antibody.

(C) Ciliated RPE1 cells were immuno-stained for FAM92A (green), Cby (red), and acetylated α-tubulin (Ac-tub) for cilia (purple). Nuclei were detected by DAPI (blue). Endogenous FAM92A protein was detected with Cby at the base of the cilia. FAM92B was undetectable by immunofluorescence staining (data not shown). Scale bar, 5 μm.

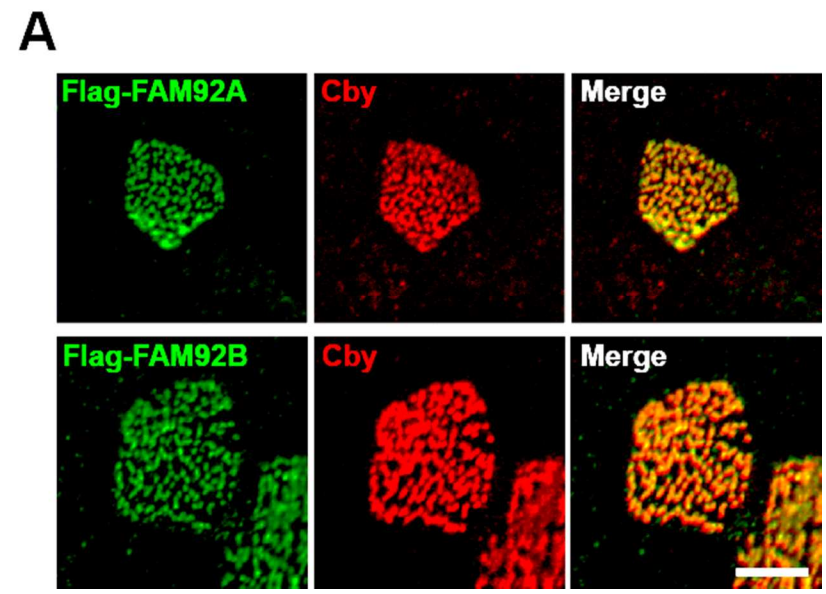
A
Flag-FAM92A
Cby
Merge
Flag-FAM92B
Cby
Merge

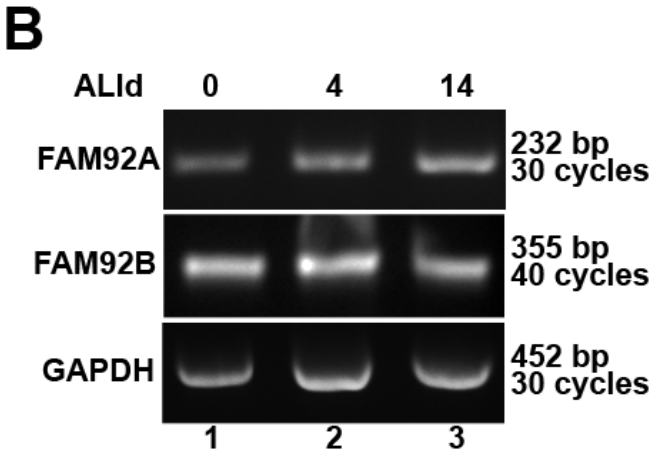
B
ALId
0
4
14
FAM92A
232 bp
30 cycles
FAM92B
355 bp
40 cycles
GAPDH
452 bp
30 cycles
1
2
3

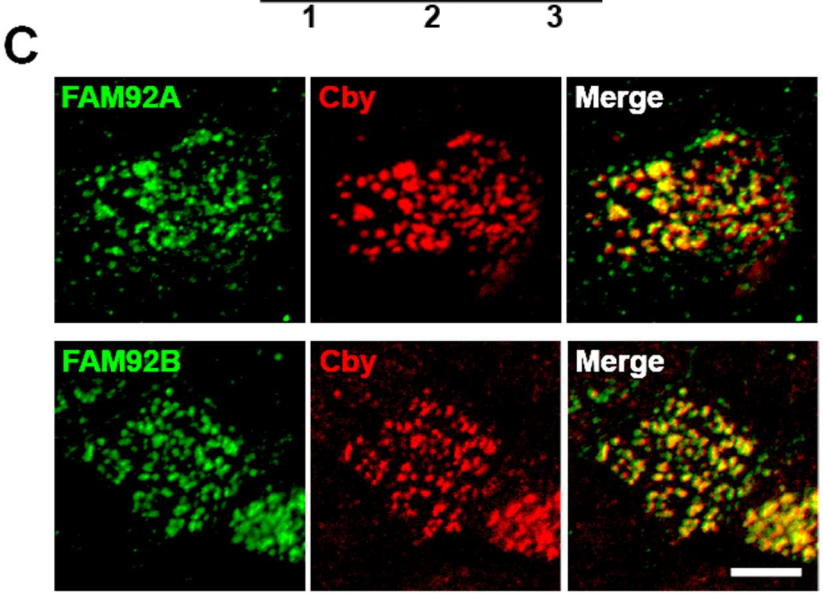
C
FAM92A
Cby
Merge
FAM92B
Cby
Merge

Figure 13. FAM92A and FAM92B co-localize with Cby at the basal body in tracheal multi-ciliated cells.

(A) Mouse tracheal epithelial cells (MTECs) were isolated and infected with the indicated lentiviruses for Flag-tagged FAM92A or FAM92B. MTECs were grown to confluence and differentiation was induced by the creation of the ALI. Immunofluorescence staining was performed on fully differentiated ALId 14 MTECs with antibodies against Flag tag for FAM92 proteins (green), and Cby (red). Ectopically expressed FAM92A and FAM92B proteins localized to the basal body with Cby. Scale bar, 5 μm.

(B) Expression of FAM92A and FAM92B mRNAs were analyzed by RT-PCR at ALId0, 4, and 14 during MTEC differentiation. GAPDH was used as an internal control. Both FAM92A and FAM92B are expressed throughout differentiation of MTECs. Both FAM92A and FAM92B are expressed throughout differentiation of MTECs. Note that FAM92B mRNA expression was detectable at higher PCR cycle numbers

(C) MTECs were fixed at ALId14 and immunofluorescence staining was performed for endogenous FAM92 proteins (green) and Cby (red). Endogenous FAM92A and FAM92B proteins co-localize with Cby at the ciliary base in multi-ciliated cells. Scale bar, 5 μm.

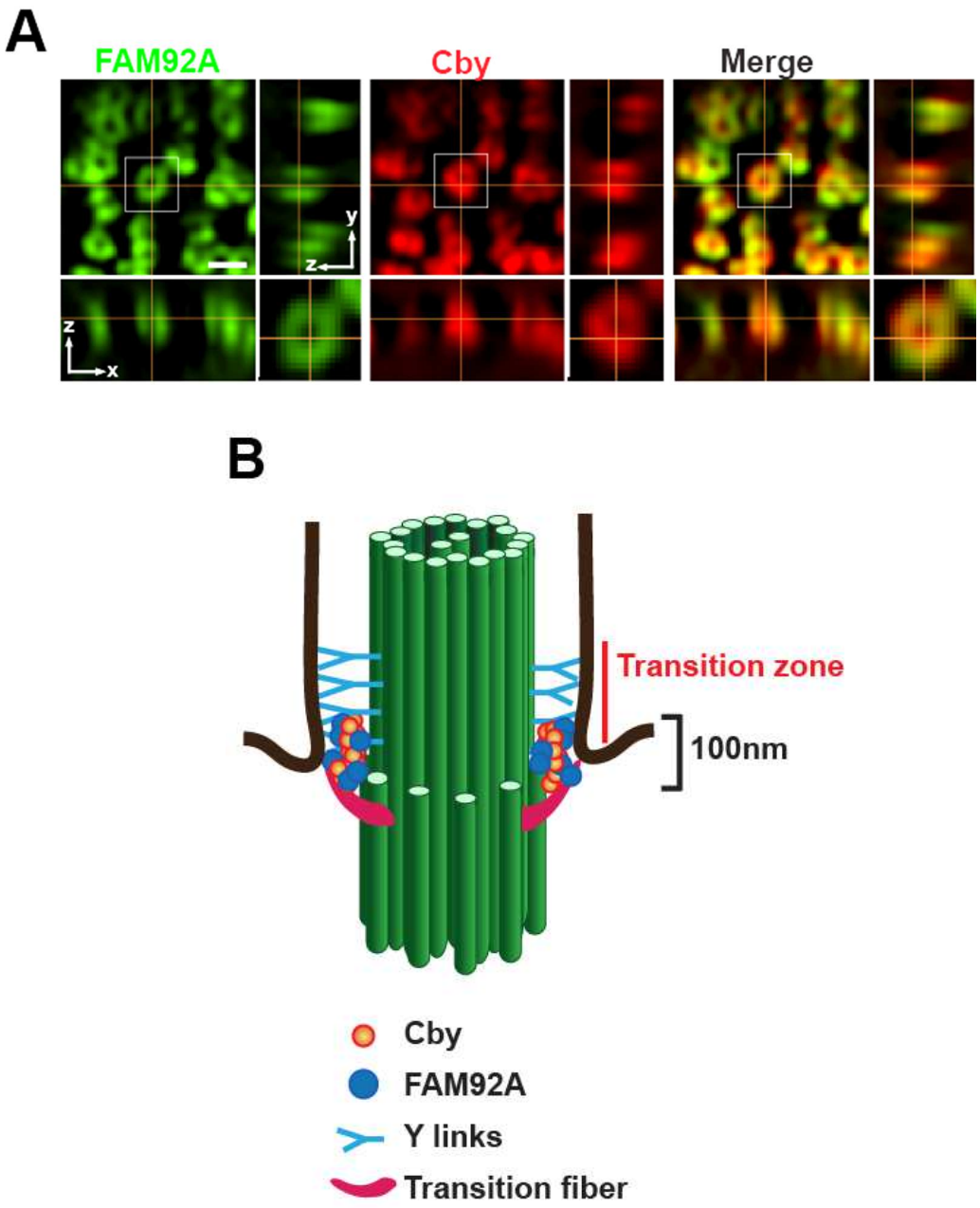

Figure 14. FAM92A localizes in a ring pattern with Cby at the base of cilia in multi-ciliated cell.

(A) MTECs were fixed at ALId 14 and immunofluorescence staining was performed with antibodies against FAM92A (green) and Cby (red). Images taken by super-resolution 3D-SIM are shown with top-down (x-y; main panel) and side (y-z on the right and x-z on the bottom; maximum projections) views. The boxed area is shown in higher magnification at the bottom right corner. Scale bar, 0.5 μm.

(B) Proposed model of FAM92A localization with Cby at the transition fibers.

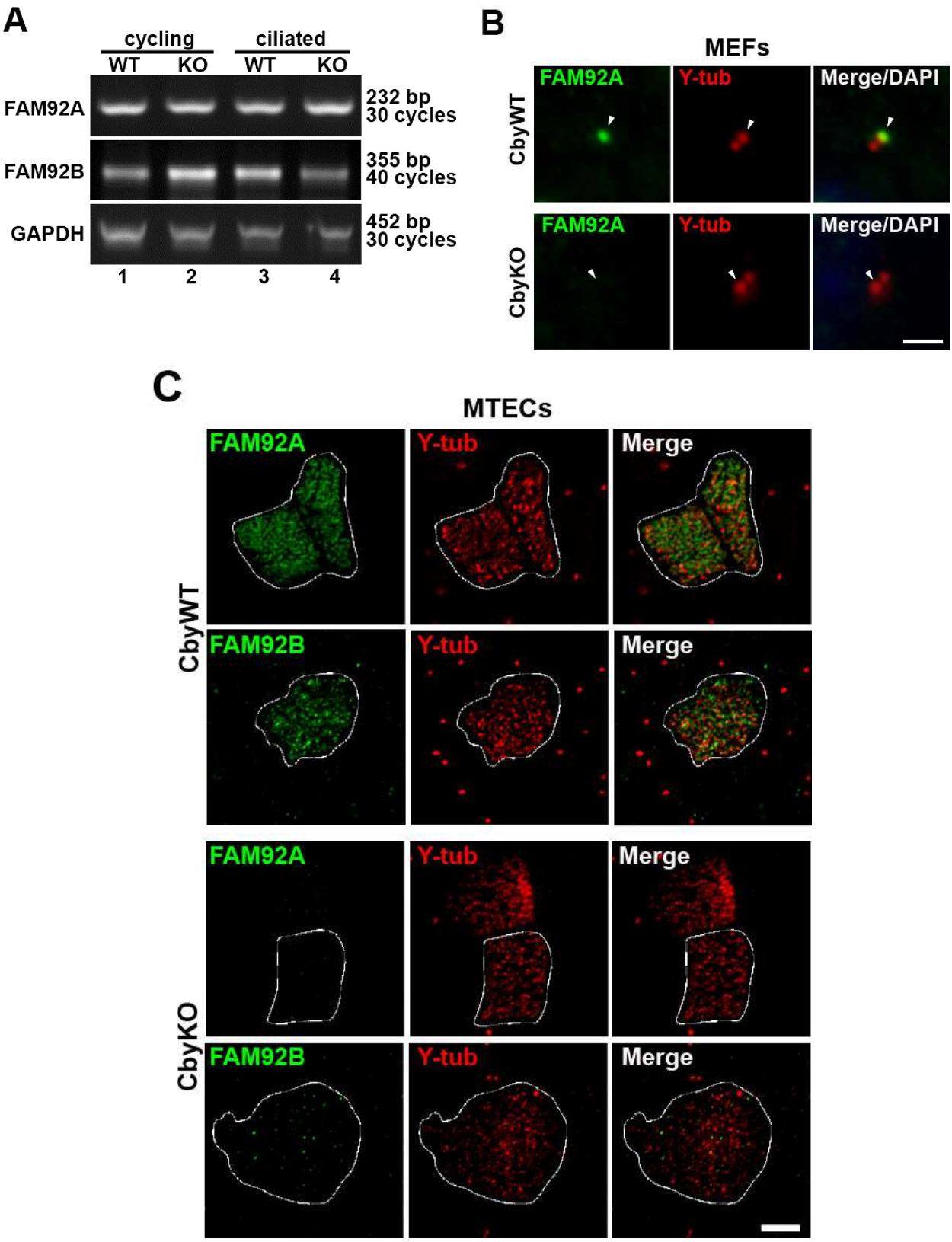
A
cycling
ciliated
WT
KO
WT
KO
FAM92A
FAM92B
GAPDH
232 bp
30 cycles
355 bp
40 cycles
452 bp
30 cycles
1
2
3
4
B
MEFs
CbyWT
CbyKO
FAM92A
Y-tub
Merge/DAPI
C
MTECs
CbyWT
CbyKO
FAM92A
FAM92B
Y-tub
Merge

Figure 15. Cby recruits FAM92 to the basal body.

(A) Expression of FAM92A and FAM92B mRNAs was analyzed by RT-PCR in CbyWT and CbyKO mouse embryonic fibroblasts (MEFs) in both the cycling and the ciliated state. GAPDH was used as an internal control.

(B) CbyWT and CbyKO MEFs were serum-starved to induce ciliation and immuno-stained for endogenous FAM92A (green) and γ-tubulin (γ-tub) for centrioles (red). Nuclei were detected by DAPI (blue). In the absence of Cby, FAM92A localization to the mother centriole (white arrow) is disrupted. FAM92B protein was not clearly detectable by immunofluorescence staining (data not shown). Scale bar, 5 μm.

(C) CbyWT and CbyKO MTECs were fixed at ALId 14 and immuno-staining was performed for FAM92 proteins (green) and γ-tubulin (γ-tub) for centrioles (red). Localization of FAM92A and FAM92B at the basal body is disrupted in CbyKO multi-ciliated cells (encircled). Scale bar, 5 μm.

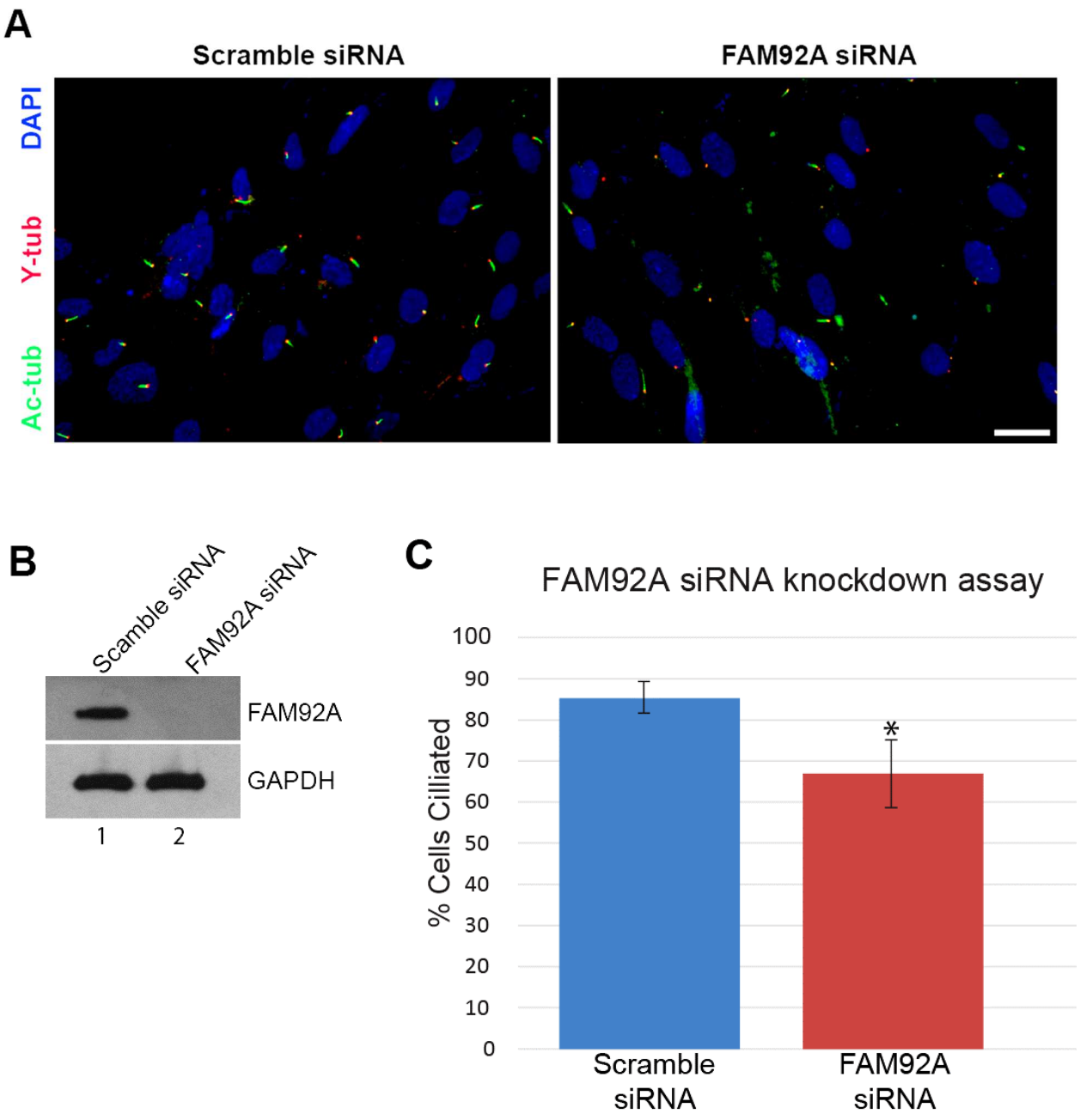

Figure 16. FAM92A functions in ciliogenesis.

(A) RPE1 cells were transfected with scramble siRNA or FAM92A siRNA and serum starved for 18 hr to induce ciliation. Immunofluorescence staining was performed with antibodies against acetylated α-tubulin (Ac-tub) for cilia (green) and γ-tubulin (γ-tub) for centrioles (red). Nuclei were detected by DAPI (blue). Scale bar, 25 μm.

(B) Western blotting demonstrating efficient depletion of FAM92A by siRNA.

(C) Effects of FAM92A depletion on primary cilia formation. FAM92A knockdown led to a significant decrease in the number of cilia in RPE1. Data represent mean ±s.d. from 6 independent experiment (n=200/experiment). Student's *t*-test, *P<0.001.

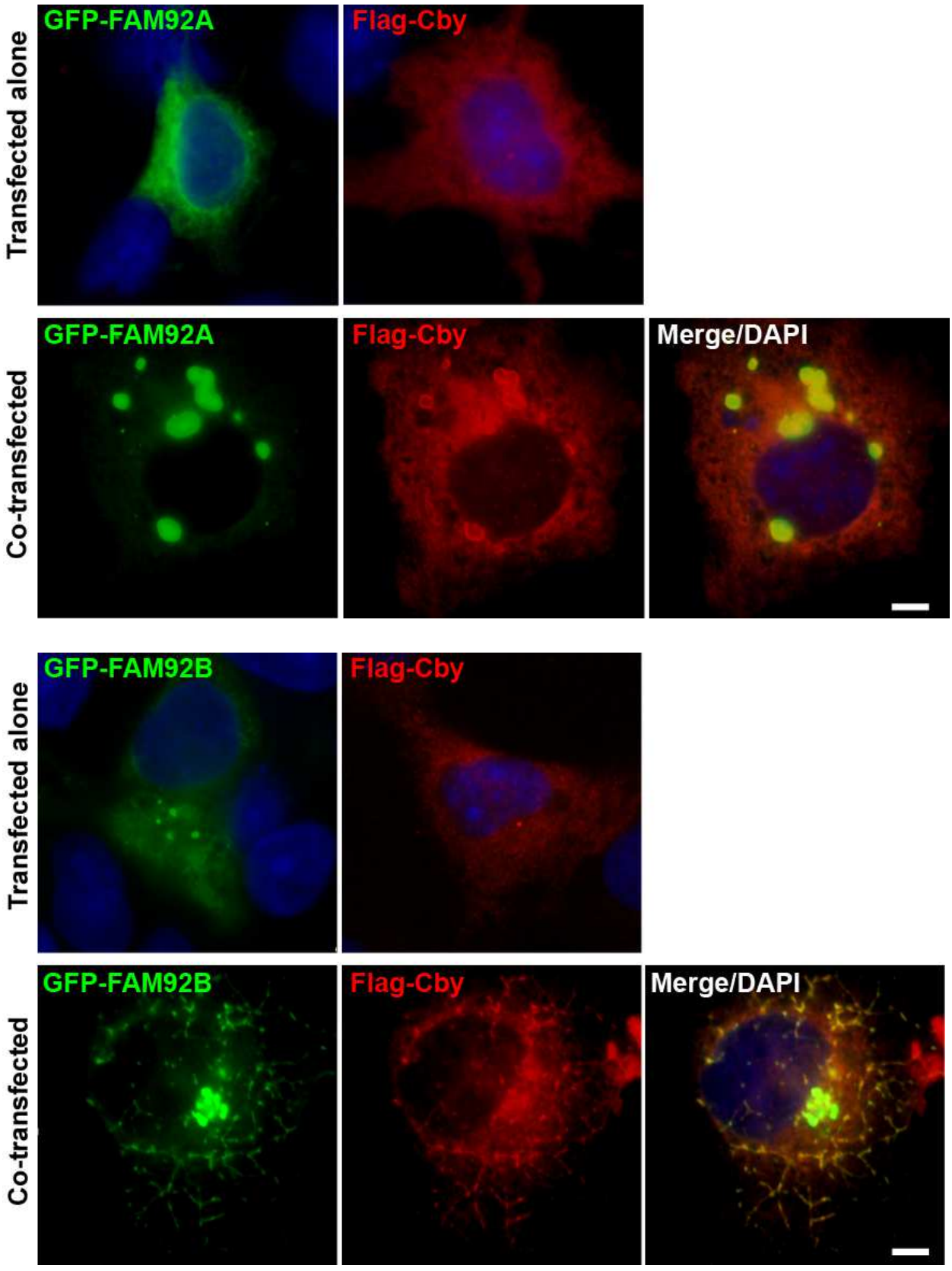
Transfected alone
GFP-FAM92A
Flag-Cby
Co-transfected
GFP-FAM92A
Flag-Cby
Merge/DAPI
Transfected alone
GFP-FAM92B
Flag-Cby
Co-transfected
GFP-FAM92B
Flag-Cby
Merge/DAPI

Figure 17: Ectopic expression of FAM92 and Cby induces membrane tubule-like structures.

COS7 cells were transiently transfected with GFP-FAM92A, GFP-FAM92B, and Flag-Cby individually or co-transfected in combination as indicated. Immuno-staining was performed for Flag tag for Cby (red). Nuclei was detected by DAPI (blue). Arrows point to potential membrane structures in the cytoplasm, containing both FAM92 and Cby. Scale bar, 5 μm.

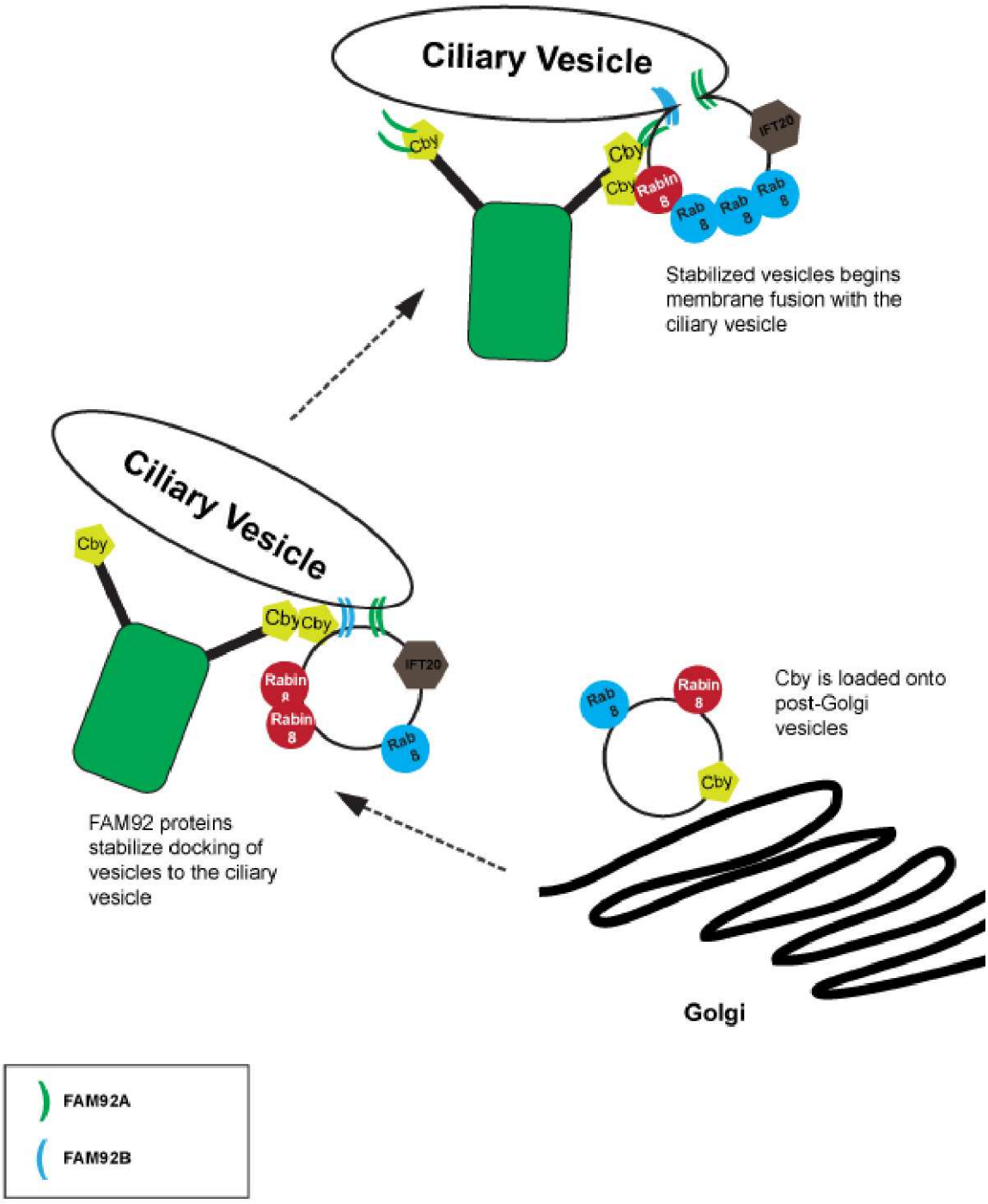
Ciliary Vesicle
Cby
Cby
Cby
Rabin 8
Rab 8
Rab 8
Rab 8
IFT20
Stabilized vesicles begins membrane fusion with the ciliary vesicle
Ciliary Vesicle
Cby
Cby
Cby
Rabin 8
Rabin 8
Rab 8
IFT20
FAM92 proteins stabilize docking of vesicles to the ciliary vesicle
Rab 8
Rabin 8
Cby
Cby is loaded onto post-Golgi vesicles
Golgi
FAM92A
FAM92B

Figure 18: Proposed model of FAM92A and FAM92B function.
FAM92A and FAM92B is recruited to the base of cilia by Cby. There, FAM92A and FAM92B act recruiters for the incoming vesicles. Cby interacts with the Rabin8, while the BAR domain of FAM92 protein sense incoming vesicle and act to stabilize it for the subsequent fusion event. FAM92 might play a role in the subsequent fusion event by creating membrane deformation to trigger membrane fusion. In absence of Cby, FAM92A and FAM92B is not recruited to the base of cilia. Incoming vesicles cannot dock effectively and cilia formation is severely reduced.

protein	unique peptides	coverage	TAP-Cby	TAP-GFP
sp|P04264|K2C1_HUMAN Keratin, type II cytoskeletal 1	78	72.00%	555	639
sp|P13645|K1C10_HUMAN Keratin, type I cytoskeletal 10	56	67.10%	440	489
SW_TRYP_PIG	37	64.90%	432	433
sp|P07437|TBB5_HUMAN Tubulin beta chain (TUBB)	41	77.00%	416	30
sp|P35908|K22E_HUMAN Keratin, type II cytoskeletal 2 epidermal	62	80.80%	320	420
sp|P68363|TBA1B_HUMAN Tubulin alpha-1B chain (TUBA1B)	29	70.30%	254	31
sp|P35527|K1C9_HUMAN Keratin, type I cytoskeletal 9	47	67.30%	227	327
sp|Q9Y3M2|CBY1_HUMAN Protein chibby homolog 1	27	82.50%	217	0
sp|P08107|HSP71_HUMAN Heat shock 70 kDa protein 1A/1B	32	56.50%	181	31
sp|P11142|HSP7C_HUMAN Heat shock cognate 71 kDa protein	31	41.50%	102	23
sp|P62258|1433E_HUMAN 14-3-3 protein epsilon	22	54.10%	80	0
sp|P13647|K2C5_HUMAN Keratin, type II cytoskeletal 5	26	39.50%	78	96
sp|P02533|K1C14_HUMAN Keratin, type I cytoskeletal 14	25	47.70%	68	95
sp|P02538|K2C6A_HUMAN Keratin, type II cytoskeletal 6A	19	31.90%	57	47
sp|P27708|PYR1_HUMAN CAD protein	17	9.80%	52	0
sp|P05787|K2C8_HUMAN Keratin, type II cytoskeletal 8	16	35.60%	45	13
sp|P68371|TBB2C_HUMAN Tubulin beta-2C chain	6	15.50%	43	2
sp|P61981|1433G_HUMAN 14-3-3 protein gamma	11	35.20%	42	0
TEV_protease	8	40.30%	36	27
sp|P68104|EF1A1_HUMAN Elongation factor 1-alpha 1	6	14.70%	34	3
sp|Q7Z794|K2C1B_HUMAN Keratin, type II cytoskeletal 1b	14	26.50%	33	3
sp|O14654|IRS4_HUMAN Insulin receptor substrate 4	12	11.60%	27	0
sp|P31946|1433B_HUMAN 14-3-3 protein beta/alpha	5	25.60%	27	0
sp|P08779|K1C16_HUMAN Keratin, type I cytoskeletal 16	11	31.90%	22	31
sp|Q04917|1433F_HUMAN 14-3-3 protein eta	8	38.20%	21	0
sp|P81605|DCD_HUMAN Dermcidin	2	20.00%	19	12
sp|P08670|VIME_HUMAN Vimentin	8	18.70%	19	0
sp|P05783|K1C18_HUMAN Keratin, type I cytoskeletal 18	9	20.00%	18	1
sp|P31689|DNJA1_HUMAN DnaJ homolog subfamily A member 1	3	12.80%	17	0
sp|P0CG48|UBC_HUMAN Polyubiquitin-C	4	6.90%	15	0
sp|Q9H1R3|MYLK2_HUMAN Myosin light chain kinase 2, skeletal/cardiac muscle	2	1.80%	14	4
sp|P62829|RL23_HUMAN 60S ribosomal protein L23	4	32.10%	14	0
sp|P63104|1433Z_HUMAN 14-3-3 protein zeta/delta	3	17.10%	13	0
sp|P02768|ALBU_HUMAN Serum albumin	3	5.60%	12	7
sp|Q04695|K1C17_HUMAN Keratin, type I cytoskeletal 17	4	9.50%	12	7
sp|P05109|S10A8_HUMAN Protein S100-A8	3	32.30%	12	4
sp|P60709|ACTB_HUMAN Actin, cytoplasmic 1	4	11.20%	12	4
sp|P06702|S10A9_HUMAN Protein S100-A9	4	40.40%	12	0
sp|P08727|K1C19_HUMAN Keratin, type I cytoskeletal 19	6	16.00%	12	0
sp|P53621|COPA_HUMAN Coatomer subunit alpha	4	4.30%	12	0
sp|O60884|DNJA2_HUMAN DnaJ homolog subfamily A member 2	3	8.70%	11	0
sp|Q13263|TIF1B_HUMAN Transcription intermediary factor 1-beta	7	9.70%	11	0
sp|Q5D862|FILA2_HUMAN Filaggrin-2	3	1.80%	10	14
sp|Q9BUF5|TBB6_HUMAN Tubulin beta-6 chain	6	12.30%	10	0
sp|A1XBS5|F92A1_HUMAN Protein FAM92A1	4	15.90%	9	0
sp|Q9Y230|RUVB2_HUMAN RuvB-like 2	5	12.30%	9	0
sp|Q13885|TBB2A_HUMAN Tubulin beta-2A chain	4	8.10%	8	0
sp|P15924|DESP_HUMAN Desmoplakin	10	3.50%	7	13
17PM_#2_PHS2_RABIT	2	2.40%	7	0
sp|O95071|UBR5_HUMAN E3 ubiquitin-protein ligase UBR5	6	2.70%	7	0
sp|P11021|GRP78_HUMAN 78 kDa glucose-regulated protein	3	5.00%	7	0
sp|P23396|RS3_HUMAN 40S ribosomal protein S3	4	18.90%	7	0
sp|Q13748|TBA3C_HUMAN Tubulin alpha-3C/D chain	2	6.00%	7	0
sp|Q86YZ3|HORN_HUMAN Hornerin	6	4.00%	6	13
sp|Q9Y265|RUVB1_HUMAN RuvB-like 1	4	11.80%	6	0
sp|Q14CN4|K2C72_HUMAN Keratin, type II cytoskeletal 72	2	4.70%	5	1
sp|Q9ULX6|AKP8L_HUMAN A-kinase anchor protein 8-like	2	3.40%	5	0
sp|P04259|K2C6B_HUMAN Keratin, type II cytoskeletal 6B	3	6.40%	4	11
sp|P83731|RL24_HUMAN 60S ribosomal protein L24	2	13.40%	4	0
sp|Q86YF9|DZIP1_HUMAN Zinc finger protein DZIP1	2	3.10%	4	0
sp|P08238|HS90B_HUMAN Heat shock protein HSP 90-beta	3	5.00%	3	0
sp|Q14683|SMC1A_HUMAN Structural maintenance of chromosomes protein 1A	3	2.70%	3	0

protein	unique peptides	coverage	TAP-Cby	TAP-GFP
sp|Q9UNF1|MAGD2_HUMAN Melanoma-associated antigen D2	2	5.30%	3	0
sp|Q02413|DSG1_HUMAN Desmoglein-1	9	12.50%	2	15
sp|Q5T749|KPRP_HUMAN Keratinocyte proline-rich protein	5	6.90%	2	8
sp|P35030|TRY3_HUMAN Trypsin-3	4	15.80%	2	6
sp|Q8TAQ2|SMRC2_HUMAN SWI/SNF complex subunit SMARCC2	2	3.00%	2	1
17PM_#14_MYG_HORSE	2	17.00%	2	0
sp|O75190|DNJB6_HUMAN DnaJ homolog subfamily B member 6	2	7.10%	2	0
sp|P42677|RS27_HUMAN 40S ribosomal protein S27	2	28.60%	2	0
sp|Q14204|DYHC1_HUMAN Cytoplasmic dynein 1 heavy chain 1	2	0.50%	2	
sp|Q9UBS4|DJB11_HUMAN DnaJ homolog subfamily B member 11	2	7.50%	2	0
sp|P14923|PLAK_HUMAN Junction plakoglobin	3	5.90%	1	6
sp|Q8N1N4|K2C78_HUMAN Keratin, type II cytoskeletal 78	4	9.00%	1	4
sp|Q6KB66|K2C80_HUMAN Keratin, type II cytoskeletal 80	2	5.10%	1	3
sp|P04406|G3P_HUMAN Glyceraldehyde-3-phosphate dehydrogenase	2	8.70%	1	2
sp|Q99456|K1C12_HUMAN Keratin, type I cytoskeletal 12	3	3.80%	1	2
sp|P05089|ARGI1_HUMAN Arginase-1	2	5.90%	1	1
sp|P62158|CALM_HUMAN Calmodulin	11	69.10%	0	38
sp|Q96P63|SPB12_HUMAN Serpin B12	3	6.70%	0	3

Table 1: Protein composition of tandem affinity purified TAP-Cby and TAP-GFP.

Summary of mass spectrometry analysis of the TAP-Cby and TAP-GFP. Proteins labeled in red are specific to Cby, while the ones labeled in black are common to both. The black box indicates FAM92A.

Chapter 4: Conclusions and Future Directions

Cilia are present on almost every cell of the human body. The motile cilia is responsible for clearing mucus from the airway, transporting o from the ovary to uterus and circulating the cerebrospinal fluids in the brain (Roy, 2009). After centuries of being ignored as a vestigial organ, the primary cilium has emerged as a prominent player in numerous physiological and development processes (Eggenschwiler and Anderson, 2007; Shah et al., 2009). The primary cilia act as 'antennae' playing crucial role in mechanosensation, photoreception and intracellular signaling (Fliegauf et al., 2007b; Goetz and Anderson, 2010). To accomplish these diverse roles, the cilia has over 1200 different proteins, many of which are known to associate with the axoneme (Pazour et al., 2005).

Ciliopathies are a genetic disorders of the cilia or basal body that result in defective ciliary function or formation. One of the best characterized ciliopathies is primary ciliary dyskinesia (PCD), a disorder in which the motile cilia of the body have defective motors. The clinical manifestation include chronic respiratory disease, male infertility and *situs inversus* (Bush and Ferkol, 2006; Schidlow, 1994). Upon characterization of our CbyKO mice, it was found that many of the CbyKO phenotypes bear striking resemblance to ciliopathic phenotypes. Subsequent investigation have concluded that Cby plays a major role in cilia formation. This dissertation isolated and characterized novel Cby interacting partners, FAM92A and FAM92B, and presented a possible link by which Cby mediate its function as a mediator of vesicle docking and fusion.

Here, I demonstrated the Cby dynamics at the base of cilia. The slow recovery of Cby from the FRAP data suggest that Cby is localized to a region of cilium that is not

readily accessible, as Cby is known to localize to the ciliary gate/transition fiber region of the ciliary axoneme (Lee et al., 2014; Burke et al., 2014). Using the microtubule depolymerization assay, I was able to visualize a subpopulation of pericentriolar Cby. This pericentriolar Cby is highly similar to PCM-1 staining in response nocodazole treatment (Lopes et al., 2011). In a co-staining with a Golgi protein marker, it was found that Cby localizes peripherally to the Golgi, which is consistent with the observation that Cby localizes with IFT20 in a pool of post-Golgi vesicles. Questions as what role this subpopulation plays remain to be answered. The fact that this subpopulation of Cby mobilize in response to microtubule depolymerization could suggest that it plays a shuttling role, delivering vital ciliary components necessary for continued ciliary function. Cby has been characterized as a shuttling protein in its role as a Wnt/β-catenin antagonist (Li et al., 2008; Takemaru et al., 2009).

Using the TAP technology, I was able to generate a list of potential Cby interacting partners. This system was used to purify and identify the BBSome complex of the basal body (Wei et al., 2012). The list included the 14-3-3ε and 14-3-3ζ protein, which is consistent with previous affinity purification (Li et al., 2008). New to the list of Cby interacting partner was the FAM92A protein. The FAM92A protein is largely uncharacterized, with a few paper that characterized its *Xenopus* homology as being important for organogenesis. Much of the project was focus on characterizing FAM92A and its related family member FAM92B, and what this interaction might mean for cilia formation.

Sequence alignment of the two FAM92 members showed homology, especially BAR domain region. The conserved nature of the BAR domain suggest shared function,

as they both interact with Cby and localize to the base of cilia in both cycling and ciliated cells. Beyond that putative BAR-domain, the FAM92 proteins gave no clue as to possible function. I demonstrated the homodimerization ability of the FAM92 bar domain proteins. Heterodimerization was suggested to be possible for two closely related BAR domain, however it was not the case for the FAM92 proteins. One interesting question is whether or not heterodimerization can be forced through point mutations of the dimer interface, as demonstrated in SNX33 and SNX9 proteins (Dislich et al., 2011).

Although FAM92A knockdown did produce a significant reduction in ciliation, the effect was moderate. Other BAR-domain proteins have been implicated in either cilia formation or maintenance. The F-BAR protein syndapin I associate with membrane areas prone to cilia formation, where it recruits Cobl which has actin binding and nucleation properties (Qualmann and Kelly, 2000). The BAR domain protein ASAP1 is thought to cause membrane deformation at the TGN that allows the release of the RTC to be trafficked to the ciliary base (Wang et al., 2012). This suggests that BAR-domain proteins could function by inducing fission. The knockdown data of FAM92A protein confirmed FAM92A as basal body protein. Future work should focus on knocking down both FAM92A and FAM92B, to minimize any genetic redundancy effect. Generating FAM92A and FAM92B knockdown will be pivotal in understand the functions of FAM92A and FAM92B.

FAM92B showed the ability to tubulate membrane, however only in the presence of Cby. FAM92B alone was not able to tubulate membranes. FAM92A when co-expressed with Cby exhibited strong puncta with a ring of Cby. Some BAR domain form vesicles instead of tubules (Boucrot et al., 2012). Depending on the physical structure of

the BAR domain, shallow hydrophobic insertions are predicted to be sufficient for vesicle formation, drive membrane fission, whereas crescent-like protein scaffolds are predicted to support the formation of continuous membrane tubules. Future work should be focused on obtaining an X-ray crystallography structure to examine the curvature of the FAM92 dimers. Additional it would be interesting to examine whether overexpression of FAM92A would have any effect on FAM92B. In conclusion, this study characterized novel basal body proteins FAM92A and FAM92B. Their BAR-domains interact with Cby and have been shown to localize to the base of cilia. Taken together, this could provide the link for the question of how Cby is able to mediate the membrane docking and fusion event so pivotal for cilia formation.

Future work should be focus on exploring the other potential Cby interacting partners listed on Table 1. One of the earliest candidate of interest were the α-tubulin and β-tubulins. The αβ-tubulin heterodimers form the basic unit of microtubule, which is the major component of the cytoskeleton providing the platform for intracellular transport and forming the core of the ciliary axoneme. This leads to the potential question of whether Cby's potential interaction with these tubulins might be involved in cilia formation. Other interesting potential include the coatomer subunit alpha, which is a component of the coatmer complex, required for budding from Golgi membrane and is essential for retrograde Golgi-to-ER transport of dilysine-tagged proteins. Cyoplasmic dynein 1, which is a motor protein involved in retrograde transport.

References

Adams, N.A., A. Awadein, and H.S. Toma. 2007. The retinal ciliopathies. *Ophthalmic Genet.* 28:113–125. doi:10.1080/13816810701537424.

Ahuja, R., R. Pinyol, N. Reichenbach, L. Custer, J. Klingensmith, M.M. Kessels, and B. Qualmann. 2007. Cordon-Bleu Is an Actin Nucleation Factor and Controls Neuronal Morphology. *Cell*. 131:337–350. doi:10.1016/j.cell.2007.08.030.

Angers, S., and R.T. Moon. 2009. Proximal events in Wnt signal transduction. *Nat Rev Mol Cell Biol*. 10:468–477. doi:10.1038/nrm2717.

Asante, D., L. Maccarthy-Morrogh, A.K. Townley, M.A. Weiss, K. Katayama, K.J. Palmer, H. Suzuki, C.J. Westlake, and D.J. Stephens. 2013. A role for the Golgi matrix protein giantin in ciliogenesis through control of the localization of dynein-2. *J Cell Sci*. 126:5189–5197. doi:10.1242/jcs.131664.

Avasthi, P., and W.F. Marshall. 2012. Stages of ciliogenesis and regulation of ciliary length. *Differentiation*. 83:S30–42. doi:10.1016/j.diff.2011.11.015.

Awata, J., S. Takada, C. Standley, K.F. Lechtreck, K.D. Bellvé, G.J. Pazour, K.E. Fogarty, and G.B. Witman. 2014. NPHP4 controls ciliary trafficking of membrane proteins and large soluble proteins at the transition zone. *J. Cell Sci.* 127:4714–27. doi:10.1242/jcs.155275.

Badano, J.L., N. Mitsuma, P.L. Beales, and N. Katsanis. 2006. The ciliopathies: an emerging class of human genetic disorders. *Annu Rev Genomics Hum Genet*. 7:125–148. doi:10.1146/annurev.genom.7.080505.115610.

Bae, Y.-K., and M.M. Barr. 2008. Sensory roles of neuronal cilia: cilia development, morphogenesis, and function in C. elegans. *Front. Biosci.* 13:5959–5974. doi:10.2741/3129.

Barandon, L., T. Couffinhal, J. Ezan, P. Dufourcq, P. Costet, P. Alzieu, L. Leroux, C. Moreau, D. Dare, and C. Duplaa. 2003. Reduction of infarct size and prevention of cardiac rupture in transgenic mice overexpressing FrzA. *Circulation*. 108:2282–2289. doi:10.1161/01.CIR.0000093186.22847.4C.

Barenz, F., D. Mayilo, and O.J. Gruss. 2011. Centriolar satellites: busy orbits around the centrosome. *Eur J Cell Biol*. 90:983–989. doi:10.1016/j.ejcb.2011.07.007.

Behrend, L., M. Stoter, M. Kurth, G. Rutter, J. Heukeshoven, W. Deppert, and U. Knippschild. 2000. Interaction of casein kinase 1 delta (CK1delta) with post-Golgi structures, microtubules and the spindle apparatus. *Eur J Cell Biol*. 79:240–251.

Behrens, J., J.P. von Kries, M. Kuhl, L. Bruhn, D. Wedlich, R. Grosschedl, and W. Birchmeier. 1996. Functional interaction of beta-catenin with the transcription factor LEF-1. *Nature*. 382:638–642. doi:10.1038/382638a0.

Benzing, T., and B. Schermer. 2011. Transition zone proteins and cilia dynamics. *Nat Genet*. 43:723–724. doi:10.1038/ng.896.

Berbari, N.F., A.D. Johnson, J.S. Lewis, C.C. Askwith, and K. Mykytyn. 2008a. Identification of ciliary localization sequences within the third intracellular loop of G protein-coupled receptors. *Mol Biol Cell*. 19:1540–1547. doi:10.1091/mbc.E07-09-0942.

Berbari, N.F., J.S. Lewis, G.A. Bishop, C.C. Askwith, and K. Mykytyn. 2008b. Bardet-Biedl syndrome proteins are required for the localization of G protein-coupled

receptors to primary cilia. *Proc Natl Acad Sci U S A*. 105:4242–4246. doi:10.1073/pnas.0711027105.
Bienz, M., and H. Clevers. 2000. Linking colorectal cancer to Wnt signaling. *Cell*. 103:311–320. doi:10.1016/S0092-8674(00)00122-7.
Boucrot, E., A.P. Ferreira, L. Almeida-Souza, S. Debard, Y. Vallis, G. Howard, L. Bertot, N. Sauvonnet, and H.T. McMahon. 2015. Endophilin marks and controls a clathrin-independent endocytic pathway. *Nature*. 517:460–465. doi:10.1038/nature14067.
Boucrot, E., A. Pick, G. Çamdere, N. Liska, E. Evergren, H.T. McMahon, and M.M. Kozlov. 2012. Membrane fission is promoted by insertion of amphipathic helices and is restricted by crescent BAR domains. *Cell*. 149:124–136. doi:10.1016/j.cell.2012.01.047.
Brown, J.M., and G.B. Witman. 2014. Cilia and Diseases. *Bioscience*. 64:1126–1137. doi:10.1093/biosci/biu174.
Brunner, E., O. Peter, L. Schweizer, and K. Basler. 1997. pangolin encodes a Lef-1 homologue that acts downstream of Armadillo to transduce the Wingless signal in Drosophila. *Nature*. 385:829–833. doi:10.1038/385829a0.
Burke, M.C., F.Q. Li, B. Cyge, T. Arashiro, H.M. Brechbuhl, X. Chen, S.S. Siller, M.A. Weiss, C.B. O'Connell, D. Love, C.J. Westlake, S.D. Reynolds, R. Kuriyama, and K. Takemaru. 2014. Chibby promotes ciliary vesicle formation and basal body docking during airway cell differentiation. *J Cell Biol*. 207:123–137. doi:10.1083/jcb.201406140.
Bush, A., and T. Ferkol. 2006. Movement: the emerging genetics of primary ciliary dyskinesia. *Am J Respir Crit Care Med*. 174:109–110. doi:10.1164/rccm.2604002.
Cajánek, L., and E. a Nigg. 2014. Cep164 triggers ciliogenesis by recruiting Tau tubulin kinase 2 to the mother centriole. *Proc. Natl. Acad. Sci. U. S. A.* 111:E2841–50. doi:10.1073/pnas.1401777111.
Cassimeris, L.U., P. Wadsworth, and E.D. Salmon. 1986. Dynamics of microtubule depolymerization in monocytes. *J Cell Biol*. 102:2023–2032.
Chavrier, P., and B. Goud. 1999. The role of ARF and Rab GTPases in membrane transport. *Curr Opin Cell Biol*. 11:466–475. doi:10.1016/S0955-0674(99)80067-2.
Cheeseman, I.M., and A. Desai. 2005. A combined approach for the localization and tandem affinity purification of protein complexes from metazoans. *Sci STKE*. 2005:pl1. doi:10.1126/stke.2662005pl1.
Chi, R.J., J. Liu, M. West, J. Wang, G. Odorizzi, and C.G. Burd. 2014. Fission of SNX-BAR-coated endosomal retrograde transport carriers is promoted by the dynamin-related protein Vps1. *J. Cell Biol.* 204:793–806. doi:10.1083/jcb.201309084.
Chia, P.Z., and P.A. Gleeson. 2014. Membrane tethering. *F1000Prime Rep*. 6:74. doi:10.12703/P6-74.
Chih, B., P. Liu, Y. Chinn, C. Chalouni, L.G. Komuves, P.E. Hass, W. Sandoval, and A.S. Peterson. 2012. A ciliopathy complex at the transition zone protects the cilia as a privileged membrane domain. *Nat Cell Biol*. 14:61–72. doi:10.1038/ncb2410.
Clevers, H. 2006. Wnt/beta-catenin signaling in development and disease. *Cell*. 127:469–480. doi:10.1016/j.cell.2006.10.018.
Corbit, K.C., A.E. Shyer, W.E. Dowdle, J. Gaulden, V. Singla, M.H. Chen, P.T. Chuang, and J.F. Reiter. 2008. Kif3a constrains beta-catenin-dependent Wnt signalling

through dual ciliary and non-ciliary mechanisms. *Nat Cell Biol*. 10:70–76. doi:ncb1670 [pii] 10.1038/ncb1670.
Coutinho-Budd, J., V. Ghukasyan, M.J. Zylka, and F. Polleux. 2012. The F-BAR domains from srGAP1, srGAP2 and srGAP3 regulate membrane deformation differently. *J. Cell Sci.* 125:3390–3401. doi:10.1242/jcs.098962.
Craige, B., C.C. Tsao, D.R. Diener, Y. Hou, K.F. Lechtreck, J.L. Rosenbaum, and G.B. Witman. 2010. CEP290 tethers flagellar transition zone microtubules to the membrane and regulates flagellar protein content. *J Cell Biol*. 190:927–940. doi:jcb.201006105 [pii] 10.1083/jcb.201006105.
Cyge, B., V. Fischer, K. Takemaru, and F.Q. Li. 2011. Generation and characterization of monoclonal antibodies against human Chibby protein. *Hybrid.* 30:163–168. doi:10.1089/hyb.2010.0098.
Dafinger, C., M.C. Liebau, S.M. Elsayed, Y. Hellenbroich, E. Boltshauser, G.C. Korenke, F. Fabretti, A.R. Janecke, I. Ebermann, G. Nurnberg, P. Nurnberg, H. Zentgraf, F. Koerber, K. Addicks, E. Elsobky, T. Benzing, B. Schermer, and H.J. Bolz. 2011. Mutations in KIF7 link Joubert syndrome with Sonic Hedgehog signaling and microtubule dynamics. *J Clin Invest*. 121:2662–2667. doi:10.1172/JCI43639 43639 [pii].
Dammermann, A., and A. Merdes. 2002. Assembly of centrosomal proteins and microtubule organization depends on PCM-1. *J Cell Biol*. 159:255–266. doi:10.1083/jcb.200204023.
Daumke, O., A. Roux, and V. Haucke. 2014. BAR domain scaffolds in dynamin-mediated membrane fission. *Cell*. 156:882–892. doi:10.1016/j.cell.2014.02.017.
Dawe, H.R., H. Farr, and K. Gull. 2007. Centriole/basal body morphogenesis and migration during ciliogenesis in animal cells. *J Cell Sci*. 120:7–15. doi:10.1242/jcs.03305.
Deane, J.A., D.G. Cole, E.S. Seeley, D.R. Diener, and J.L. Rosenbaum. 2001. Localization of intraflagellar transport protein IFT52 identifies basal body transitional fibers as the docking site for IFT particles. *Curr Biol*. 11:1586–1590.
Deretic, D., and J. Wang. 2012a. Molecular assemblies that control rhodopsin transport to the cilia. *Vision Res.* 75:5–10. doi:10.1016/j.visres.2012.07.015.
Deretic, D., and J. Wang. 2012b. Molecular assemblies that control rhodopsin transport to the cilia. *Vis. Res*. 75:5–10. doi:10.1016/j.visres.2012.07.015.
Dharmalingam, E., A. Haeckel, R. Pinyol, L. Schwintzer, D. Koch, M.M. Kessels, and B. Qualmann. 2009. F-BAR proteins of the syndapin family shape the plasma membrane and are crucial for neuromorphogenesis. *J. Neurosci.* 29:13315–13327. doi:10.1523/JNEUROSCI.3973-09.2009.
Dislich, B., M.E. Than, and S.F. Lichtenthaler. 2011. Specific amino acids in the BAR domain allow homodimerization and prevent heterodimerization of sorting nexin 33. *Biochem J*. 433:75–83. doi:10.1042/BJ20100709.
Eggenschwiler, J.T., and K. V Anderson. 2007. Cilia and Developmental Signaling. *Annu. Rev. Cell Dev. Biol.* 23:345–373. doi:10.1146/annurev.cellbio.23.090506.123249.
Essner, J.J., K.J. Vogan, M.K. Wagner, C.J. Tabin, H.J. Yost, and M. Brueckner. 2002. Conserved function for embryonic nodal cilia. *Nature*. 418:37–38. doi:10.1038/418037a.

Fischer, V., D.A. Brown-Grant, and F.Q. Li. 2012. Chibby suppresses growth of human SW480 colon adenocarcinoma cells through inhibition of beta-catenin signaling. *J Mol Signal*. 7:6. doi:10.1186/1750-2187-7-6.

Fliegauf, M., T. Benzing, and H. Omran. 2007a. When cilia go bad: cilia defects and ciliopathies. *Nat. Rev. Mol. Cell Biol.* 8:880–893. doi:10.1038/nrm2317.

Fliegauf, M., T. Benzing, and H. Omran. 2007b. When cilia go bad: cilia defects and ciliopathies. *Nat Rev Mol Cell Biol*. 8:880–893. doi:10.1038/nrm2278.

Fliegauf, M., J. Horvath, C. von Schnakenburg, H. Olbrich, D. Muller, J. Thumfart, B. Schermer, G.J. Pazour, H.P. Neumann, H. Zentgraf, T. Benzing, and H. Omran. 2006. Nephrocystin specifically localizes to the transition zone of renal and respiratory cilia and photoreceptor connecting cilia. *J Am Soc Nephrol*. 17:2424–2433. doi:ASN.2005121351 [pii] 10.1681/ASN.2005121351.

Foley, A.C., and M. Mercola. 2005. Heart induction by Wnt antagonists depends on the homeodomain transcription factor Hex. *Genes Dev*. 19:387–396. doi:10.1101/gad.1279405.

Follit, J.A., L. Li, Y. Vucica, and G.J. Pazour. 2010. The cytoplasmic tail of fibrocystin contains a ciliary targeting sequence. *J Cell Biol*. 188:21–28. doi:10.1083/jcb.200910096.

Follit, J.A., R.A. Tuft, K.E. Fogarty, and G.J. Pazour. 2006. The intraflagellar transport protein IFT20 is associated with the Golgi complex and is required for cilia assembly. *Mol Biol Cell*. 17:3781–3792. doi:E06-02-0133 [pii] 10.1091/mbc.E06-02-0133.

Frost, A., R. Perera, A. Roux, K. Spasov, O. Destaing, E.H. Egelman, P. De Camilli, and V.M. Unger. 2008. Structural Basis of Membrane Invagination by F-BAR Domains. *Cell*. 132:807–817. doi:10.1016/j.cell.2007.12.041.

Frost, A., V.M. Unger, and P. De Camilli. 2009. The BAR domain superfamily: membrane-molding macromolecules. *Cell*. 137:191–196. doi:10.1016/j.cell.2009.04.010.

Gad, S., D. Teboul, A. Lievre, N. Goasguen, A. Berger, P. Beaune, and P. Laurent-Puig. 2004. Is the gene encoding Chibby implicated as a tumour suppressor in colorectal cancer ? *BMC Cancer*. 4:31. doi:10.1186/1471-2407-4-31 1471-2407-4-31 [pii].

Gallop, J.L., C.C. Jao, H.M. Kent, P.J. Butler, P.R. Evans, R. Langen, and H.T. McMahon. 2006. Mechanism of endophilin N-BAR domain-mediated membrane curvature. *EMBO J*. 25:2898–2910. doi:10.1038/sj.emboj.7601174.

Gallop, J.L., and H.T. McMahon. 2005. BAR domains and membrane curvature: bringing your curves to the BAR. *Biochem. Soc. Symp.* 223–231.

Gerdes, J.M., Y. Liu, N.A. Zaghloul, C.C. Leitch, S.S. Lawson, M. Kato, P.A. Beachy, P.L. Beales, G.N. DeMartino, S. Fisher, J.L. Badano, and N. Katsanis. 2007. Disruption of the basal body compromises proteasomal function and perturbs intracellular Wnt response. *Nat Genet*. 39:1350–1360. doi:ng.2007.12 [pii] 10.1038/ng.2007.12.

Gherman, A., E.E. Davis, and N. Katsanis. 2006. The ciliary proteome database: an integrated community resource for the genetic and functional dissection of cilia. *Nat. Genet.* 38:961–2. doi:10.1038/ng0906-961.

Giles, R.H., J.H. Van Es, and H. Clevers. 2003. Caught up in a Wnt storm: Wnt signaling in cancer. *Biochim. Biophys. Acta - Rev. Cancer*. 1653:1–24. doi:10.1016/S0304-419X(03)00005-2.

Goel, R., K.R. Murthy, S.M. Srikanth, S.M. Pinto, M. Bhattacharjee, D.S. Kelkar, A.K. Madugundu, G. Dey, S.S. Mohan, V. Krishna, T.K. Prasad, S. Chakravarti, H. Harsha, and A. Pandey. 2013. Characterizing the normal proteome of human ciliary body. *Clin. Proteomics*. 10:9. doi:10.1186/1559-0275-10-9.

Goetz, S.C., and K. V Anderson. 2010. The primary cilium: a signalling centre during vertebrate development. *Nat Rev Genet*. 11:331–344. doi:10.1038/nrg2774.

Gouy, M., S. Guindon, and O. Gascuel. 2010. SeaView version 4: A multiplatform graphical user interface for sequence alignment and phylogenetic tree building. *Mol Biol Evol*. 27:221–224. doi:10.1093/molbev/msp259.

Graser, S., Y.D. Stierhof, S.B. Lavoie, O.S. Gassner, S. Lamla, M. Le Clech, and E.A. Nigg. 2007. Cep164, a novel centriole appendage protein required for primary cilium formation. *J Cell Biol*. 179:321–330. doi:jcb.200707181 [pii] 10.1083/jcb.200707181.

Greer, Y.E., and J.S. Rubin. 2011. Casein kinase 1 delta functions at the centrosome to mediate Wnt-3a-dependent neurite outgrowth. *J Cell Biol*. 192:993–1004. doi:10.1083/jcb.201011111.

Greer, Y.E., C.J. Westlake, B. Gao, K. Bharti, Y. Shiba, C.P. Xavier, G.J. Pazour, Y. Yang, and J.S. Rubin. 2014. Casein kinase 1delta functions at the centrosome and Golgi to promote ciliogenesis. *Mol Biol Cell*. 25:1629–1640. doi:10.1091/mbc.E13-10-0598.

Gunay-Aygun, M. 2009. Liver and kidney disease in ciliopathies. *Am. J. Med. Genet. Part C Semin. Med. Genet.* 151:296–306. doi:10.1002/ajmg.c.30225.

Gustafsson, M.G.L., L. Shao, P.M. Carlton, C.J.R. Wang, I.N. Golubovskaya, W.Z. Cande, D.A. Agard, and J.W. Sedat. 2008. Three-dimensional resolution doubling in wide-field fluorescence microscopy by structured illumination. *Biophys. J.* 94:4957–4970. doi:10.1529/biophysj.107.120345.

Habermann, B. 2004. The BAR-domain family of proteins: a case of bending and binding? *EMBO Rep*. 5:250–255. doi:10.1038/sj.embor.7400105.

Hagiwara, H., N. Ohwada, T. Aoki, and K. Takata. 2000. Ciliogenesis and ciliary abnormalities. *Med. Electron Microsc.* 33:109–114. doi:10.1007/s007950000009.

Hay, J.C., and R.H. Scheller. 1997. SNAREs and NSF in targeted membrane fusion. *Curr Opin Cell Biol*. 9:505–512.

Hidaka, S., V. Konecke, L. Osten, and R. Witzgall. 2004. PIGEA-14, a novel coiled-coil protein affecting the intracellular distribution of polycystin-2. *J Biol Chem*. 279:35009–35016. doi:10.1074/jbc.M314206200 M314206200 [pii].

Hildebrandt, F., T. Benzing, and N. Katsanis. 2011. Ciliopathies. *N. Engl. J. Med.* 364:1533–1543. doi:10.1056/NEJMra1010172.

Hildebrandt, F., and W. Zhou. 2007. Nephronophthisis-Associated Ciliopathies. *J Am Soc Nephrol*. 18:1855–1871. doi:10.1681/asn.2006121344.

Hirayama, S., Y. Yamazaki, A. Kitamura, Y. Oda, D. Morito, K. Okawa, H. Kimura, D.M. Cyr, H. Kubota, and K. Nagata. 2008. MKKS is a centrosome-shuttling protein degraded by disease-causing mutations via CHIP-mediated ubiquitination. *Mol. Biol. Cell*. 19:899–911. doi:10.1091/mbc.E07-07-0631.

Hsiao, Y.C., K. Tuz, and R.J. Ferland. 2012. Trafficking in and to the primary cilium. *Cilia*. 1:4. doi:10.1186/2046-2530-1-4.
Huang, P., and A.F. Schier. 2009. Dampened Hedgehog signaling but normal Wnt signaling in zebrafish without cilia. *Development*. 136:3089–3098. doi:10.1242/dev.041343.
Huangfu, D., A. Liu, A.S. Rakeman, N.S. Murcia, L. Niswander, and K. V Anderson. 2003. Hedgehog signalling in the mouse requires intraflagellar transport proteins. *Nature*. 426:83–87. doi:10.1038/nature02061.
Huber, D., S. Geisler, S. Monecke, and S. Hoyer-Fender. 2008. Molecular dissection of ODF2/Cenexin revealed a short stretch of amino acids necessary for targeting to the centrosome and the primary cilium. *Eur J Cell Biol*. 87:137–146. doi:10.1016/j.ejcb.2007.10.004.
Hurtado, L., C. Caballero, M.P. Gavilan, J. Cardenas, M. Bornens, and R.M. Rios. 2011. Disconnecting the Golgi ribbon from the centrosome prevents directional cell migration and ciliogenesis. *J Cell Biol*. 193:917–933. doi:10.1083/jcb.201011014.
Inglis, P.N., G. Ou, M.R. Leroux, and J.M. Scholey. 2007. The sensory cilia of Caenorhabditis elegans. *WormBook*. 1–22. doi:10.1895/wormbook.1.126.2.
Ishikawa, H., A. Kubo, and S. Tsukita. 2005. Odf2-deficient mother centrioles lack distal/subdistal appendages and the ability to generate primary cilia. *Nat Cell Biol*. 7:517–524. doi:ncb1251 [pii] 10.1038/ncb1251.
Ishikawa, H., and W.F. Marshall. 2011. Ciliogenesis: building the cell's antenna. *Nat. Rev. Mol. Cell Biol.* 12:222–234. doi:10.1038/nrm3085.
Jacob, L., and L. Lum. 2007. Hedgehog signaling pathway. *Sci. STKE*. 2007:cm6. doi:10.1126/stke.4072007cm6.
Jiang, J., and C.-C. Hui. 2008. Hedgehog signaling in development and cancer. *Dev. Cell*. 15:801–812. doi:10.1016/j.devcel.2008.11.010.
Jin, H., and M. V Nachury. 2009. The BBSome. *Curr Biol*. 19:R472–3. doi:10.1016/j.cub.2009.04.015.
Jin, H., S.R. White, T. Shida, S. Schulz, M. Aguiar, S.P. Gygi, J.F. Bazan, and M. V Nachury. 2010. The conserved Bardet-Biedl syndrome proteins assemble a coat that traffics membrane proteins to cilia. *Cell*. 141:1208–1219. doi:10.1016/j.cell.2010.05.015.
Jones, C., V.C. Roper, I. Foucher, D. Qian, B. Banizs, C. Petit, B.K. Yoder, and P. Chen. 2008. Ciliary proteins link basal body polarization to planar cell polarity regulation. *Nat Genet*. 40:69–77. doi:10.1038/ng.2007.54.
Joo, K., C.G. Kim, M.S. Lee, H.Y. Moon, S.H. Lee, M.J. Kim, H.S. Kweon, W.Y. Park, C.H. Kim, J.G. Gleeson, and J. Kim. 2013. CCDC41 is required for ciliary vesicle docking to the mother centriole. *Proc Natl Acad Sci U S A*. 110:5987–5992. doi:10.1073/pnas.1220927110.
Jost, A., and R. Heintzmann. 2013. Superresolution Multidimensional Imaging with Structured Illumination Microscopy. *Annu. Rev. Mater. Res.* 43:261–282. doi:10.1146/annurev-matsci-071312-121648.
Kim, J., S.R. Krishnaswami, and J.G. Gleeson. 2008. CEP290 interacts with the centriolar satellite component PCM-1 and is required for Rab8 localization to the primary cilium. *Hum Mol Genet*. 17:3796–3805. doi:10.1093/hmg/ddn277.

Kim, J., J.E. Lee, S. Heynen-Genel, E. Suyama, K. Ono, K. Lee, T. Ideker, P. Aza-Blanc, and J.G. Gleeson. 2010. Functional genomic screen for modulators of ciliogenesis and cilium length. *Nature*. 464:1048–1051. doi:10.1038/nature08895.

Kim, J.C., J.L. Badano, S. Sibold, M.A. Esmail, J. Hill, B.E. Hoskins, C.C. Leitch, K. Venner, S.J. Ansley, A.J. Ross, M.R. Leroux, N. Katsanis, and P.L. Beales. 2004. The Bardet-Biedl protein BBS4 targets cargo to the pericentriolar region and is required for microtubule anchoring and cell cycle progression. *Nat Genet*. 36:462–470. doi:10.1038/ng1352.

Kim, S., and B.D. Dynlacht. 2013a. Assembling a primary cilium. *Curr Opin Cell Biol*. 25:506–511. doi:10.1016/j.ceb.2013.04.011.

Kim, S., and B.D. Dynlacht. 2013b. Assembling a primary cilium. *Curr Opin Cell Biol*. 25:506–511. doi:10.1016/j.ceb.2013.04.011.

Klaus, A., and W. Birchmeier. 2008. Wnt signalling and its impact on development and cancer. *Nat Rev Cancer*. 8:387–398. doi:10.1038/nrc2389.

Klinger, M., W. Wang, S. Kuhns, F. Barenz, S. Drager-Meurer, G. Pereira, and O.J. Gruss. 2014. The novel centriolar satellite protein SSX2IP targets Cep290 to the ciliary transition zone. *Mol Biol Cell*. 25:495–507. doi:10.1091/mbc.E13-09-0526.

Knödler, A., S. Feng, J. Zhang, X. Zhang, A. Das, J. Peränen, and W. Guo. 2010. Coordination of Rab8 and Rab11 in primary ciliogenesis. *Proc. Natl. Acad. Sci. U. S. A.* 107:6346–6351. doi:10.1073/pnas.1002401107.

Kubo, A., H. Sasaki, A. Yuba-Kubo, S. Tsukita, and N. Shiina. 1999. Centriolar satellites: molecular characterization, ATP-dependent movement toward centrioles and possible involvement in ciliogenesis. *J Cell Biol*. 147:969–980.

Lee, L. 2011. Mechanisms of mammalian ciliary motility: Insights from primary ciliary dyskinesia genetics. *Gene*. 473:57–66. doi:10.1016/j.gene.2010.11.006.

Lee, Y.L., J. Sante, C.J. Comerci, B. Cyge, L.F. Menezes, F.Q. Li, G.G. Germino, W.E. Moerner, K. Takemaru, and T. Stearns. 2014. Cby1 promotes Ahi1 recruitment to a ring-shaped domain at the centriole-cilium interface and facilitates proper cilium formation and function. *Mol Biol Cell*. 25:2919–2933. doi:10.1091/mbc.E14-02-0735.

Leprince, C. 2003. Sorting nexin 4 and amphiphysin 2, a new partnership between endocytosis and intracellular trafficking. *J. Cell Sci.* 116:1937–1948. doi:10.1242/jcs.00403.

Li, F.Q., A. Mofunanya, V. Fischer, J. Hall, and K. Takemaru. 2010. Nuclear-cytoplasmic shuttling of Chibby controls beta-catenin signaling. *Mol Biol Cell*. 21:311–322. doi:10.1091/mbc.E09-05-0437.

Li, F.Q., A. Mofunanya, K. Harris, and K. Takemaru. 2008. Chibby cooperates with 14-3-3 to regulate beta-catenin subcellular distribution and signaling activity. *J Cell Biol*. 181:1141–1154. doi:10.1083/jcb.200709091.

Li, F.Q., A.M. Singh, A. Mofunanya, D. Love, N. Terada, R.T. Moon, and K. Takemaru. 2007. Chibby promotes adipocyte differentiation through inhibition of beta-catenin signaling. *Mol Cell Biol*. 27:4347–4354. doi:10.1128/MCB.01640-06.

Li, Y., Q. Zhang, Q. Wei, Y. Zhang, K. Ling, and J. Hu. 2012. SUMOylation of the small GTPase ARL-13 promotes ciliary targeting of sensory receptors. *J Cell Biol*. 199:589–598. doi:10.1083/jcb.201203150.

Lienkamp, S., A. Ganner, and G. Walz. 2012. Inversin, Wnt signaling and primary cilia. *Differentiation*. 83:S49–55. doi:10.1016/j.diff.2011.11.012.
Liu, C., T.R. Cummins, L. Tyrrell, J.A. Black, S.G. Waxman, and S.D. Dib-Hajj. 2005. CAP-1A is a novel linker that binds clathrin and the voltage-gated sodium channel Nav1.8. *Mol. Cell. Neurosci.* 28:636–649. doi:10.1016/j.mcn.2004.11.007.
Loktev, A. V, Q. Zhang, J.S. Beck, C.C. Searby, T.E. Scheetz, J.F. Bazan, D.C. Slusarski, V.C. Sheffield, P.K. Jackson, and M. V Nachury. 2008. A BBSome subunit links ciliogenesis, microtubule stability, and acetylation. *Dev Cell*. 15:854–865. doi:10.1016/j.devcel.2008.11.001.
Lopes, C.A., S.L. Prosser, L. Romio, R.A. Hirst, C. O'Callaghan, A.S. Woolf, and A.M. Fry. 2011. Centriolar satellites are assembly points for proteins implicated in human ciliopathies, including oral-facial-digital syndrome 1. *J Cell Sci*. 124:600–612. doi:10.1242/jcs.077156.
Love, D., F.Q. Li, M.C. Burke, B. Cyge, M. Ohmitsu, J. Cabello, J.E. Larson, S.L. Brody, J.C. Cohen, and K. Takemaru. 2010. Altered lung morphogenesis, epithelial cell differentiation and mechanics in mice deficient in the Wnt/beta-catenin antagonist Chibby. *PLoS One*. 5:e13600. doi:10.1371/journal.pone.0013600.
Marshall, W.F., H. Qin, M. Rodrigo Brenni, and J.L. Rosenbaum. 2005. Flagellar length control system: testing a simple model based on intraflagellar transport and turnover. *Mol Biol Cell*. 16:270–278. doi:10.1091/mbc.E04-07-0586.
Mattila, P.K., A. Pykäläinen, J. Saarikangas, V.O. Paavilainen, H. Vihinen, E. Jokitalo, and P. Lappalainen. 2007. Missing-in-metastasis and IRSp53 deform PI(4,5)P2-rich membranes by an inverse BAR domain-like mechanism. *J. Cell Biol.* 176:953–964. doi:10.1083/jcb.200609176.
Mazelova, J., L. Astuto-Gribble, H. Inoue, B.M. Tam, E. Schonteich, R. Prekeris, O.L. Moritz, P.A. Randazzo, and D. Deretic. 2009. Ciliary targeting motif VxPx directs assembly of a trafficking module through Arf4. *EMBO J*. 28:183–192. doi:10.1038/emboj.2008.267.
Miaczynska, M., S. Christoforidis, A. Giner, A. Shevchenko, S. Uttenweiler-Joseph, B. Habermann, M. Wilm, R.G. Parton, and M. Zerial. 2004. APPL proteins link Rab5 to nuclear signal transduction via an endosomal compartment. *Cell*. 116:445–456.
Milenkovic, L., M.P. Scott, and R. Rohatgi. 2009. Lateral transport of Smoothened from the plasma membrane to the membrane of the cilium. *J Cell Biol*. 187:365–374. doi:10.1083/jcb.200907126.
Millard, T.H., G. Bompard, M.Y. Heung, T.R. Dafforn, D.J. Scott, L.M. Machesky, and K. Fütterer. 2005. Structural basis of filopodia formation induced by the IRSp53/MIM homology domain of human IRSp53. *EMBO J.* 24:240–250. doi:10.1038/sj.emboj.7600535.
Mim, C., and V.M. Unger. 2012. Membrane curvature and its generation by BAR proteins. *Trends Biochem Sci*. 37:526–533. doi:10.1016/j.tibs.2012.09.001.
Mofunanya, A., F.Q. Li, J.C. Hsieh, and K. Takemaru. 2009. Chibby forms a homodimer through a heptad repeat of leucine residues in its C-terminal coiled-coil motif. *BMC Mol Biol*. 10:41. doi:10.1186/1471-2199-10-41.
Moritz, O.L., B.M. Tam, L.L. Hurd, J. Peranen, D. Deretic, and D.S. Papermaster. 2001. Mutant rab8 Impairs docking and fusion of rhodopsin-bearing post-Golgi

membranes and causes cell death of transgenic Xenopus rods. *Mol Biol Cell*. 12:2341–2351.
Moss, D.K., G. Bellett, J.M. Carter, M. Liovic, J. Keynton, A.R. Prescott, E.B. Lane, and M.M. Mogensen. 2007. Ninein is released from the centrosome and moves bi-directionally along microtubules. *J. Cell Sci.* 120:3064–3074. doi:10.1242/jcs.010322.
Nachury, M. V. 2008. Tandem affinity purification of the BBSome, a critical regulator of Rab8 in ciliogenesis. *Methods Enzym.* 439:501–513. doi:10.1016/S0076-6879(07)00434-X.
Nachury, M. V, A. V Loktev, Q. Zhang, C.J. Westlake, J. Peranen, A. Merdes, D.C. Slusarski, R.H. Scheller, J.F. Bazan, V.C. Sheffield, and P.K. Jackson. 2007. A core complex of BBS proteins cooperates with the GTPase Rab8 to promote ciliary membrane biogenesis. *Cell*. 129:1201–1213. doi:S0092-8674(07)00534-X [pii] 10.1016/j.cell.2007.03.053.
Nauli, S.M., and J. Zhou. 2004. Polycystins and mechanosensation in renal and nodal cilia. *Bioessays*. 26:844–856. doi:10.1002/bies.20069.
Nie, Z., D.S. Hirsch, R. Luo, X. Jian, S. Stauffer, A. Cremesti, J. Andrade, J. Lebowitz, M. Marino, B. Ahvazi, J.E. Hinshaw, and P.A. Randazzo. 2006. A BAR domain in the N terminus of the Arf GAP ASAP1 affects membrane structure and trafficking of epidermal growth factor receptor. *Curr. Biol.* 16:130–9. doi:10.1016/j.cub.2005.11.069.
Nie, Z., and P.A. Randazzo. 2006. Arf GAPs and membrane traffic. *J. Cell Sci.* 119:1203–1211. doi:10.1242/jcs.02924.
Nonaka, S., Y. Tanaka, Y. Okada, S. Takeda, A. Harada, Y. Kanai, M. Kido, and N. Hirokawa. 1998a. Randomization of left-right asymmetry due to loss of nodal cilia generating leftward flow of extraembryonic fluid in mice lacking KIF3B motor protein. *Cell*. 95:829–837.
Nonaka, S., Y. Tanaka, Y. Okada, S. Takeda, A. Harada, Y. Kanai, M. Kido, and N. Hirokawa. 1998b. Randomization of left-right asymmetry due to loss of nodal cilia generating leftward flow of extraembryonic fluid in mice lacking KIF3B motor protein. *Cell*. 95:829–837. doi:10.1016/S0092-8674(00)81705-5.
Nusse, R., C. Fuerer, W. Ching, K. Harnish, C. Logan, A. Zeng, D. ten Berge, and Y. Kalani. 2008. Wnt signaling and stem cell control. *Cold Spring Harb Symp Quant Biol*. 73:59–66. doi:10.1101/sqb.2008.73.035.
Ocbina, P.J.R., M. Tuson, and K. V. Anderson. 2009. Primary cilia are not required for normal canonical Wnt signaling in the mouse embryo. *PLoS One*. 4. doi:10.1371/journal.pone.0006839.
Di Paolo, G., and P. De Camilli. 2006. Phosphoinositides in cell regulation and membrane dynamics. *Nature*. 443:651–657. doi:10.1038/nature05185.
Pazour, G.J., N. Agrin, J. Leszyk, and G.B. Witman. 2005. Proteomic analysis of a eukaryotic cilium. *J Cell Biol*. 170:103–113. doi:10.1083/jcb.200504008.
Pazour, G.J., N. Agrin, B.L. Walker, and G.B. Witman. 2006. Identification of predicted human outer dynein arm genes: candidates for primary ciliary dyskinesia genes. *J. Med. Genet.* 43:62–73. doi:10.1136/jmg.2005.033001.
Pazour, G.J., S.A. Baker, J.A. Deane, D.G. Cole, B.L. Dickert, J.L. Rosenbaum, G.B. Witman, and J.C. Besharse. 2002. The intraflagellar transport protein, IFT88, is

essential for vertebrate photoreceptor assembly and maintenance. *J Cell Biol*. 157:103–113. doi:10.1083/jcb.200107108.
Pazour, G.J., and J.L. Rosenbaum. 2002. Intraflagellar transport and cilia-dependent diseases. *Trends Cell Biol*. 12:551–555.
Pearson, C.G., T.H. Giddings Jr., and M. Winey. 2009a. Basal body components exhibit differential protein dynamics during nascent basal body assembly. *Mol Biol Cell*. 20:904–914. doi:10.1091/mbc.E08-08-0835.
Pearson, C.G., D.P.S. Osborn, T.H. Giddings, P.L. Beales, and M. Winey. 2009b. Basal body stability and ciliogenesis requires the conserved component Poc1. *J. Cell Biol.* 187:905–920. doi:10.1083/jcb.200908019.
Pedersen, L.B., and J.L. Rosenbaum. 2008. Intraflagellar transport (IFT) role in ciliary assembly, resorption and signalling. *Curr Top Dev Biol*. 85:23–61. doi:10.1016/S0070-2153(08)00802-8.
Pedersen, L.B., I.R. Veland, J.M. Schrøder, and S.T. Christensen. 2008. Assembly of primary cilia. *Dev. Dyn.* 237:1993–2006. doi:10.1002/dvdy.21521.
Peter, B.J., H.M. Kent, I.G. Mills, Y. Vallis, P.J. Butler, P.R. Evans, and H.T. McMahon. 2004. BAR domains as sensors of membrane curvature: the amphiphysin BAR structure. *Science (80-.).* 303:495–499. doi:10.1126/science.1092586.
Pinto, D., and H. Clevers. 2005. Wnt, stem cells and cancer in the intestine. *Biol Cell*. 97:185–196. doi:10.1042/BC20040094.
Price, A., W. Wickner, and C. Ungermann. 2000. Proteins needed for vesicle budding from the Golgi complex are also required for the docking step of homotypic vacuole fusion. *J Cell Biol*. 148:1223–1229.
Puig, O., F. Caspary, G. Rigaut, B. Rutz, E. Bouveret, E. Bragado-Nilsson, M. Wilm, and B. Seraphin. 2001. The tandem affinity purification (TAP) method: a general procedure of protein complex purification. *Methods*. 24:218–229. doi:10.1006/meth.2001.1183.
Qualmann, B., and R.B. Kelly. 2000. Syndapin isoforms participate in receptor-mediated endocytosis and actin organization. *J. Cell Biol.* 148:1047–1061. doi:10.1083/jcb.148.5.1047.
Qualmann, B., D. Koch, and M.M. Kessels. 2011. Let's go bananas: revisiting the endocytic BAR code. *EMBO J*. 30:3501–3515. doi:10.1038/emboj.2011.266.
Ramjaun, A.R., J. Philie, E. De Heuvel, and P.S. McPherson. 1999. The N terminus of amphiphysin II mediates dimerization and plasma membrane targeting. *J. Biol. Chem.* 274:19785–19791. doi:10.1074/jbc.274.28.19785.
Ren, G., P. Vajjhala, J.S. Lee, B. Winsor, and A.L. Munn. 2006. The BAR domain proteins: molding membranes in fission, fusion, and phagy. *Microbiol Mol Biol Rev*. 70:37–120. doi:10.1128/MMBR.70.1.37-120.2006.
Renard, H.F., M. Simunovic, J. Lemiere, E. Boucrot, M.D. Garcia-Castillo, S. Arumugam, V. Chambon, C. Lamaze, C. Wunder, A.K. Kenworthy, A.A. Schmidt, H.T. McMahon, C. Sykes, P. Bassereau, and L. Johannes. 2015. Endophilin-A2 functions in membrane scission in clathrin-independent endocytosis. *Nature*. 517:493–496. doi:10.1038/nature14064.
Rigaut, G., A. Shevchenko, B. Rutz, M. Wilm, M. Mann, and B. Seraphin. 1999. A generic protein purification method for protein complex characterization and proteome exploration. *Nat Biotechnol*. 17:1030–1032. doi:10.1038/13732.

Roberts-Galbraith, R.H., and K.L. Gould. 2010. Setting the F-BAR: functions and regulation of the F-BAR protein family. *Cell Cycle*. 9:4091–4097.
Rolland, T., M. Tasan, B. Charloteaux, S.J.J. Pevzner, Q. Zhong, N. Sahni, S. Yi, I. Lemmens, C. Fontanillo, R. Mosca, A. Kamburov, S.D.D. Ghiassian, X. Yang, L. Ghamsari, D. Balcha, B.E.E. Begg, P. Braun, M. Brehme, M.P.P. Broly, A.-R.R. Carvunis, D. Convery-Zupan, R. Corominas, J. Coulombe-Huntington, E. Dann, M. Dreze, A. Dricot, C. Fan, E. Franzosa, F. Gebreab, B.J.J. Gutierrez, M.F.F. Hardy, M. Jin, S. Kang, R. Kiros, G.N.N. Lin, K. Luck, A. MacWilliams, J. Menche, R.R.R. Murray, A. Palagi, M.M.M. Poulin, X. Rambout, J. Rasla, P. Reichert, V. Romero, E. Ruyssinck, J.M.M. Sahalie, A. Scholz, A.A.A. Shah, A. Sharma, Y. Shen, K. Spirohn, S. Tam, A.O.O. Tejeda, S.A.A. Trigg, J.-C.C. Twizere, K. Vega, J. Walsh, M.E.E. Cusick, Y. Xia, A.L. Barabasi, L.M.M. Iakoucheva, P. Aloy, J. De Las Rivas, J. Tavernier, M.A.A. Calderwood, D.E.E. Hill, T. Hao, F.P.P. Roth, M. Vidal, M. Taşan, B. Charloteaux, S.J.J. Pevzner, Q. Zhong, N. Sahni, S. Yi, I. Lemmens, C. Fontanillo, R. Mosca, A. Kamburov, S.D.D. Ghiassian, X. Yang, L. Ghamsari, D. Balcha, B.E.E. Begg, P. Braun, M. Brehme, M.P.P. Broly, A.-R.R. Carvunis, D. Convery-Zupan, R. Corominas, J. Coulombe-Huntington, E. Dann, M. Dreze, A. Dricot, C. Fan, E. Franzosa, F. Gebreab, et al. 2014. A proteome-scale map of the human interactome network. *Cell*. 159:1212–1226. doi:10.1016/j.cell.2014.10.050.
Rosenbaum, J. 2002. Intraflagellar transport. *Curr Biol*. 12:R125.
Rosenbaum, J.L., and G.B. Witman. 2002. Intraflagellar transport. *Nat Rev Mol Cell Biol*. 3:813–825. doi:10.1038/nrm952.
Rothman, J.E., and G. Warren. 1994. Implications of the SNARE hypothesis for intracellular membrane topology and dynamics. *Curr Biol*. 4:220–233.
Roy, S. 2009. The motile cilium in development and disease: emerging new insights. *Bioessays*. 31:694–699. doi:10.1002/bies.200900031.
Satir, P., and S.T. Christensen. 2007. Overview of structure and function of mammalian cilia. *Annu Rev Physiol*. 69:377–400. doi:10.1146/annurev.physiol.69.040705.141236.
Schermelleh, L., R. Heintzmann, and H. Leonhardt. 2010. A guide to super-resolution fluorescence microscopy. *J. Cell Biol.* 190:165–175. doi:10.1083/jcb.201002018.
Schidlow, D. V. 1994. Primary ciliary dyskinesia (the immotile cilia syndrome). *Ann. Allergy*. 73:457–468; quiz 468–470. doi:10.1016/B978-1-4377-0755-7.00396-1.
Schmidt, T.I., J. Kleylein-Sohn, J. Westendorf, M. Le Clech, S.B. Lavoie, Y.D. Stierhof, and E.A. Nigg. 2009. Control of Centriole Length by CPAP and CP110. *Curr. Biol.* 19:1005–1011. doi:10.1016/j.cub.2009.05.016.
Schuierer, M.M., E. Graf, K. Takemaru, W. Dietmaier, and A.K. Bosserhoff. 2006. Reduced expression of beta-catenin inhibitor Chibby in colon carcinoma cell lines. *World J Gastroenterol*. 12:1529–1535.
Sebio, A., M. Kahn, and H.J. Lenz. 2014. The potential of targeting Wnt/beta-catenin in colon cancer. *Expert Opin Ther Targets*. 18:611–615. doi:10.1517/14728222.2014.906580.
Seeley, E.S., and M. V Nachury. 2010. The perennial organelle: assembly and disassembly of the primary cilium. *J. Cell Sci.* 123:511–518. doi:10.1242/jcs.061093.

Shah, A.S., Y. Ben-Shahar, T.O. Moninger, J.N. Kline, and M.J. Welsh. 2009. Motile cilia of human airway epithelia are chemosensory. *Science (80-.).* 325:1131–1134. doi:10.1126/science.1173869.

Sharma, N., N.F. Berbari, and B.K. Yoder. 2008. Chapter 13 Ciliary Dysfunction in Developmental Abnormalities and Diseases. *Curr. Top. Dev. Biol.* 85:371–427. doi:10.1016/S0070-2153(08)00813-2.

Shinozaki-Narikawa, N., T. Kodama, and Y. Shibasaki. 2006. Cooperation of phosphoinositides and BAR domain proteins in endosomal tubulation. *Traffic*. 7:1539–1550. doi:10.1111/j.1600-0854.2006.00480.x.

Simons, M., J. Gloy, A. Ganner, A. Bullerkotte, M. Bashkurov, C. Kronig, B. Schermer, T. Benzing, O.A. Cabello, A. Jenny, M. Mlodzik, B. Polok, W. Driever, T. Obara, and G. Walz. 2005. Inversin, the gene product mutated in nephronophthisis type II, functions as a molecular switch between Wnt signaling pathways. *Nat Genet*. 37:537–543. doi:ng1552 [pii] 10.1038/ng1552.

Singh, A.M., F.Q. Li, T. Hamazaki, H. Kasahara, K. Takemaru, and N. Terada. 2007. Chibby, an antagonist of the Wnt/beta-catenin pathway, facilitates cardiomyocyte differentiation of murine embryonic stem cells. *Circulation*. 115:617–626. doi:CIRCULATIONAHA.106.642298 [pii] 10.1161/CIRCULATIONAHA.106.642298.

Sonnen, K.F., L. Schermelleh, H. Leonhardt, and E.A. Nigg. 2012. 3D-structured illumination microscopy provides novel insight into architecture of human centrosomes. *Biol. Open*. 1:965–976. doi:10.1242/bio.20122337.

Sorokin, S. 1962. Centrioles and the formation of rudimentary cilia by fibroblasts and smooth muscle cells. *J Cell Biol*. 15:363–377.

Sorokin, S.P. 1968. Centriole formation and ciliogenesis. *Aspen Emphysema Conf*. 11:213–216.

Steere, N., V. Chae, M. Burke, F.Q. Li, K. Takemaru, and R. Kuriyama. 2012. A Wnt/beta-catenin pathway antagonist Chibby binds Cenexin at the distal end of mother centrioles and functions in primary cilia formation. *PLoS One*. 7:e41077. doi:10.1371/journal.pone.0041077.

Suetsugu, S. 2010. The proposed functions of membrane curvatures mediated by the BAR domain superfamily proteins. *J. Biochem.* 148:1–12. doi:10.1093/jb/mvq049.

Szymanska, K., and C.A. Johnson. 2012. The transition zone: an essential functional compartment of cilia. *Cilia*. 1:10. doi:10.1186/2046-2530-1-10.

Takemaru, K., V. Fischer, and F.Q. Li. 2009. Fine-tuning of nuclear-catenin by Chibby and 14-3-3. *Cell Cycle*. 8:210–213.

Takemaru, K., S. Yamaguchi, Y.S. Lee, Y. Zhang, R.W. Carthew, and R.T. Moon. 2003. Chibby, a nuclear beta-catenin-associated antagonist of the Wnt/Wingless pathway. *Nature*. 422:905–909. doi:10.1038/nature01570.

Tanos, B.E., H.J. Yang, R. Soni, W.J. Wang, F.P. Macaluso, J.M. Asara, and M.F. Tsou. 2013. Centriole distal appendages promote membrane docking, leading to cilia initiation. *Genes Dev*. 27:163–168. doi:10.1101/gad.207043.112.

Tarricone, C., B. Xiao, N. Justin, P.A. Walker, K. Rittinger, S.J. Gamblin, and S.J. Smerdon. 2001. The structural basis of Arfaptin-mediated cross-talk between Rac and Arf signalling pathways. *Nature*. 411:215–219. doi:10.1038/35075620.

Thompson, J.D., D.G. Higgins, and T.J. Gibson. 1994. CLUSTAL W: improving the sensitivity of progressive multiple sequence alignment through sequence weighting,

position-specific gap penalties and weight matrix choice. *Nucleic Acids Res*. 22:4673–4680.
Tobin, J.L., and P.L. Beales. 2009. The nonmotile ciliopathies. *Genet. Med.* 11:386–402. doi:10.1097/GIM.0b013e3181a02882.
Tsang, W.Y., C. Bossard, H. Khanna, J. Peranen, A. Swaroop, V. Malhotra, and B.D. Dynlacht. 2008. CP110 suppresses primary cilia formation through its interaction with CEP290, a protein deficient in human ciliary disease. *Dev Cell*. 15:187–197. doi:S1534-5807(08)00283-9 [pii] 10.1016/j.devcel.2008.07.004.
Varmark, H., S. Llamazares, E. Rebollo, B. Lange, J. Reina, H. Schwarz, and C. Gonzalez. 2007. Asterless Is a Centriolar Protein Required for Centrosome Function and Embryo Development in Drosophila. *Curr. Biol.* 17:1735–1745. doi:10.1016/j.cub.2007.09.031.
Vladar, E.K., and S.L. Brody. 2013. Analysis of ciliogenesis in primary culture mouse tracheal epithelial cells. *Methods Enzymol.* 525:285–309. doi:10.1016/B978-0-12-397944-5.00014-6.
Vladar, E.K., and T. Stearns. 2007. Molecular characterization of centriole assembly in ciliated epithelial cells. *J Cell Biol*. 178:31–42. doi:jcb.200703064 [pii] 10.1083/jcb.200703064.
Voronina, V.A., K. Takemaru, P. Treuting, D. Love, B.R. Grubb, A.M. Hajjar, A. Adams, F.Q. Li, and R.T. Moon. 2009a. Inactivation of Chibby affects function of motile airway cilia. *J Cell Biol*. 185:225–233. doi:10.1083/jcb.200809144.
Voronina, V.A., K.-I. Takemaru, P. Treuting, D. Love, B.R. Grubb, A.M. Hajjar, A. Adams, F.-Q.Q. Li, and R.T. Moon. 2009b. Inactivation of Chibby affects function of motile airway cilia. *J. Cell Biol.* 185:225–233. doi:10.1083/jcb.200809144.
Wagner, M.K., and H.J. Yost. 2000. Left-right development: The roles of nodal cilia. *Curr. Biol.* 10. doi:10.1016/S0960-9822(00)00328-6.
Wang, J., Y. Morita, J. Mazelova, and D. Deretic. 2012. The Arf GAP ASAP1 provides a platform to regulate Arf4- and Rab11–Rab8-mediated ciliary receptor targeting. *EMBO J.* 31:4057–4071. doi:10.1038/emboj.2012.253.
Wang, Q., M.V.A.S. Navarro, G. Peng, E. Molinelli, S.L. Goh, B.L. Judson, K.R. Rajashankar, and H. Sondermann. 2009. Molecular mechanism of membrane constriction and tubulation mediated by the F-BAR protein Pacsin/Syndapin. *Proc. Natl. Acad. Sci. U. S. A.* 106:12700–12705. doi:10.1073/pnas.0902974106.
Waters, A.M., and P.L. Beales. 2011. Ciliopathies: an expanding disease spectrum. *Pediatr Nephrol*. 26:1039–1056. doi:10.1007/s00467-010-1731-7.
Van Weering, J.R., P. Verkade, and P.J. Cullen. 2010. SNX-BAR proteins in phosphoinositide-mediated, tubular-based endosomal sorting. *Semin Cell Dev Biol*. 21:371–380. doi:10.1016/j.semcdb.2009.11.009.
Wei, Q., Y. Zhang, Y. Li, Q. Zhang, K. Ling, and J. Hu. 2012. The BBSome controls IFT assembly and turnaround in cilia. *Nat Cell Biol*. 14:950–957. doi:10.1038/ncb2560.
Westlake, C.J., L.M. Baye, M. V Nachury, K.J. Wright, K.E. Ervin, L. Phu, C. Chalouni, J.S. Beck, D.S. Kirkpatrick, D.C. Slusarski, V.C. Sheffield, R.H. Scheller, and P.K. Jackson. 2011. Primary cilia membrane assembly is initiated by Rab11 and transport protein particle II (TRAPPII) complex-dependent trafficking of Rabin8 to the centrosome. *Proc Natl Acad Sci U S A*. 108:2759–2764. doi:10.1073/pnas.1018823108.

Williams, C.L., C. Li, K. Kida, P.N. Inglis, S. Mohan, L. Semenec, N.J. Bialas, R.M. Stupay, N. Chen, O.E. Blacque, B.K. Yoder, and M.R. Leroux. 2011. MKS and NPHP modules cooperate to establish basal body/transition zone membrane associations and ciliary gate function during ciliogenesis. *J Cell Biol*. 192:1023–1041. doi:10.1083/jcb.201012116.

Wolf, M.T.F., and F. Hildebrandt. 2011. Nephronophthisis. *Pediatr. Nephrol.* 26:181–194. doi:10.1007/s00467-010-1585-z.

Yin, Y., A. Arkhipov, and K. Schulten. 2009. Simulations of Membrane Tubulation by Lattices of Amphiphysin N-BAR Domains. *Structure*. 17:882–892. doi:10.1016/j.str.2009.03.016.

Yoshimura, S., J. Egerer, E. Fuchs, A.K. Haas, and F.A. Barr. 2007. Functional dissection of Rab GTPases involved in primary cilium formation. *J Cell Biol*. 178:363–369. doi:10.1083/jcb.200703047.

Yuan, S., and Z. Sun. 2013. Expanding horizons: ciliary proteins reach beyond cilia. *Annu. Rev. Genet.* 47:353–76. doi:10.1146/annurev-genet-111212-133243.

Zerial, M., and H. McBride. 2001. Rab proteins as membrane organizers. *Nat Rev Mol Cell Biol*. 2:107–117. doi:10.1038/35052055.

Zhao, H., A. Pykalainen, and P. Lappalainen. 2011. I-BAR domain proteins: linking actin and plasma membrane dynamics. *Curr Opin Cell Biol*. 23:14–21. doi:10.1016/j.ceb.2010.10.005.

Zhao, X., D. Wang, X. Liu, L. Liu, Z. Song, T. Zhu, G. Adams, X. Gao, R. Tian, Y. Huang, R. Chen, F. Wang, D. Liu, X. Yu, Y. Chen, Z. Chen, M. Teng, X. Ding, and X. Yao. 2013. Phosphorylation of the Bin, Amphiphysin, and RSV161/167 (BAR) domain of ACAP4 regulates membrane tubulation. *Proc. Natl. Acad. Sci. U. S. A.* 110:11023–8. doi:10.1073/pnas.1217727110.